Development of a contrast enhanced ultrasound technique for the measurement of cerebral blood flow in patients with acute brain injury at the intensive care unit

Master Thesis

Author:
E.J. Vinke

Supervisors:
Dr. C. Hoedemaekers
Prof. Dr. Ir. C.H. Slump
Dr. C.L. de Korte
Drs. P.A. van Katwijk

Wednesday, 19 August 2015

UNIVERSITY OF TWENTE.

Radboudumc

Acknowledgements

This thesis is the result of my graduation assignment for Technical Medicine, master track Medical Sensing and Stimulation. In the past year I conducted this research at the Intensive Care department of the Radboudumc. I would like to thank *Astrid Hoedemaekers* for her supervision during the internship and giving me the opportunity to participate in clinical practice. Your views on the clinical context helped to ensure the clinical relevance of my research. Furthermore your help, critical comments, enthusiasm and support in setting up the pilot study helped make this thesis possible. At several times you had more confidence in me and in the study than I did myself. Even after it became clear that you literally could not withstand microbubbles, your confidence and enthusiasm remained. I would also like to thank *Chris de Korte* and *Gert Weijers* for your support in the use of the ultrasound device and data analysis.

Furthermore I would like to thank *Kees Slump* for his technical supervision and his help securing the scientific aspects of my study. *Paul van Katwijk*, I would like to thank you for your support and critical remarks that aided my learning process in this and previous internships. *Jeanette Hofmeijer*, thank you for taking the time to participate in my graduation colloquium and for your support in my previous internship.

I would like to thank *Bernard Geurts and Christoph Brune* for the valuable input from the mathematical point of view. Thanks to all the people at the intensive care department of the Radboudumc for the guidance during my clinical internship and for cooperating during the measurements of the pilot study. A special thanks to all the members of what we called the "SonoVue-experts-team", with a special thanks to *Judith van den Brule*. Furthermore I would also like to thank all the volunteers who participated in the pilot study. A special thanks to *Sytse de Jong*, for your company, help and support during my internship.

Finally I would like to thank all my friends and family for their moral support and motivation.

Content

1 Abstract

Background: Neurocritical care is focused on the prevention and the minimization of secondary brain damage and enabling neurological recovery. Since adequate supply of blood containing oxygen and glucose is crucial for the recovery and survival of brain tissue, monitoring the cerebral blood flow (CBF) is an essential part of neurocritical care. However, easy, non-invasive and reliable direct bedside monitoring of the CBF is not feasible at this moment in the ICU. Contrast enhanced ultrasound (CEUS) is a promising technique for this purpose. A literature study was performed to investigate promising CEUS techniques for becoming a CBF monitoring technique for patients with acute brain injury at the ICU. Following the conclusions of this systematic review a pilot study was performed. From the systematic review it is clear that studies using CEUS to measure CBF had many different aims, furthermore it was concluded that the flash-replenishment technique was the most promising technique for becoming a CBF monitoring technique. However the repeatability of the different CEUS techniques has not yet been assessed. Therefore the aim of this study is to determine the repeatability of the bolus kinetic and to determine the correlation between the blood flow velocity measured with duplex and the perfusion parameters of the bolus technique at different CBF.
Method: A study was performed on 10 young healthy volunteers. The bolus kinetic technique was performed three times during baseline. After the baseline measurements, a CEUS measurement during mild hyperventilation was performed to measure a change in CBF within the same subject. The degree of hyperventilation was monitored with end-tidal CO_2 measurements. Duplex was used as a reference, measuring the cerebral blood flow velocity (CBFV) of the middle cerebral artery (MCA) before each CEUS measurement.

Four regions of interest (ROIs) were selected, one in the MCA and three in the parenchyma. From the ROIs, time intensity curves were calculated and bolus curves were fitted. The outcome parameters of the bolus kinetic technique that were analysed were: peak intensity (PI), time peak intensity (T_{PI}) time to peak (TTP), area under the curve (AUC) and full width of half the maximum (FWHM). The outcome parameters from the Duplex were the mean CBFV ($CBFV_{mean}$) and the peak systolic velocity (PSV).

Repeatability was determined by calculating coefficient of variation (CV) in the three baseline CEUS measurements. Adequate repeatability was defined as a CV <10%. Pearson's correlation coefficients of the duplex and the CEUS outcome parameters were calculated. Furthermore CEUS perfusion parameter values and CV of the CEUS perfusion parameters in the different ROIs were analysed with a paired-T-test.
Results: the CEUS parameter with the lowest CV in the MCA region is the T_{PI} with a value of 13.7%. In the three parenchyma regions the parameter with the lowest CV is T_{PI} with a value of 6.1% in $ROI_{POSTipsi}$ and 9.7% in the other parenchyma regions. Other parameters in the MCA and parenchyma all had a CV >10%. An average decrease of 21.2% of the baseline end-tidal CO_2 was reached during mild hyperventilation. An average decrease of 10,9% of the PSV and 16,7% of the $CBFV_{mean}$ was determined. The correlation of each of the CEUS parameters and the PSV or $CBFV_{mean,}$ was significant in a maximum of two subjects.
Discussion/Conclusion: We conclude that the CEUS parameters have poor repeatability, except for the T_{PI} in the parenchyma regions. However the CV of the TTP is more representative for the variation of the arrival time than the T_{PI} . The poor repeatability corresponds with the high variation in CEUS outcome already described in literature. For the quantification of the CBF we believe that the poor repeatability within the same individual is the most important limitation of this technique.
Future perspective: Quantification of the CBF with CEUS is still far out of reach due to the high variability of the CEUS outcome. However, with the growth of our understanding of the microbubble behaviour, development of microbubbles which are uniform in size and coating, developments in the areas of ultrasound system, transducer design and signal processing, we believe that quantification of the CBF will be possible in the future. However, for the ultimate application at the ICU there are essential additional steps that need to be made in case quantification for this population becomes possible.

2 Introduction

Acute brain injury (ABI) has a high mortality and morbidity.[1] ABI is caused by stroke or traumatic brain injury (TBI). The extend of the brain damage depends on both the primary brain damage following the injury and the secondary brain damage. Brain ischemia is the major common pathway of secondary brain damage, but hyperperfusion may also include brain damage.[2] Neurocritical care is focused on the prevention and the minimization of secondary brain damage and enabling neurological recovery.[2] Since adequate supply of blood containing oxygen and nutrients is crucial for the recovery and survival of brain tissue, monitoring the cerebral blood flow (CBF) is an essential part of neurocritical care. However, easy, non-invasive, reliable and bedside monitoring of the CBF does not exist in the ICU at this moment.

In order to limit the risk of secondary brain damage in patients with ABI, changes in the brain perfusion should be detected before irreversible damage has occurred. Furthermore, the effects of the interventions have to be monitored in order to adjust therapy. Therefore, monitoring of the CBF is essential. Several methods exist to measure or image the CBF or related parameters. Imaging methods that can be used include positron emission tomography (PET), Perfusion weighted MRI (PWI), stable xenon computed tomography (Xenon CT), single-photon emission computed tomography (SPECT) and computed tomography perfusion scan (CTP).[2] These techniques give a quantitative, qualitative or semi-quantitative measure of the regional CBF. The use of these techniques in ICU patients is however limited due to the risk involved in transportation of the patient, the use or radioactive compounds or other contrast agents and/or the restrictions of the MRI environment. Other techniques measuring the CBF are thermal diffusion flowmetry (TDF), laser Doppler flowmetry (LDF), transcranial Doppler ultrasonography (TCD), jugular venous oximetry ($SjvO_2$), brain tissue oxygen monitoring ($PbrO_2$), Near-infrared spectroscopy (NIRS) and intracerebral microdialysis (ICM). Although these techniques can be used at the bedside, their use has a number of important limitations: the measures are only indirectly related to CBF, the technique measures only flow in a very restricted region of the brain or the technique is invasive.[2] A non-invasive bedside technique which is able to monitor the CBF continuously is ideal, currently no device can be singled out as an ideal CBF monitor.

Cerebral contrast enhanced ultrasound (CEUS) has been suggested as a promising method to measure CBF in patients with ABI at the ICU. Ultrasound is an attractive technique because it is non-invasive, has a high temporal resolution and can be used at the bedside. Ultrasound contrast agents (UCAs) have been used for visualization of the cerebral arteries to overcome the low level of acoustic intensity due to the ultrasound absorption of the skull leading to a poor signal-to-noise ratio.

This master thesis is focussed on the development of a CBF monitoring technique at the ICU using CEUS.

3 Clinical background

3.1 Clinical relevance

ABI has a high mortality and morbidity.[1] Traumatic brain injury (TBI) and acute stroke are the main disorders that result in acute brain injury. The incidence of TBI is approximately 85,000 per year in the Netherlands, from which the majority (85-90%) sustain a mild or moderate head injury. In 2011 approximately 21,000 TBI patients were submitted to the hospital in the Netherlands.[3] The incidence of acute stroke is 45,000 respectively 20,000 patients each year.[4] There are two types of stroke: ischemic stroke, caused by an obstruction of cerebral blood vessels or hypoperfusion, and hemorrhagic stroke, caused by a intracerebral haemorrhage or subarachnoid haemorrhage (SAH). Since adequate supply of blood containing oxygen and glucose is crucial for the recovery and survival of brain tissue, monitoring the cerebral blood flow (CBF) is an essential part of neurocritical care.

Imaging modalities measuring the CBF that cannot be performed at the ICU but are executed in some cases are PCT, DSA or CT angiography (CTA). These modalities give a measure of the CBF over the total brain, where PCT gives an indication of the microcirculation of the parenchyma and DSA and CTA give an indication of the state of the cerebral macrocirculation.[5] Because these techniques cannot be used bedside at the ICU, transportation of the patient is needed. Due to the possible deleterious effect of transportation in this patient population as indicated by Peerdeman et al., transportation should be avoided if possible.[6] Furthermore there is a radiation exposure during these measurements. Therefore the use of these imaging modalities for patients with ABI is limited and only performed when considered absolutely necessary.

3.2 Cerebral blood flow

Although the weight of the brain is only 2% of the total human body weight, CBF in the normal brain is approximately 50 ml/100 g/min, which is 15% of the cardiac output. The cerebral oxygen consumption is 20% and glucose consumption is 25% of the whole body consumption. The brain is able to withstand only very short periods of lack of blood supply due to its limited capacity for anaerobic metabolism and limited capacity of energy stores, which makes the brain extremely sensitive to ischemia.

The total CBF depends on the cerebral perfusion pressure (CPP) and the cerebrovascular resistance (CVR) (Equation 3-1). Furthermore the CPP equals the difference between the mean arterial pressure (MAP) and the intracranial pressure (ICP) (Equation 3-2).

$$\boldsymbol{CBF = \frac{CPP}{CVR}} \qquad \textbf{3-1}$$

$$\boldsymbol{CPP = MAP - ICP} \qquad \textbf{3-2}$$

As is explained by Poisseuille's law in Equation 3-3, a decrease in vessel diameter with constant perfusion pressure will decrease the blood flow. F represents the flow through a cylindrical tube with length L and radius R. ΔP represents the perfusion pressure in the tube and η the viscosity of the fluid flowing through the tube.

$$\boldsymbol{F = \Delta P \frac{\pi}{8\eta L} R^4} \qquad \textbf{3-3}$$

The regulation of the CBF involves a wide spectrum of overlapping regulatory mechanisms that together provide an adequate CBF to ensure optimal oxygen and nutrient delivery.[7] The principal regulators of the CBF are the carbon dioxide partial pressure (P_{aCO2}), mean arterial pressure, cerebral metabolism and the autonomic nervous system. With these mechanisms an adequate CBF over a wide range of cerebral perfusion pressures can be achieved using vasodilatation and vasoconstriction of the cerebral arterioles

located between the large arteries and the capillaries. However the regulatory mechanisms and the interaction between them have not yet been fully established.

3.2.1 Brain injury and cerebral blood flow

The primary brain damage caused by acute brain injury is often largely irreversible. Primary brain damage initiates metabolic, immunological and biochemical changes that can result in secondary brain damage.[2] The course of these changes are described regarding the type of damage.

Ischemia

In a patient with primary brain damage due to acute ischemic stroke, the damage regions can be divided in ischemic penumbra and the core of infarction. The cerebral damage in the core of infarction is irreversible, however the damage in the penumbra is potentially viable before it becomes completely infarcted as the core.[8] Factors which influence the viability of the penumbra are for example the cerebrovascular collateral circulation that maintains flow in the penumbra area and the CPP. Many patients have an acute hypertensive response during an acute stroke.[8]

The phenomenon of secondary ischemia after a SAH is called delayed cerebral ischemia (DCI). DCI is a common clinical syndrome which occurs in 30% of patients who suffered from SAH.[9] The widely held concept of DCI is that extravasated blood from aneurysm rupture leads to a chain reaction of cerebral artery vasoconstriction, tissue infarction, and clinical deterioration.[9] This vasoconstriction of the large arteries is called vasospasm. The exact contribution of the cerebral vasoconstriction in DCI remains unclear. For example after SAH, patients can develop cerebral infarction in a vascular distribution unaffected by angiographic vasoconstriction, however not every patient with angiographic vasospasm develops symptomatic vasospasm.[9]

Hyperperfusion

Cerebral hyperperfusion is frequently encountered following reperfusion of the ischemic brain. Reperfusion injury is defined as the structural and physiologic failure of brain tissue following an acute reperfusion or after a long-standing hyperperfusion. Mechanisms of this reperfusion injury could be related to tissue plasminogen activator toxicity, oxidative stress, and hyperperfusion due to impaired cerebral autoregulation in already maximally dilated cerebral vasculature. Presentation of this reperfusion injury include headache, seizure, status epilepticus, cerebral edema, intracranial hemorrhage, or subarachnoid hemorrhage.[10]

Edema

Edema is an important factor leading to secondary brain damage, especially in TBI. Cerebral edema can be classified in two main categories: cellular edema or vasogenic edema.[11] Cellular oedema is characterized by a water shift from the extracellular space to the intracellular space, resulting in cell swelling. Cellular edema itself does not result in an increase in brain water content or brain swelling and no rise in ICP. It does however impact the cellular function by altering intracellular metabolite concentration. Vasogenic edema is the result of the movement of water from the vasculature to the extracellular space in response to an osmotic gradient generated by the leakage of vascular components through the blood-brain barrier (BBB) into the brain parenchyma. Increase brain water content results in tissue swelling and an increase in ICP. The two types of edema can occur simultaneously. An increased ICP leads to compression of the blood vessels, decrease of CPP, which leads to a decrease in CBF as explained in Equation 3-2. Eventually, high ICP results in compression and shifts of brain tissue, which may affect vital brain areas.[11]

Cerebral autoregulation disturbance

Cerebral autoregulation is the maintenance of a constant CBF despite variations in the mean arterial pressure (MAP). The classical assumption regarding the cerebral autoregulation was that under normal conditions the CBF remains constant over a range of approximately 50-150 mmHg by adjustment of the cerebrovascular resistance. Recent studies have shown a more pressure-passive relationship between MAP and CBF in healthy individuals with a smaller plateau region.[7]

Regulatory mechanisms of CBF may be impaired or its limits may be exceeded following acute brain injury.[12] Events that may occur after acute brain injury are: ischemia and hyperperfusion. These events occur during ischemia and the reperfusion and activate a cascade of events resulting in (secondary) ischemia. Reperfusion after ischemia may also be destructive for the brain parenchyma and vessels. Ischemia will lead to damage of the endothelial cell wall of the vessels and with reperfusion molecular mechanisms and signal pathways further damaging the brain are activated.[13] Furthermore, with ischemia the resistance vessels maximally dilate and become less responsive. As a result, the arterial blood pressure is not dampened in the resistance vessels during reperfusion, resulting in capillary damage and brain edema during reperfusion.[13] This brain edema increases the ICP, influencing the CBF.[11] All these events together can result in an impaired CBF autoregulation due to the less responsive and damaged vessels, which again can result in secondary ischemia in case of hypotension or raised ICP.
CBF distribution in the brain is strongly heterogeneous. These regional differences are likely to become more pronounced in pathophysiologic conditions, because autoregulatory mechanisms may be affected heterogeneously. The range of cerebral perfusion pressure necessary to maintain adequate CBF is highly variable between individuals and changes over time. Therefore, the current opinion is that the individual cerebral perfusion thresholds should be used instead of a fixed general threshold.[12]

3.3 Neuromonitoring at the ICU

Neurocritical care aims to limit secondary brain injury and prevent systemic complications in patients with ABI. Therefore measurements of CBF or related parameters are performed on the ICU of the macro- and microcirculation. In this section a number of neuromonitoring techniques used at the ICU will be further explained. However the optimal target values of the perfusion related parameters are unknown.

3.3.1 Invasive neuromonitoring

Invasive neuromonitoring techniques include intracranial pressure (ICP) measurement, thermal diffusion flowmetry (TDF), laser Doppler flowmetry (LDF), brain tissue oxygen monitoring ($PbrO_2$) Jugular venous oximetry ($SjvO_2$) and intracerebral microdialysis (ICM). The application and the relation between the outcome parameters and the CBF are described below.

ICP
The ICP can be monitored using a catheter introduced in the ventricles or parenchym.[14] As described in Equation 3-1 and Equation 3-2, the ICP influences the CPP and therefore the CBF. Current guidelines for treatment of ABI aims to keep the ICP <20 mmHg.[15,16] In case the ICP exceeds this threshold, several treatment options exist to lower the ICP. Furthermore it is important to realize that the ICP can only be measured at one region in the brain, the region in which the catheter is placed. The measured ICP does not represent the ICP of the total brain.

TDF
The temperature difference between the neutral plate and the heated element of the probe positioned in the parenchyma reflects the local CBF. Studies have found good correlation with other methods such as Xenon CT. The main limitation of TDF are provision of only a single focal CBF measurement from the area near the probe and potential complications of acute tissue damage, bleeding and infection.[2,17] When positioned near the large vessels it may produce inaccurate measurements. Also loss of tissue contact and fever may affect the reliability of the measurements.[2]

LDF
LDF continuously measures regional CBF changes real-time. This technique has been used to assess autoregulation, CO_2 reactivity, detect ischemic insults and responses to therapeutic interventions. LD measures erythrocyte flux rather than actual CBF and therefore the quantitative CBF is expressed in units.[2] Limitations of this technique are the invasiveness and small region of which the CBF is measured.[2,17]

$PbrO_2$

A $PbrO_2$ probe is an electrode inserted into the brain parenchyma measuring pO_2. Threshold for critical cerebral ischemia is considered to be 10 mmHg. With placement near the injury or penumbra, values will reflect the local measure of brain tissue oxygen to guide therapy. $PbrO_2$ monitoring is considered useful in a variety of clinical situations where cerebral ischemia is at risk.[2,17] In patients with TBI $PbrO_2$ has shown to be a good indicator of treatment effects and correlates well with clinical outcome measures. Furthermore $PbrO_2$-guided therapy is associated with better outcome than conventional therapy.[17] This additional $PbrO_2$ monitoring to ICP/CPP directed management enabled the investigators to tolerate higher ICPs and avoid ICP management side-effects.[2] Limitations of the technique are: the invasiveness of the technique, placement of the probe within a contusion or clot will give incorrect readings and only the pO_2 near the probe can be monitored.

$SjvO_2$

Cannulation of the jugular bulb enables the assessment of the global oxygenation status of the brain and therefore the adequacy of CBF. Normal $SjvO_2$ ranges between 55 and 75%.[2,17] The ischemic threshold has been reported to be a $SjvO_2$ <50% for at least 10 minutes.[18] Low $SjvO_2$ indicates either an increase in oxygen demand or a reduction in oxygen delivery. A high $SjvO_2$ indicates the opposite and may be consistence with benign hyperaemia or decreased metabolic demand. $SjvO_2$ monitoring has been commonly used in patients with TBI or SAH for detection of reduced cerebral perfusion. A significant association exists between jugular venous desaturation and poor neurological outcome. However it has a low sensitivity and a large volume of tissue (approximately 13%) must be affected before $SjvO_2$ levels decrease below 50%.[2,17] Another limitation is the risk of complications of catheter insertion.[2]

ICM

ICM is a frequently used technique continuously monitoring biochemical markers for occurrence of hypoxia and/or ischemia. ICM can only measure the local metabolic parameters in the area of the catheter, so the catheter should ideally be placed in 'at-risk' tissue.[2,19] The most commonly measured interstitial brain analytes are lactate, pyruvate, glucose, glutamate and glycerol.[2,17] Low glucose values correlate with increased tissue injury and poor outcome. The lactate to pyruvate ratio indicates energy failure and ischemia. Glycerol is a marker for cellular stress, low oxygen or low glucose levels.[2,19] Glutamate is an excitatory amino acid neurotransmitter that is likely a marker of late injury. Due to considerable patient variation, trend interpretation is more useful than absolute measures.[2] Furthermore ICM only provides a focal measurement, therefore interpretation should be on the basis of the location.[17]

3.3.2 Non-invasive neuromonitoring

Non-invasive neuromonitoring techniques are: transcranial Doppler (TCD) and near-infrared spectroscopy (NIRS).

TCD

TCD is frequently used in the neuro-ICU for the detection of vasospasms.[17] With TCD the CBFV of the large cerebral arteries can be measured non-invasively using ultrasound. Many studies have focused on the correlation between the CBFV and the prediction of the occurrence of vasospasms. Mean flow velocities over 200 cm/s are highly suggestive for severe vasospasm, whereas velocities less than 100 cm/s are rarely associated with substantial vasospasm.[20,21] The sensitivity of TCD for diagnosis of vasospasm is 50-60% for mean flow velocities over 120 cm/s to 150 cm/s and the specificity is over 90%.[21,22]

NIRS

NIRS measures the light reflected from haemoglobin in the brain to derive the regional oxygen saturation. The values are closely related to the cerebral venous oxygen saturation as can be measured with $SjvO_2$. NIRS has been utilized for non-invasive cerebral autoregulation assessment. Establishing a consensus value for NIRS-derived thresholds for ischemia/hypoxia can be difficult due to many individual factors influencing the outcome value. Furthermore extracranial blood contamination, ambient light and probes positioning are other limitations.[2,17]

3.3.3 CEUS: a promising CBF monitoring technique

The main limitations of the techniques described in this chapter are: the invasiveness, focal or global measurements, outcome parameters are only related to the CBF or the metabolic state or oxygenation are measured. However a CBF monitoring technique at the ICU must fulfil the following requirements:

- **Applicable bedside at the ICU:** A lot of equipment is connected to the patients at the ICU and they are continuously monitored. Therefore transport of these patients is not practical, time consuming and has its risks. The study of Peerdeman et al. in 2002 indicates possible negative side effects of transportation in critically ill, mechanically ventilated head-injured patients. Therefore transportation of these patients should be avoided if possible.[6]
- **Repeatable measurement:** Optimizing the (patient specific) therapy is an ongoing process at the ICU. To know the effect of therapy on the CBF and to be able to detect changes in the CBF over time, it is not sufficient to have a single measurement of the CBF. The measurement must be repeatable at least every few hours and comparable. A low inter observer variability and a low operator dependency is preferred.
- **Safe measurement:** Inherent to the previous point, the measurement has to be safe and without side effects for the patients.
- **Semi-quantitative or quantitative outcome:** the goal of the CBF measurement is early detection of alteration of the CBF before irreversible (secondary) damage occurs. Furthermore the CBF measurements can monitor the effects of interventions in order to adjust therapy. Therefore, it is important that relative changes over time can be measured in an individual patient.
- **Suitable measurement characteristics:** The technique should have sufficient temporal, spatial resolution and accuracy.

Taking these requirements in account CEUS is a promising method because it is non-invasive, can measure the brain region that is insonated with the ultrasound probe and it measures perfusion parameters correlated with the blood volume and blood velocity. Multiplication of these perfusion parameters then correlates with the CBF.

4 Technical Background

4.1 Introduction to contrast enhanced ultrasound

Contrast enhanced ultrasound (CEUS) is an imaging technique that is frequently used to detect abnormal flow during cardiograms and for the characterization of liver lesions. CEUS has also been suggested as a promising method to measure CBF in patients with ABI at the ICU. Ultrasound is an attractive technique because it is non-invasive, has a high temporal resolution and can be used at the bedside. To visualize cerebral arteries, ultrasound contrast agents (UCAs) are necessary to overcome the low level of acoustic intensity due to the ultrasound absorption of the skull leading to a poor signal-to-noise ratio.

Several CEUS methods have been used in order to measure the CBF. The main approaches to measure the blood flow in the microcirculation with UCAs are the bolus kinetics, depletion kinetics and refill kinetics. Besides different UCA techniques, different contrast specific imaging modes have been used to quantify CBF.

The different CEUS methods have specific limitations and measure different parameters related to CBF. In the search for a bedside neuromonitoring technique at the ICU, not only measuring the most accurate perfusion parameter is required. The technique must also be: safe, feasible at the ICU, repeatable, reproducible and accurate.

4.2 Ultrasound contrast agents (UCAs)

Current ultrasound contrast agents consist of microbubbles, which are gas-filled particles of 1-10 µm diameter with various types of shells for stabilization. Because of their small size, they are able to pass through the microcirculation. When the microbubbles are dissolved, the gas is removed from the blood via exhalation.[23]

Microbubbles increase the reflectivity of blood due to its very low acoustic impedance with respect to blood. Furthermore microbubbles demonstrate a non-linear behaviour. An acoustic wave applies alternating positive and negative pressures resulting in compression and expansion of the microbubbles. Because microbubbles are able to expand much more than they can compress, an asymmetric non-linear bubble oscillation is produced. Consequently the backscattered signal contains a range of frequencies in addition to that of the incident ultrasound field. These additional frequency components are usually integer or fractional multiples of the incident frequency, called harmonics. Since tissue is less non-linear, these harmonics can be used to distinguish the microbubble echoes from tissue echoes.[24]

When microbubbles are expanded with a strong negative pressure, the shell stabilizing the bubble can break. The mechanical index (MI), originally defined to predict the onset of cavitation in fluids, gives an indication of the likelihood of bubble disruption. The probability of microbubble rupture increases with increasing MI, where MI is defined as:

$$MI = \frac{P -}{\sqrt{f}} \qquad \textbf{4-1}$$

Where P- is the negative pressure and f the ultrasound frequency. The probability of the microbubble rupture increases with a higher peak negative pressure and a lower ultrasound frequency. The threshold between a low MI and high MI is not clearly defined. In extracranial organs, ultrasound intensities with an MI >0.5 are referred to as high MI imaging. In cerebral imaging an MI >1.0 is needed for the destruction of the microbubbles to compensate for the ultrasound absorption of the skull.[25] With a MI of 0.1 or less in extracranial imaging, the microbubbles are not significantly destroyed, but give a good harmonic contrast signal. In transcranial imaging, an MI up to 0.2 is used to compensate for skull attenuation.[26]

4.3 UCA safety

There are several UCAs currently approved by the European Medicines Agency for use in European countries. The UCAs differ in type of shell and the gas within the shell. The UCA that is currently widely used in Europe is SonoVue.[27] In general, UCAs are safe with a low incidence of side effects. They are not nephrotoxic and do not interact with the thyroid gland. Mild, temporary side effects have been reported, such as nausea, flushing, pruritus and backache. The incidence of severe hypersensitivity or anaphylactoid reactions is lower than with current X-ray agents and is comparable to that of MR contrast agents. Life threatening anaphylactoid reactions have been reported with a rate of less than 0.002%.[28]

Theoretically the interaction of ultrasound and microbubbles could produce bioeffects. Cellular effects that have been observed in vitro are sonoporation, haemolysis and cell death. Such effects may have relevance for the in vivo situation. Data from small animal models have already suggested that haemorrhage and microvascular rupture could occur when microbubbles are insonated with high MI.[29] However Studies investigating the integrity of the blood brain barrier (BBB) in humans after using standard contrast-enhanced ultrasound perfusion imaging did not lead to MRI detectable BBB changes or focal brain damage.[30,31] Therefore users should balance the potential clinical benefit of the use of UCAs against the theoretical possibility of associated adverse bioeffects in humans.[28]

4.4 UCA detection

As described in the previous section, one of the methods to distinguish microbubbles from tissue is by using its harmonic behaviour. Next to this non-linear imaging, also linear scattering and bubble destruction can be used for imaging of contrast agents. The different contrast agent detection methods are described below.

Harmonic B-mode imaging (HI)
Harmonic B-mode imaging is a single pulse modality based on the stronger non-linear oscillation of contrast agents compared to the surrounding tissue. The non-linear oscillation results in harmonics in the frequency domain of the scattered signals ,therefore the signals of tissue and microbubbles can be separated using a band pass filter.

Multi-pulse ultrasound techniques
Multi-pulse techniques use multiple pulses with differences in amplitude (Power Modulation, PM), phase (Pulse Inversion, PI; Pulse Inversion Harmonic Imaging, PIHI) or both amplitude and phase (Contrast Pulse Sequencing, CPS; Power modulated PIHI, PMPI) in order to detect the harmonic response. By sending several of these pulses and subtracting the responses the linear response reduces and the harmonic response remains.

Power Doppler
Power Doppler uses the Doppler shift in frequency induced by the movement of the scattering objects, but instead of displaying this frequency shift, it displays the amplitude of the Doppler signal, which can also be colour coded. Microbubble destruction signals are being interpreted as moving objects with strong scattering power. The monochrome colour intensity is characteristic for microbubble concentration. This technique can also be combined with a harmonic bandpass filter (Harmonic power Doppler).

Contrast burst imaging (CBI) and Time Variance Imaging (TVI)
Contrast Burst Imaging and Time Variance Imaging are derived from Power Doppler in which pulses are broadband with high acoustic power. CBI detects the changes in the acoustic properties of microbubbles that are caused by ultrasound-induced shrinking, splitting and destruction, while suppressing tissue and clutter signals by multiple echo measurements. TVI also depicts the time variant acoustic properties of microbubbles by analysing multiple pulse echo measurements, but TVI uses a contrast agent specific analysis strategy to improve the suppression of noise and artefacts.[32]

4.5 From microbubble to perfusion parameters

In CEUS, next to the different contrast specific imaging modes, three different approaches are used to measure the cerebral perfusion. These approaches are based on the bolus, refill (replenishment) and depletion kinetics. In CEUS, the CBF has mainly been assessed with the bolus kinetic approach.

4.5.1 Bolus kinetics

After a bolus injection, microbubbles enter the insonation field and the acoustic intensity in this plane increases. The acoustic intensity over time can be represented by a time intensity curve (TIC) as shown in Figure 1. Microbubbles entering the insonation field are destroyed by ultrasound energy. To allow inflow into the parenchyma, a frame rate of 0.25-1 Hz must be used. Different parameters of the TIC can be extracted, such as: time-to-peak (TTP), time-to-peak intensity (T_{PI}), peak intensity (PI), peak width (PW, full width at 90% of the maximum intensity), full width at half of the maximum intensity increase (FWHM), area under the curve (AUC) and positive gradient (PG, slope of the wash-in phase).

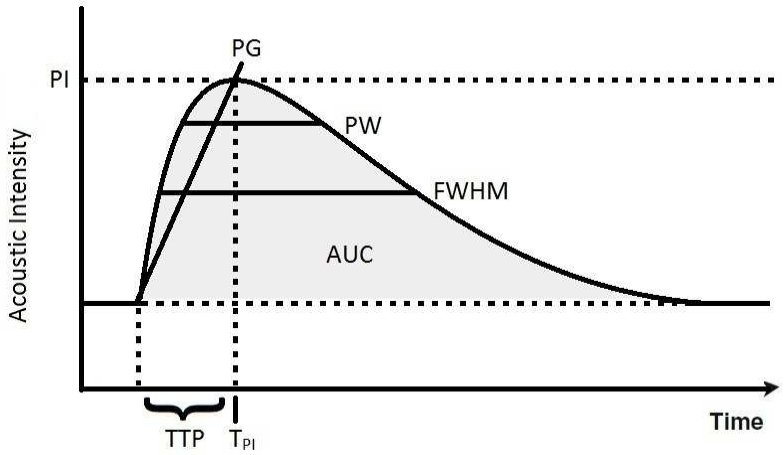

Figure 1: Time intensity curve of the bolus kinetic CEUS approach, with time-to-peak (TTP), time-to-peak intensity (TPI), peak intensity (PI), peak width (PW, full width at 90% of the maximum intensity), full width at half of the maximum intensity increase (FWHM), positive gradient (PG), and area under the curve (AUC).

4.5.2 Refill kinetics

Refill kinetics is based on the reappearance of echo-contrast after complete destruction of the microbubbles, when a constant UCA infusion is given. By destroying the contrast agent within the scanning plane using a high MI flash image, a negative bolus of contrast agent is created locally and new microbubbles enter the plane with a certain velocity within a certain tissue volume. The refill intensity curve can be achieved using two methods. In Figure 2, the flash-replenishment method is shown where low MI ultrasound imaging is used to monitor replenishment kinetics in real-time following UCA destruction. The second method, called the increasing intervals method, detects the intensity gain between destructive ultrasound frames at increasing pulsing intervals, from 50 ms to 8000 ms.[25]

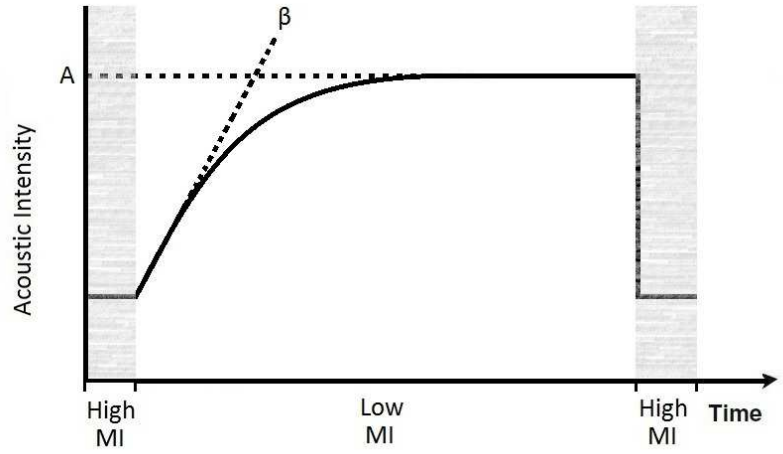

Figure 2: Intensity curve of the refill kinetics, resulting from high MI pulses followed by low MI pulses, with parameters A and β .

After bubble destruction, microbubble tissue replenishment can be described as an exponential curve with the corresponding equation:

$$y = A(1 - e^{-\beta t}) \qquad \textbf{4-2}$$

Where y is the acoustic intensity, *t* represents time after the high MI flashes (flash-replenishment imaging) or pulsing interval (increasing intervals method), β represents the rise rate of the acoustic intensity over time and A is the plateau of acoustic intensity, reflecting the microvascular cross-sectional area. β is directly related to the blood flow velocity and A to the blood volume. Therefore, the product of both (A×β) is related with the blood flow.[33]

4.5.3 Depletion kinetics

Depletion kinetics is based on the destruction of contrast agent at a constant frame rate with a high MI. The TIC decreases to a new equilibrium, determined by a balance between destruction and reperfusion of the UCA between the high MI frames. Three mathematical models have been applied for analysing the depletion curve: an exponential decay model, a complex exponential model, which separates the curve into destruction and reperfusion phases, providing a perfusion and destruction coefficient, and a simple linear model (Figure 3). Because of the short sampling time needed (1- 10 seconds), depletion kinetics can be analysed using either bolus injection or infusion.[25]

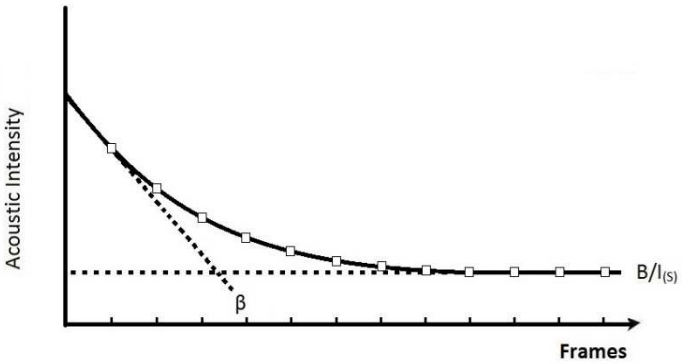

Figure 3: Scheme of contrast depletion kinetics of brain perfusion assessment. $\beta = \ln 2/T_{halflife}$, B = baseline intensity (exponential model), equivalent to I(S) = intensity at the steady state (linear model). The dotted line indicates the two components of the complex exponential model.

4.5.4 Perfusion parameters

The parameters retrieved from the intensity curves from the bolus, depletion and refill kinetics can be used to quantify the cerebral perfusion. The value of these parameters depend on the relation with CBF. From the theoretical point of view, time dependent parameters like TTP (bolus kinetics), perfusion coefficient (depletion kinetics) or β (refill kinetics) are more useful than amplitude dependent parameters. This because the amplitude depends on the insonation depth and contrast concentration and therefore depends on the attenuation of the skull. Time dependent parameters are independent from amplitude and insonation depth and are expected to be linearly related to the blood flow velocity.[34–36]

In order to extract the perfusion parameters from the TICs measured with CEUS, curve fitting must be applied due to the noise, scattering and probe movement artefacts. This will be further explained in section 4.6.2 and in section 6.4.1.

4.6 General aspects of CEUS

CEUS is frequently used for the diagnosis and the characterization of focal liver lesions. The appearance of focal liver lesions during the CEUS procedure are described in terms of degree of enhancement and phase of enhancement (arterial phase, portal venous phase and the late phase). Other applications of CEUS in the liver are inter operative CEUS during liver resection and monitoring ablation therapy.[27] Over the years CEUS has also been applied to several other medical fields as an enhancement on the conventional US and Doppler ultrasound. Overall CEUS is used for diagnosing and characterizing lesions, tumours and vascular disorders in several organs.[28,37]

However, to overcome the subjective evaluation of the enhancement of normal and abnormal parenchyma, or between a focal lesion and surrounding tissue, quantitative measures of the blood flow are needed. Depending on the organ and the goal of the CEUS measurement quantification is focussed on the blood volume or on the CBF. So far the main use of CEUS quantification is for monitoring therapeutic response to drugs implying an effect on tumour vascularization, which focusses on the quantification of the blood volume.[38]

4.6.1 CEUS outcome variability

High variability of CEUS outcome is the key challenge of quantification of this technique. The causes of this high variability have not yet been completely understood.[39] The sources of this variability that are described can be divided in four categories: CEUS operator, scanner settings, patient based factors and microbubble based factors. Variation due to these different factors may be effectively reduced by standardizing the data acquisition and processing protocols. However these protocols can only effectively reduce the variations to a certain extent. Protocols cannot deal with variation caused by physiological or pathological variation of the patients.[37,38]

CEUS operator

CEUS is operator dependent, due to differences between operators according to microbubble handling, probe positioning, selection of the regions of interest, sonographic interpretation and personal preferences in scanner settings. In order to reduce operator based variation it is recommended that only one experienced operator does the measurements in both clinical and study applications.[39]

Scanner settings

Imaging parameters and specific equipment settings greatly influence the quantification outcomes. All CEUS examinations should be performed on systems with nonlinear imaging modes designed to suppress tissue echoes and detecting microbubbles echoes as described in section 4.4. Furthermore a dual image display format is recommended. In this display format a tissue image and a microbubble contrast image are displayed side-by-side. This is necessary due to the fact that before contrast administration the contrast image is totally black and it is difficult to keep the region of interest steady in the image plane. Other settings that must be chosen with caution are: the acoustic power (MI and the number and positions of focal zones) and depth. These parameters alter the spatial profile of the ultrasound beam and therefore influence the distribution of the acoustic power and the local MI. Another

important parameter is the dynamic range, also called compression[38,39], which is further explained in section 4.6.2.

Patient based factors

There are different factors and conditions that influence the kinetics of UCAs in a patient, such as posture, resting time, heart rate, blood pressure, body and ambient temperature, and metabolic factors. Blood pressure for example affects the signals from bubbles both by altering their equilibrium radius and their stability. Blood pressure itself varies across a large range depending on location, phase of a heart cycle and the condition of the patient. Furthermore, interactions of microbubbles with the body can create additional variability. Lung filtration results in a lowering of the microbubble concentration, particularly of large microbubbles. This lung filtration alters the size distribution and therefore the echogenicity of the contrast agent suspension. The filtration of large microbubbles may impact the acoustic signal even more because passage of the microbubbles through the lungs and exposure to low blood pressure with high oxygen and nitrogen concentration can cause diffusion of these gases into the bubbles, resulting in an increased size of microbubbles.[39] Another influence concerning passage through the lungs may be the effect of phagocytosis by the pulmonary macrophages, as hypothesized by Skrok et al.[40] They investigated the effect of a second injection of SonoVue after complete disappearance of the enhancement of the first injection. They showed an increased PI in the second injection. They hypothesized that the increase in intensity was caused by saturation of pulmonary macrophages by the first injection.

Recirculation of the microbubbles also influences the shape of the TIC. A bubble could circulate around the body in less than a minute, influencing the tail of the TIC. However the extend of the effect of recirculation remains difficult to quantify. One factor is the gradual spatial spreading of the contrast agents within the vessels over time. [39]

Also tissue motion caused by for example a pumping heart or breathing causes variation in the CEUS measurements. The extend of this variation depends on what kind of features move in and out of the ROI. For example, when main source of the backscattering remains within the ROI the extend of variation will be less than when this source moves in and out of the ROI. Tissue attenuation influences the TIC directly, whereas the peak intensity of the TIC decreases as the depth increases.[38,39] Other factors that are described are temperature and the blood density (haematocrit).[41]

It is recommended to keep detailed record of patient based settings and surrounding factors to help explain discrepancies in unexpected findings taken at different sessions during follow up.

Microbubble based factors

The microbubble based factors depend on the bubble type, the administration of the microbubble and the dosage. As described in section 4.3, there are several different UCAs available for clinical use. These agents differ both in terms of their composition and size distribution, determining the properties for perfusion studies.[39] Currently all the commercial available contrast agents have broad size distributions and the mean size differs significantly between contrast agents, making comparison between contrast agents difficult. Even for the same agent, the way it is reconstituted prior to the administration may introduce significant variations in both size and concentration owing to manual shaking of vials. Such variations during reconstitution, together with further variations caused by administration and the physical and physiological conditions in the immediate environment means the size distribution of commercial agents provided by the manufacturers does not provide a sufficient accurate indication of the bubble distribution in vivo.[39] Furthermore the bubble coating is an important factor determining the acoustic response. Its mechanical properties determine the bubble resonance frequency, amplitude and linearity of oscillation. Even two SonoVue bubbles with a similar initial diameter showed significantly different behaviour, indicating significant difference in their coating.[39]

Preparation and administration of microbubbles influence the microbubble properties. The time between the preparation of the microbubbles and the administration, the diameter of the needle, the needle orientation and the time to administer the UCA have significant impact on the size distribution, stability and the concentration of the UCAs and therefore on the perfusion parameters. At high UCA doses, multiple scattering can occur, with the sound waves scattered by one bubble affecting the oscillation and hence scattering from its neighbours. This will alter the echoes obtained from highly concentrated

bubble populations and render the relationship between the UCA concentration and signal intensity nonlinear.[39]

4.6.2 Data analysis

Variability of CEUS outcome can also be caused by different data analysis approaches. Important steps in the data analysis are the linearization of the data, the extraction of the perfusion parameters by the quantification software and the corresponding presentation of the results.

Linearizing image data

Quantification data are taken at various stages of the image processing chain. A key underlying assumption for quantification is that image intensity is linearly proportional to the concentration of bubbles and thus blood flow. Although it is recommended to directly analyse raw linear data, this option is not always available. In the image processing chain logarithmic compression is applied. However the underlying assumption for quantification based on TICs is that image intensity is linearly related to the concentration of UCA. Some ultrasound scanners offer the opportunity to save the data in a "native" format that allows accurate removal of the logarithmic compression, others offer an approximate linearization algorithm.[38,39] Furthermore linearization scheme can also experimentally be derived from measurements of tissue phantoms.[39]

Quantification software

Several different software packages are used for CEUS quantification. Some are implemented into the ultrasound machines and some are accessible as stand-alone software. These quantification software packages use different curve fitting algorithms, perfusion parameter names, type of image data and quantification machine settings.[38]

Results are processed using manually selected ROIs and the corresponding averaged TICs and their fitted curves. The shape of the fitted curves of the regions of interest are then compared. Another approach to evaluate and present the results is parametric mapping. Parametric maps are constructed in a way that the brightness or colour of each pixel represents the value of a certain parameter from the TIC of that pixel. This approach allows global visualization of the hemodynamics in the whole image. The two presentations may be combined by visualizing the parameter image in the selected ROIs.

4.6.3 CBF quantification using CEUS

In section 4.6.1 and 4.6.2 the challenges in quantification of CEUS have been described. In this section these challenges will be further specified regarding the CBF quantification. First the basic cerebral CEUS procedure is described to emphasize the different factors influencing the CEUS outcome. In the systematic review in Appendix IV the different transcranial CEUS procedures that have been used in literature are described, however in this section an example of an transcranial CEUS procedure is described. Then the difficulties regarding CBF quantification will be further explained.

Transcranial CEUS Procedure

The patient is placed in supine position with the head in midline and elevated at 30 degrees. The ultrasound probe is then positioned at the temporal bone window. By small manipulations of the probe the correct insonation plane is found. There are two standardized insonation planes which are frequently used in the transcranial ultrasonography. The first is the mesencephalic plane, an untilted axial section in which the butterfly shaped mesencephalic brain stem with surrounding hypoechogenic basal cisterns are visualized. By tilting ~10 degrees towards the parietal lobe, the third ventricle and the thalamus are visualized in the so called diencephalic plane. In this plane the third ventricle is used as a landmark for orientation and the adjacent thalamus is visualized as a semicircular hyperechogenic structure.[32,42] The position of the two planes are visualized relative to the orbitomeatal line (OML) in Figure 4. In Figure 5 the ultrasound images of the standardized axial planes with the corresponding MRI section is shown, adapted from Berg et al.[43]

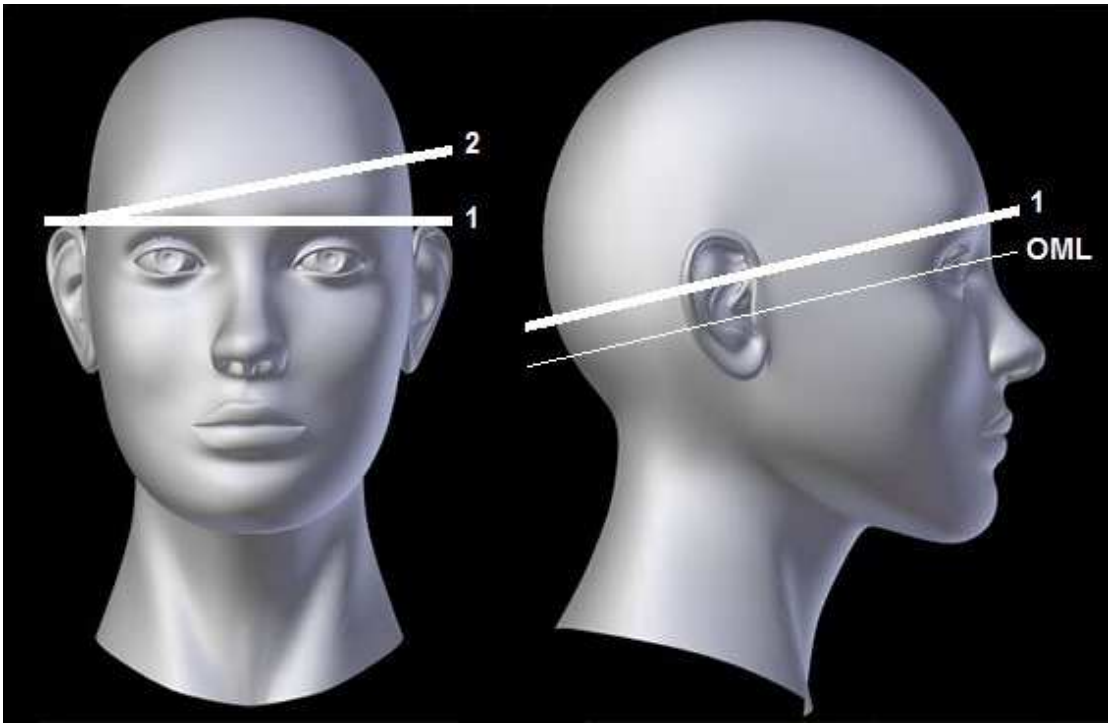

Figure 4: Schematic illustration of the two standardized ultrasound insonation planes, with the orbitomeatal line (OML), the mesencephalic plane (1) and the diencephalic plane (2).

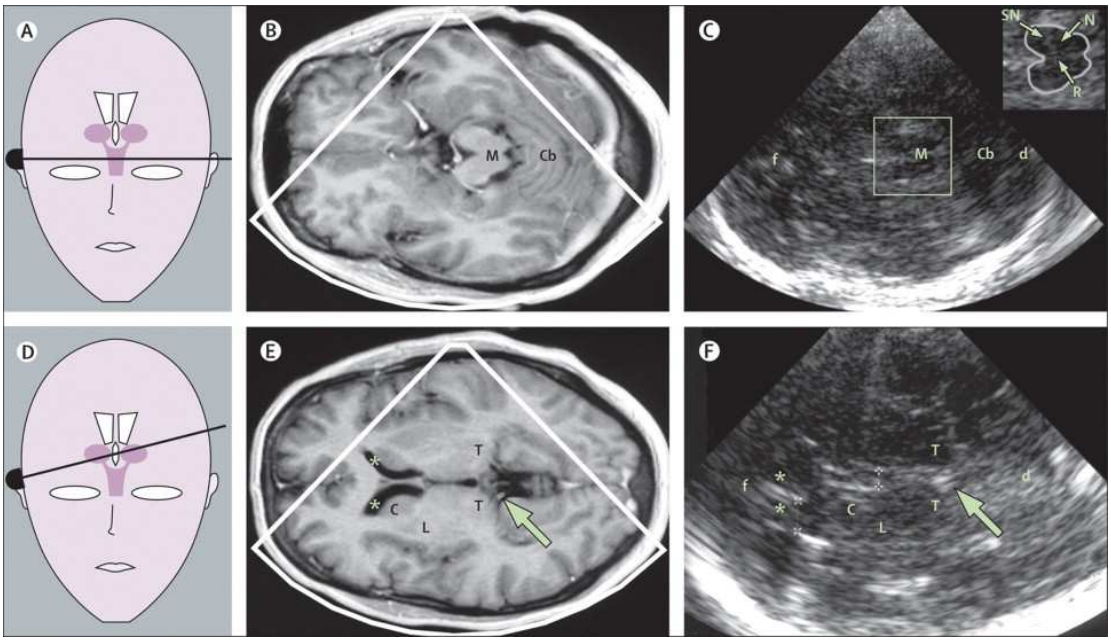

Figure 5: overview of the axial insonation planes. A) schematic illustration of the axial mesencephalic scanning plane; B) MRI of axial section ad midbrain level; C) transcranial ultrasound image of the mesencephalic scanning plane, corresponding to (B); D) schematic illustration of the axial diencephalic scanning plane; E) MRI of axial section at the level of the thalamus; F) transcranial ultrasound image of the diencephalic scanning plane, corresponding to (E); The arrows in (E) and (F) indicate the pineal gland that can be regularly shown on the ultrasound image as a sonographic landmark or high echogenicity owing to calcification. C= head of caudate nucleus; Cb= cerebellum; d= dorsal. f= frontal; L= lenticular nucleus. M= mesencephalon. N= red nucleus. R = raphe; T= thalamus; *=frontal horn of lateral ventricle; +=measuring points of widths of third ventricle; x=measuring points of widths of frontal horn. Adapted from Berg et al. 2008.[43]

When the probe is correctly positioned for the mesencephalic or diencephalic plane, the probe is kept stable during the administration of the UCA and during the measurement. The UCA is then administered using a bolus injection or a continuous infusion. After the bolus injection the bolus kinetic CEUS

measurement is started simultaneously and lasts for 2 minutes. Five minutes after the start of an UCA infusion, the flash-replenishment or depletion measurement is performed. After these five minutes the concentration of UCA is expected to be constant. After the bolus or infusion measurement a wash-out period of ~15 minutes is taken to ensure clearance of the UCA from the blood. Then the measurement is finished.

Challenges of CBF quantification

Many studies used comparison of TICs of ROIs to conclude whether there were perfusion deficits. This is usually done by comparing the same ROI in the healthy and the suspected pathologic hemisphere. The perfusion parameters of the corresponding ROIs are compared, resulting in a semi-quantitative outcome. However diffuse changes of the perfusion affecting both hemispheres will remain undetected using this approach.

The factor that makes CBF quantification even more difficult than in extracranial organs, is the presence of the skull. CEUS is performed through the temporal acoustic window, the thinnest part of the skull. However, the thickness of the temporal acoustic window is expected to be heterogeneous within and between patients. Therefore the acoustic window increases the inhomogeneity of the acoustic power distribution in the brain. This results in an even greater variance in perfusion parameters in different ROIs. Another difficulty concerning the skull is the correct placement of the CEUS probe and keeping it steady. Especially due to the varying acoustic window thickness within the same acoustic window of patients.

When CBF is indeed quantified using CEUS, the next challenge approaches. This challenge is not caused by the characteristics of the CEUS technique, but by the physiological differences in CBF between patients. The CBF thresholds for ischemia or hyperaemia is difficult due to the intra- and inter-individual variation of appropriate CBF in the brain. The variation in CBF is caused by metabolic demands of the brain. Deciding what CBF is needed to achieve a healthy perfusion at a certain brain region is difficult and also remains a subject of debate in the application of other (imaging) techniques measuring CBF, such as CT-perfusion and PWI.[14]

5 Systematic Review

In order to develop a neuromonitoring technique at the ICU using CEUS, it is important to know the relevance and the usability of the measured parameters, but also to know to what extend the measuring technique meets the requirements of a monitoring technique at the ICU. Therefore the first objective of this study was to write a systematic review about CEUS techniques measuring the CBF. We have analysed the studies performing CEUS for the assessment of the CBF from 1994 to October 2014. By comparing the methods and results of the studies, we investigated which CEUS method is most suitable for becoming a CBF monitoring technique at the ICU. The systematic review, "The potential of contrast enhanced ultrasound as a bedside monitoring technique of the cerebral blood flow at the intensive care unit", is included in Appendix IV. The method, results and conclusions of the review are summarized in this chapter.

5.1 Method

The search strategy and study selection are described in Appendix II. In order to compare potential for becoming a bedside monitoring technique of the different ultrasound techniques, the studies were categorized according to the ultrasound detection kinetic principle that was used: bolus kinetics, refill kinetics and depletion kinetics. For each category the execution and data analyses characteristics were compared. Execution characteristics included: operator, study population, UCA type, UCA dosage, UCA side-effects, duration of measurement, and insonation approach. Data analysis characteristics including reference method, ultrasound method, acquisition time, temporal and spatial resolution, and outcome parameters were recorded. Safety was assessed by registration of side effects of both the UCA and the contrast-imaging modes.

5.2 Results

A total of 38 studies were included in the study. In these studies 4 cases of mild local side effects of the UCA Optison was described on a total of 623 subjects undergoing the measurement.
In the ongoing development of CEUS, studies had different aims concerning the use of CEUS for measurement of the CBF. Some studies investigated the potential of the CEUS techniques for cerebral perfusion measurement. The potential was studied by evaluating whether there was accurate contrast in different cerebral structures[44–46] or whether it was possible to visualize cerebral perfusion deficits[47–59]. Furthermore, the three different CEUS methods (bolus, depletion, refill) were evaluated by looking at the dependence of the measured parameters on dose or infusion rate, UCA, frame rate and insonation depth.[60–64] Next to the three different kinetics, different contrast-specific imaging modes were used in the different studies. Some studies compared different contrast-specific imaging modes.[32,42,53,65–67] In twenty-seven studies the CBF was assessed with the bolus kinetic technique, six studies used the depletion kinetics and five studies used the refill kinetics technique. Differences between these three approaches were particularly the contrast administration, acquisition time, MI, frame rate and outcome parameters. An overview of these characteristics are shown in Table 1. In all the techniques an outcome parameter was related to the CBFV and another parameter to the cerebral blood volume (CBV).

Table 1: Overview of the microbubble detection techniques characteristics.

Approach	UCA intravenous	Mechanical Index (MI)	Acquisition time	Frame rate
Bolus	Bolus	High (> 1)	1-2 minutes	0.5 – 1 Hz
Depletion	Bolus or infusion	High (> 1)	1-10 seconds	>1 Hz
Refill *Increasing interval*	Infusion	High (> 1) with increasing pulse interval	Several minutes	0.125 Hz – 20 Hz
Refill *Flash replenishment*	Infusion	High (> 1) followed by low (< 0.3)	10 seconds	15 Hz

5.3 Discussion

Several studies have performed different CEUS methods and measured corresponding perfusion parameters. The techniques have been performed in patients with different cerebral perfusion pathologies over the last 20 years and several perfusion parameters have been proven to be sensitive to detect these perfusion deficits. Due to high intra- and inter-individual variation of the perfusion parameters quantification of the CBF has not yet been performed. However no study has assessed the repeatability of the different CEUS techniques.

Contrast detection method
Studies using the bolus kinetic approach and the depletion kinetic approach are based on using a high MI. This high MI results in a temporal resolution of ~1 second. Furthermore the high MI is accompanied with the shadowing effect. With the refill kinetics on the other hand, a better temporal resolution can be used, because after the bubble destruction at start, the MI is low and no microbubbles will be destructed during the replenishment, which also results in no shadowing effect. This high temporal resolution will also result in less movement artefacts due to movement of the probe or the patient. Therefore the refill kinetic approach seems to be the contrast imaging technique with the most potential for being a bedside monitoring technique of the cerebral perfusion.

An important question that remains unanswered is whether a high MI is needed to increase the signal-to-noise ratio. All the studies using the bolus kinetic approach used a high MI. Therefore, low MI CEUS (in for example low MI bolus kinetics or refill kinetics) might be more sensitive to artefacts or limited backscattering of microbubbles are detected. However, to date no study has compared the different CEUS techniques using low and high MI.

Outcome parameters
From the theoretical point of view, time dependent parameters like TTP (bolus kinetics), perfusion coefficient (depletion kinetics) or β (refill kinetics) are the most useful for the quantification of the cerebral perfusion. Studies agree on focusing on the time dependent parameters, which seem to be the most reliable perfusion parameters. However it remains unknown which of the time parameters is the most reliable for the estimation of the CBF. Bolognese et al. compared the time parameters of the low MI bolus and refill kinetics and concluded that rt-TTP and β were both sensitive parameters for the detection of perfusion changes in acute MCA stroke.[68] Based on the outcome parameters, no superior technique can be indicated. For all methods the focus should be on the time dependent parameters.

5.4 Conclusion

The flash-replenishment contrast ultrasound method, using the refill kinetics using high MI flashes followed by low MI ultrasound has the highest potential for being a bedside monitoring technique of the cerebral blood flow at the intensive care unit. This because of the high temporal resolution, short acquisition time (~10 seconds after optimal positioning of the transducer) and the use of low MI, which avoids the shadowing effect and movement artefacts. With this technique both the time dependent and theoretically depth independent real-time TTP (of the bolus kinetics) and β (of the refill kinetics) are measured, which may increase the possibility of quantifying the cerebral perfusion.

5.5 Recommendations

It is important perform a study which compares the CEUS techniques regarding the outcome variability and the correlation of the perfusion parameters with CBF. Although the flash-replenishment technique is concluded to have the highest potential for becoming a bedside monitoring technique based on the characteristics of the technique, it remains unclear whether the flash- replenishment outcome parameters and their intra- and inter-individual variation also reflects this high potential. Therefore it is suggested that the flash-replenishment technique should be compared with the frequently used bolus kinetic technique to assess the outcome variability and the correlation of the perfusion parameters with CBF.

6 Repeatability study

From the systematic review it is clear that studies using CEUS to measure CBF are very heterogeneous in methodology. Although this technique is frequently referred to as a technique that can potentially quantify CBF, studies on the validity of CEUS as a quantitative measure of CBF are lacking. The systematic review failed to identify studies that systematically and prospectively tested the validity of the technique by assessing repeatability, reproducibility and accuracy.

For the quantification of the CBF with CEUS it is important to assess the variation within a subject in a stable situation. When the variation in CEUS parameters within a subject during stable CBF is known, it can be estimated to what extend quantification of the CBF with CEUS is feasible.

It is also important to investigate whether changes in CBF can be detected with CEUS parameters . Previous studies have shown that perfusion deficits can be distinguished using CEUS. However the question is whether CEUS can be used to monitor the actual CBF and detect significant changes in CBF. No study has been performed in which different CBF states were assessed within one subject.

6.1 Study approach

The first steps that will be taken towards the development of a CBF monitoring technique are focussed on the repeatability of CEUS and the detection of a CBF change with CEUS. The bolus kinetics technique is chosen because it is the most frequently used technique so far. In addition, the technique is expected to be easier to perform compared to the refill or depletion kinetics.

6.2 Study objectives

The primary and secondary objectives of this study are described below:

Primary objective:

- *To determine the repeatability of the bolus kinetic technique*

Secondary objectives

- *To determine the correlation between the CEUS parameters and the CBFV measured with duplex.*
- *To determine the differences in the perfusion parameter values, the repeatability and the correlation between the contra- and ipsilateral parenchyma and the MCA?*

6.3 Method

In Appendix II the complete study protocol is described as submitted and approved by the local medical ethical committee. In this chapter the method regarding the bolus kinetic approach used in this study protocol is described.

6.3.1 Study population

The population consists of a total of 10 young healthy volunteers, between 18-35 years old. Before inclusion, subjects must meet all inclusion criteria and none of the exclusion criteria.

Inclusion criteria

- Healthy men or women of 18-35 years old

Exclusion criteria

- Hypersensitivity to the active substance(s) or to any of the excipients in SonoVue
- Right-to-left shunt cardiac shunt
- Severe pulmonary hypertension (pulmonary artery pressure >90 mmHg)
- Uncontrolled systemic hypertension
- Pregnancy
- Lactation
- Participation in another clinical trial within 3 months prior to the experimental day.
- History, signs, or symptoms of cardiovascular disease or pulmonary disease
- History, signs or symptoms of neurological disease
- History, signs or symptoms of renal disease
- History of hyperventilation

6.3.2 Study protocol

Duplex and CEUS measurements were performed on the subjects during rest (baseline) and during hyperventilation. In Figure 6 an overview of the study design regarding the bolus kinetic technique is shown. The measurements consisted of bilateral duplex measurements of the MCA followed by a CEUS measurement of the MCA, which was performed three times during baseline. Furthermore a duplex measurement during baseline and hyperventilation was performed on one side, followed by a CEUS measurement during hyperventilation.

6.3.3 Temporal bone window assessment

Subjects were placed on a bed in a horizontal position with the head in midline and elevated at 30 degrees. In each patient the most optimal temporal window was determined by comparing the duplex signal and the skull bone artefacts in the contrast mode. The side with the most optimal temporal window was therefore called the ipsilateral side and the other side the contralateral side.

6.3.4 CBFV measurement with duplex

For the baseline measurements the blood flow velocity of the MCA was measured at both sides, followed by the ipsilateral side with duplex. For the hyperventilation measurements only the blood flow velocity of the MCA at the ipsilateral side was measured.
The CBFV of the MCA was measured through the temporal window. With the colour mode the MCA was visible in the mesencephalic plane. The default setting of the gain of the colour mode was 66%. The gain of the colour mode determines the range of flow velocities that are visible in the colour range. By increasing the gain lower flow velocities are visible which could lead to noise from the parenchymal perfusion. The gain settings were adjusted in such a way that the MCA was clearly visible, but no parenchymal noise was present. A correct insonation plane for was defined as an insonation plane in which the MCA is clearly The blood flow velocity was measured using the pulse wave mode. According to the shape of the pulse wave, the depth, the position of the artery relative to other structures and the mean and peak velocities, the MCA was identified. During the CBFV

measurement in the MCA the mean blood flow velocity ($CBFV_{mean}$) and the peak systolic velocity (PSV) were measured and recorded.

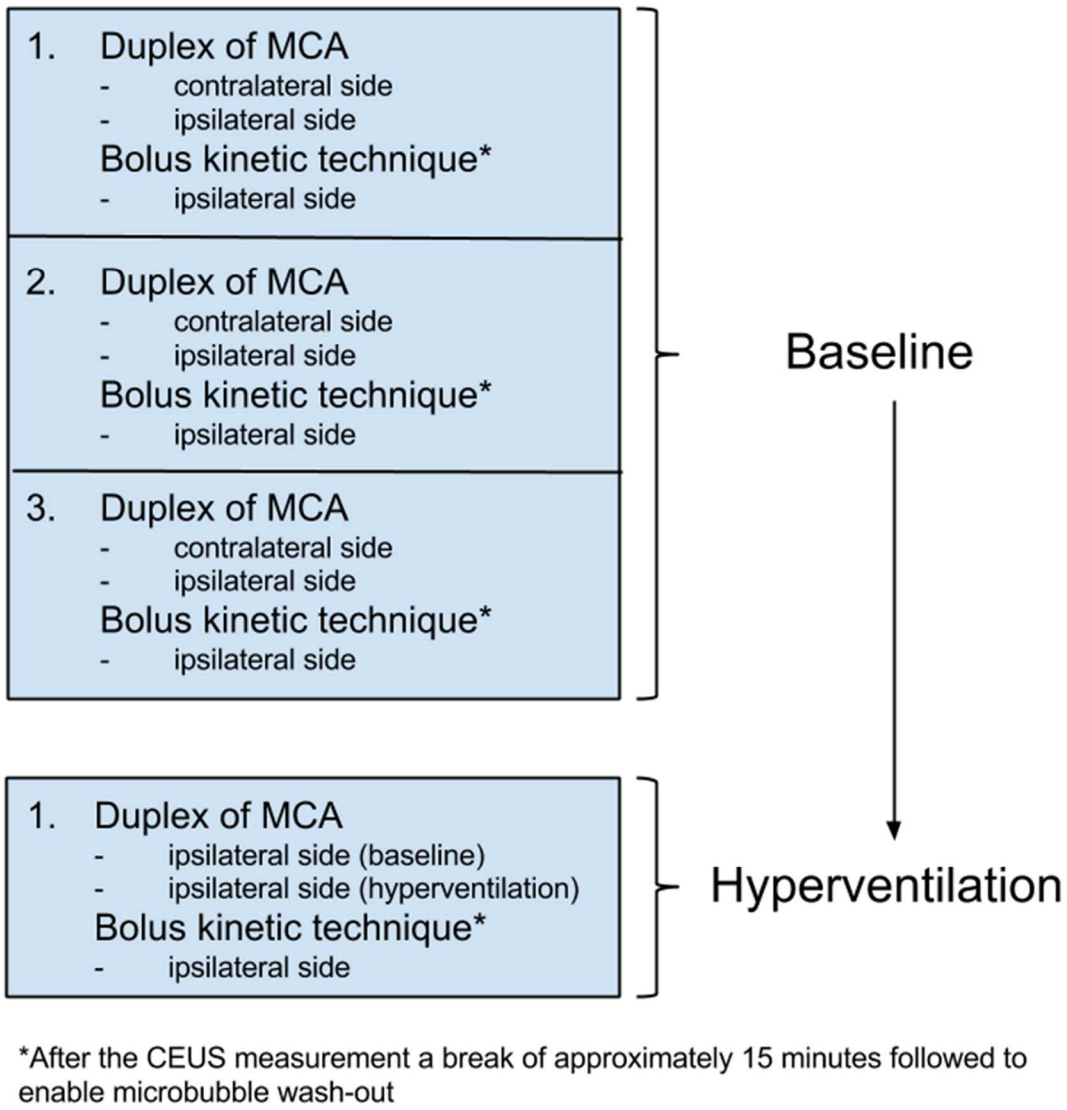

Figure 6: Study design overview.

6.3.5 CEUS

A standard venous catheter (18 G or 20 G venflon) was placed in the left or right fossa cubiti. After identification of the correct insonation plane by duplex, the duplex mode was switched to the contrast mode. An intravenous injection of 2.4 ml the UCA SonoVue (Bracco Imaging Europe BV, Amsterdam, 8 µL/ml) was given as a bolus followed by a 10 ml flush of NaCl 0.9% through the venous catheter. A two minutes recording of the bolus measurement was started at the start of the bolus injection. After these 2 minutes the contrast mode was switched back to the duplex mode to evaluate the position of the probe. A screenshot of the insonation plane in the duplex mode was taken.
This bolus kinetic method was performed during baseline and hyperventilation in each subject. Consecutive measurements were separated by an interval of at least 15 minutes, to ensure wash-out of the microbubbles. Complete wash-out was assessed by evaluating the appropriate settings for the duplex measurement. In case the gain of 66% had to be decreased below 55% in order to visualize the MCA without parenchymal noise, it was assumed the microbubbles had not yet been washed out.

6.3.6 Hyperventilation

After the baseline measurements, an additional measurement during mild hyperventilation was performed. This in order to get a measurement of a changed CBF within the same patient. Previously, it was shown that an increase of minute ventilation by 20% in patients after cardiac arrest changes mean CBFV by 15% .[69]

Patients were asked to breath normally through a short oral tube and to pinch their nose to prevent air leakage. The end-tidal CO_2 pressure was measured at the end of the tube and continuously displayed on the monitor. After baseline duplex measurements at the ipsilateral side, volunteers were asked to increase the minute ventilation by 20%, reflected by 20% decrease in end-tidal CO_2. Then a duplex measurement during hyperventilation was performed, followed by a CEUS measurement. The end-tidal CO_2 values measured during the baseline duplex measurement, the start of the bolus kinetic measurement during mild hyperventilation and at the end of the bolus kinetic measurement during mild hyperventilation were noted.

6.3.7 Ultrasound device

The iU22 xMATRIX ultrasound system (Philips Medical Systems B.V., Eindhoven, The Netherlands) was used as with an S5-1 probe for all duplex and CEUS measurements. For the duplex measurement the TCD preset was used with an image depth of 15 cm. With the colour mode the flow velocities were visible in colour. The gain of the colour mode was 66% (default setting). The colour gain was adjusted when evaluating the probe position or the microbubble wash-out. In the contrast mode an MI of 1.09 with a gain of 76% was used. The image depth was 15 cm, with a focus at 7.7 cm (range 5.3- 9.7 cm). The linearization scheme and the automatic gain correction curve were experimentally derived from measurements of tissue phantoms.

6.4 Data analysis

For the data analysis of the CEUS measurements in-house software was developed in MATLAB. With this software the DICOM files were visualized, parameter images were calculated, ROI selected from which TIC were calculated and bolus curves were fitted. For the data analysis only the first minute of the two minute recordings were analysed to reduce the calculation time. First the method for extracting the perfusion parameters is described. Then this application according to our data analysis is described.

6.4.1 Extraction and calculation of perfusion parameters

To calculate the perfusion parameters from a TIC, the method of least squares was used. The method of least squares assumes that the best-fit curve of a given type is the curve that has the minimal sum of the deviations squared from a given dataset. The sum of squared error (SSE) is defined as described in Equation 6-1, where *y* is the raw dataset and *f* the fitted function for the data points *i=1 to n.*

$$\boldsymbol{SSE = \sum_{i=1}^{n} (y_i - f(x_i, a_i))^2} \qquad \textbf{6-1}$$

With the function *fminsearch* in MATLAB, the bolus curve fitting was performed.

$$y = a + \frac{b\, e^{-c\, t}}{1 + e^{-d(t-e)}} \qquad \textbf{6-2}$$

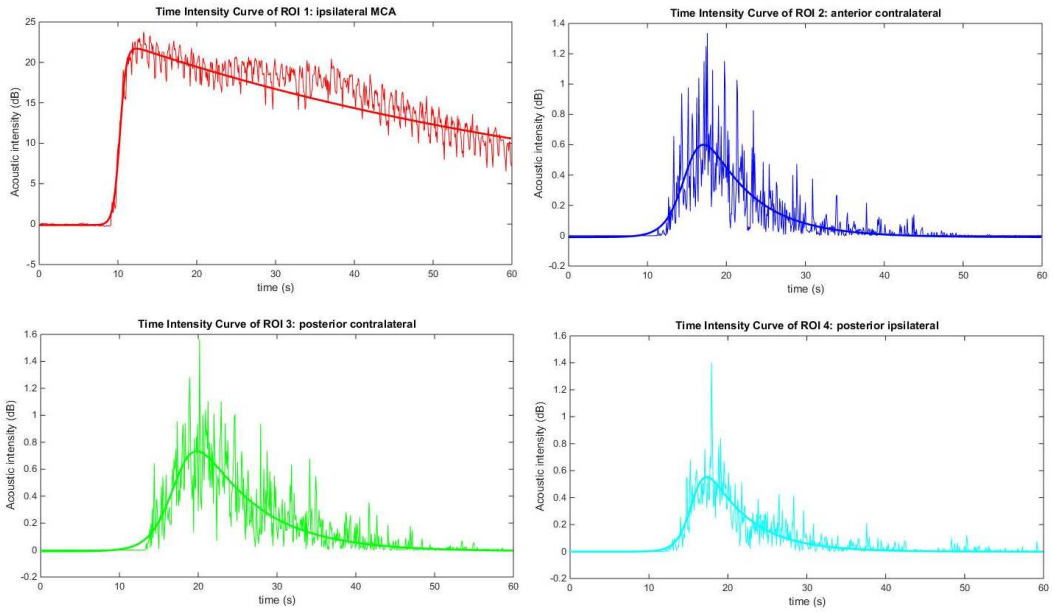

Figure 7: Example of the bolus curve fit of 4 different TICs, with thin lines the original TICs and the thick lines the curve fits.

The function that was fitted to the bolus TICs is shown in Equation 6-2. This function was previously described by Postert et al.[32] and used in several clinical studies.[49,55,57,67,70,71] The following perfusion parameters of the bolus curve were extracted: PI, TTP, T_{PI}, AUC, PW, FWHM. PI is defined as the maximum amplitude the curve reaches in the first 30 seconds of the measurement. TTP is defined as the time at which the curve reaches its PI (T_{PI}), minus the start of the bolus curve. The start of the curve is defined as the time at which > 2% of the PI was reached. The AUC is calculated by a summation of all the acoustic intensities starting from the start of the bolus curve. PW is defined as the time the acoustic intensity is ≥ 90% of the PI. FWHM is defined as the time the acoustic intensity is ≥ 50% of the PI.

The error of the fit is defined as the root mean square error (RMSE), based on the SSE as defined in Equation 6-1. The function for the RMSE is described in Equation 6-4, where *n* the amount of data points. Furthermore $RMSE_{PI}$ was used as RMSE corrected for the PI of the curve fit as defined in Equation 6-5.

$$RMSE = \sqrt{\frac{SSE}{n}} \qquad \textbf{6-4}$$

$$RMSE_{PI} = \frac{\sqrt{\frac{SSE}{n}}}{PI} = \frac{RMSE}{PI} \qquad \textbf{6-5}$$

In this study the SSE is defined as the sum of squared errors of the fit from the start of the bolus curve until the end of the measurement (60 seconds). RMSE is the mean error of each data point and $RMSE_{PI}$ the mean error of each data point as a percentage of the PI.

In total the perfusion parameters (PI, TTP, T_{PI}, AUC, PW, FWHM) and the fit error parameters (SSE, RMSE, $RMSE_{PI}$) were calculated for each TIC. TICs were first normalized by subtraction of the first data point of the TIC.

6.4.2 Parametric images and ROIs

The curve fitting approaches that were used in this study is the parameter images approach and the is the ROI selection. In the parameter images approach the perfusion and fit error parameters were calculated for each pixel and an image of all the values of a single parameter was then visualized as a parameter image. In order to visualize fits with high errors with respectively unreliable parameter values, a correction of the parameter images was performed. This correction was performed by changing the badly fitted pixel values into the value -5. Because all the parameter values of the perfusion parameters were positive, these pixels could easily be distinguished from appropriate fits by choosing sufficient grey scale limits. A fit was defined as a bad fit in case the $RMSE_{PI}$ >100%. A RMSE of 100% means that the mean error between the fit curve and the TIC is 100% of the PI.

The second approach that was used is selecting a ROI consisting of multiple pixels and calculating the perfusion parameters of this specific region. The mean TIC of the pixels within the ROI was calculated. TICs from which the bolus fit resulted in a bad fit were not included in the calculation of the mean TIC. Then the parameter values were calculated after a bolus fit of the mean TIC.

6.4.3 ROI selection

For the ROI selection the PI parameter image and the screen shot of the duplex recording was used. In the screen shot of the duplex recording the position of the CBFV measurement is visible between the two green lines, as shown in Figure 8. Four ROIs were selected manually on the corresponding PI parameter images. The screen shot of the duplex recording was used for choosing the ROI in the MCA. Looking at the position at which the CBFV recording with the duplex was performed the corresponding region was manually selected in the PI parameter image. Figure 9 shows the anatomical position and characteristics of the circle of Willis. Figure 10 shows the PI parameter image on which the ROIs were selected.

A total of four regions of interest were selected in the PI parameter image as shown in Figure 9. One ROI was selected in the ipsilateral MCA and three in the parenchyma. First the ROI of the ipsilateral MCA ($ROI_{MCAipsi}$) was selected by clicking of the position of the 4 corners at a depth of 4 to 5 cm. It was pursued to select a ROI which was positioned within the MCA at the position as measured with the duplex. When the $ROI_{MCAipsi}$ was selected the remaining three regions were selected by clicking on the position of the left upper corner. Then automatically the shape of the $ROI_{MCAipsi}$ was used to create a ROI in that parenchyma position. The second region of interest ($ROI_{POSTipsi}$) was selected in the parenchyma at the ipsilateral side on a depth of 4 to 5 cm posterior to the ipsilateral MCA region. The third region of interest ($ROI_{POSTcontr}$) was selected at the contralateral side at a depth of 9-10 cm at the same posterior level as $ROI_{POSTipsi}$. The fourth region of interest ($ROI_{ANTcontr}$) was also selected at the contralateral side a depth of 9-10 cm at the same anterior level as the $ROI_{MCAipsi}$. In case of reflections, large arteries, artefacts or many bad fits, the position was chosen as close to the position as possible.

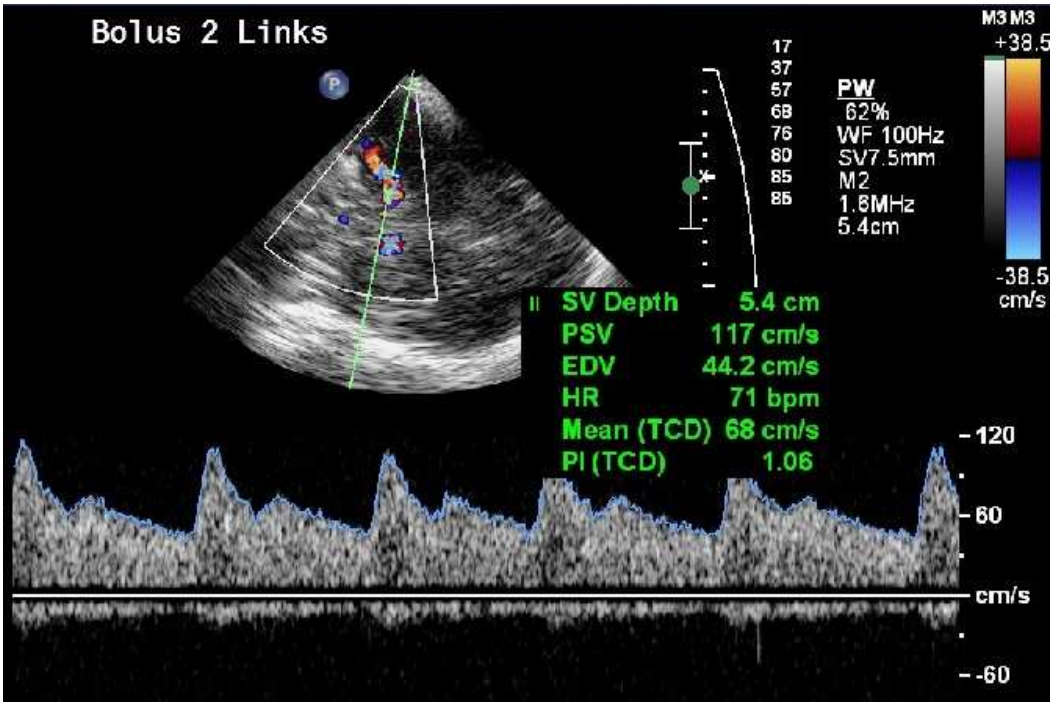

Figure 8: Example of a screen shot of a duplex measurement of the ipsilateral MCA.

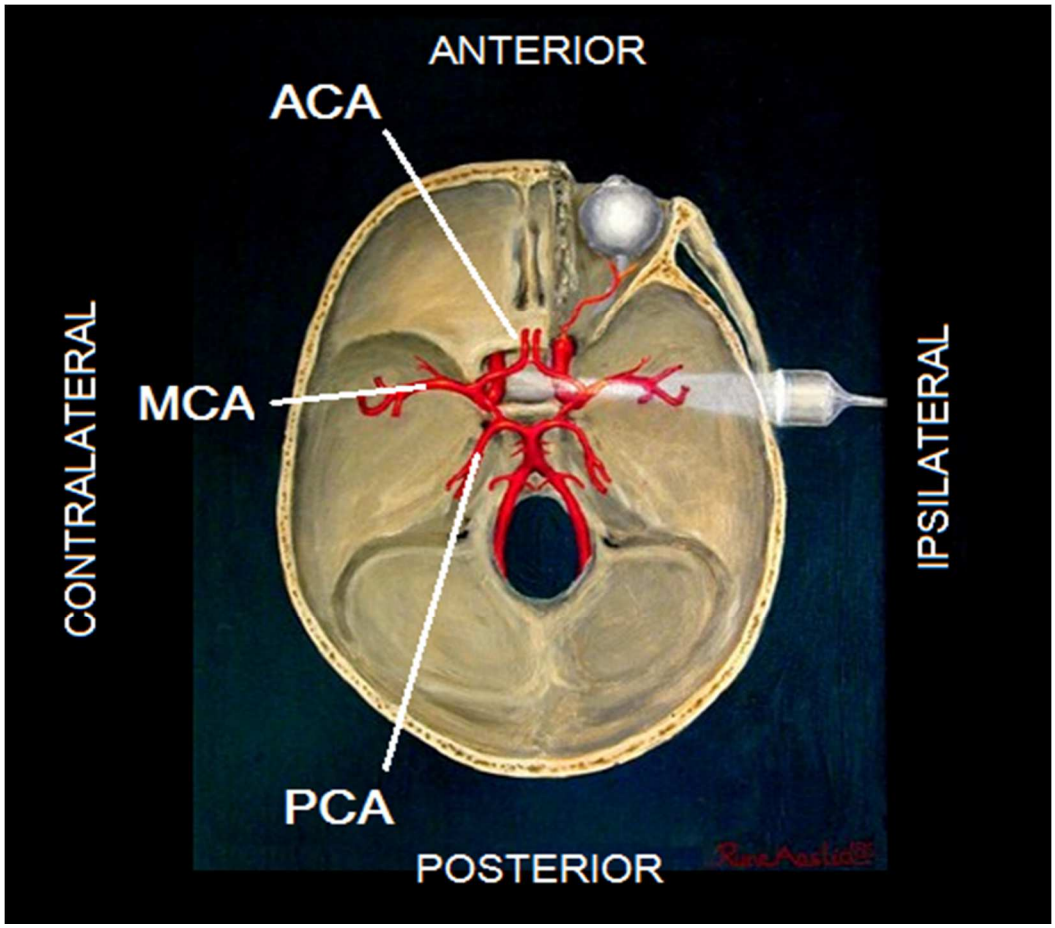

Figure 9: Visualization of the Circle of Willis with the large cerebral arteries: anterior cerebral artery (ACA), middle cerebral artery (MCA) and the posterior cerebral artery (PCA). Furthermore the side at which the probe is positioned is called the ipsilateral side, whereas the other side is called the contralateral side.

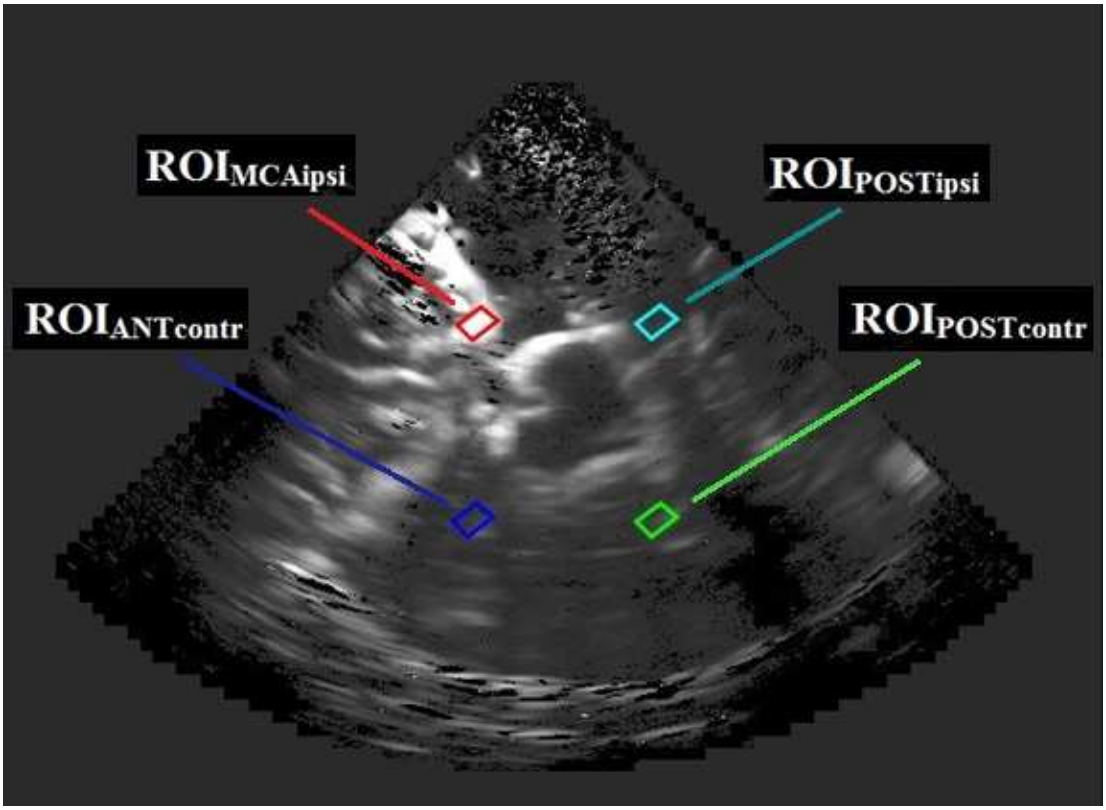

Figure 10: Example of the four selected ROIs, with the corresponding names, on the parametric image of the PI. Black pixels represent a bad bolus curve fit.

6.5 Statistical analysis

6.5.1 Primary objective

Each CEUS measurement resulted in one TIC for each ROI with the perfusion parameters TTP, PI, T_{PI}, PW, FWHM, and AUC for the bolus kinetic measurements. The repeatability of these parameters were determined by calculation of the coefficient of variation (CV), expressed in % of the mean. A CV <10% from the mean was considered to indicate adequate repeatability.
The repeatability of the mean CBFV and the PSV from the duplex measurements are also determined by calculation of the CV as described. Also a CV <10% CBFV was considered to indicate adequate repeatability.

6.5.2 Secondary objectives

The correlation between the CEUS perfusion parameters (TTP, PI, T_{PI}, PW, FWHM and AUC) and the $CBFV_{mean}$ and the PSV in the MCA and parenchyma regions was determined by linear regression analysis with the calculation of the Pearson's correlation coefficient. A p value < 0.05 was considered to indicate statistical significance.
CEUS perfusion parameter values and CV of the CEUS perfusion parameters in the different ROIs were analysed with a paired-T-test. The end-tidal CO_2, CBFVmean and PSV during baseline and hyperventilation were also analysed with a paired T-test. A p value < 0.05 was considered to indicate statistical significance.

7 Results

Thirteen healthy volunteers were screened for the participation in the study. One volunteer was excluded due to an ECG abnormality and two volunteers were excluded due to insufficient temporal bone windows. Ten healthy volunteers signed informed consent and underwent the measurements of this study. No adverse events occurred. The data of the first subject were not analysed due to technical issues in the duplex recordings and due to different settings of the CEUS device than described in section 6.3.7. In all the CEUS bolus measurements it was possible to image the ipsilateral MCA.

7.1 Demographic data

The data of nine subjects were used in this study. Five subjects were male (age: 21.2±2.6) and four subjects were female (age: 21.5±2.9). Blood pressure of the subjects before the start of the measurements was a systolic pressure of 120.7±9.4 mmHg and a diastolic pressure of 70.4±9.3 mmHg, with a heart rate of 65.7±12.3 beats per minute.

7.2 CEUS repeatability

To determine the repeatability of the perfusion parameters and the duplex parameters, CV expressed in percentage of the mean baseline was calculated. The results of the CEUS parameters in the four ROIs are shown in Table 2, Table 3, Figure 11 and Figure 12.These results are mean values of the total group. In Appendix III, Table 12 to Table 15 show the mean, standard deviation and coefficient of variation for each subject of the four ROIs.

7.2.1 Parameter values

As shown in Table 3 and Figure 11, the PI, PW and AUC in the MCA were significantly higher than in all parenchyma regions. The T_{PI} was significantly lower in the MCA than in the parenchyma. Furthermore the TTP was significantly lower in the MCA compared to the two contralateral parenchyma regions. The FWHM was significantly higher in the MCA compared to the contralateral parenchyma regions.

As shown in Figure 11, there was no significant difference between the PI of the parenchyma regions. However the TTP of the $ROI_{POSTipsi}$ was significantly lower than in the contralateral parenchyma regions. T_{PI} was significantly lower in the $ROI_{POSTipsi}$ than in the $ROI_{POSTcontr}$. AUC of the $ROI_{POSTcontr}$ was significantly higher than in the $ROI_{ANTcontr}$. PW of the $ROI_{POSTcontr}$ was significantly higher than in the $ROI_{ANTcontr}$ and $ROI_{POSTipsi}$. The FWHM of the three parenchyma regions were all significantly different.

7.2.2 Coefficient of variation

As shown in Table 2, the CEUS parameter with the lowest CV in the MCA region is the T_{PI} with a value of 13.7%. Other parameters in the MCA region had a CV higher than the T_{PI}. In the three parenchyma regions the parameter with the lowest CV is T_{PI} with a value of 6.1% in $ROI_{POSTipsi}$ and 9.7% in the other parenchyma regions. Other parameters in the parenchyma all had a CV >10%.

As shown in Figure 12, comparing the CV of the MCA with the parenchyma regions the CV of the PI was significantly lower in the MCA than in the $ROI_{POSTipsi}$. The CV of the TTP and TPI in the MCA was not significantly different than the parenchyma regions. The CV of the AUC in the MCA was significantly lower than in all the parenchyma regions. The CV of the PW in the MCA was significantly higher than all parenchyma regions. The CV of the FWHM was not significantly different than the parenchyma regions. The CV values of all parameters of the parenchyma regions were not significantly different from each other except for the T_{PI}. The CV of the T_{PI} in the $ROI_{POSTipsi}$ was significantly lower than the other parenchyma regions.

The results of the $CBFV_{mean}$ and the PSV measurements are shown in Table 4. For the $CBFV_{mean}$ values the CV was 7.0% and 6.5% for the PSV. In Figure 15 and Figure 16 the mean and standard deviation of the baseline $CBFV_{mean}$ and the PSV values are shown. In Table 11 in Appendix III the PSV and

$CBFV_{mean}$ values of the individual duplex measurements are shown with the corresponding mean, standard deviation and CV.

Table 2: Coefficient of variation (CV) of the CEUS parameters in the four ROIs.

CV (% of mean baseline)	PI	TTP	TPI	AUC	PW	FWHM
ROI MCA ipsilateral	16,6	25,2	13,7	22,3	44,4	26,7
ROI anterior contralataral	53,0	19,1	9,7	65,0	20,2	20,9
ROI posterior contralateral	46,8	25,0	9,7	64,3	24,6	28,0
ROI posterior ipsilateral	52,3	14,2	6,1	63,9	18,6	22,6

Table 3: Mean baseline, mean standard deviation (SD) and coefficient of variation (CV) of the perfusion parameters in the four different ROIs.

ROI MCA ipsilateral	PI	TTP	TPI	AUC	PW	FWHM
Mean baseline	24,3	5,9	14,1	10465,9	11,0	38,2
SD baseline	5,2	3,6	3,2	2878,1	7,4	11,7
CV (% of mean baseline)	16,6	25,2	13,7	22,3	44,4	26,7
Hyper (% of mean baseline)	89,2	139,1	100,3	53,6	54,0	48,5
ROI anterior contralateral	PI	TTP	TPI	AUC	PW	FWHM
Mean baseline	2,5	8,1	17,3	358,1	2,8	8,9
SD baseline	1,3	2,0	2,3	246,6	0,7	2,6
CV (% of mean baseline)	53,0	19,1	9,7	65,0	20,2	20,9
Hyper (% of mean baseline)	44,1	70,6	86,6	57,8	81,4	91,6
ROI posterior contralateral	PI	TTP	TPI	AUC	PW	FWHM
Mean Baseline	3,1	7,5	17,8	606,2	3,4	11,7
SD Baseline	1,7	2,1	2,2	526,2	1,2	5,2
CV (% of mean baseline)	46,8	25,0	9,7	64,3	24,6	28,0
Hyper (% of mean baseline)	51,0	92,7	90,2	49,3	83,5	81,6
ROI posterior ipsilateral	PI	TTP	TPI	AUC	PW	FWHM
Mean Baseline	2,7	6,4	16,8	424,1	2,7	9,3
SD Baseline	1,5	1,3	1,9	326,0	0,7	3,3
CV (% of mean baseline)	52,3	14,2	6,1	63,9	18,6	22,6
Hyper (% of mean baseline)	46,2	81,9	89,1	43,7	73,7	75,0

Table 4: Mean, standard deviation (SD) and coefficient of variation (CV) of the duplex parameters PSV and $CBFV_{mean}$.

MCA ipsilateral	PSV	$CBFV_{mean}$
Mean Baseline	104,2	61,7
SD Baseline	12,4	8,0
CV (% of mean)	6,5	7,0

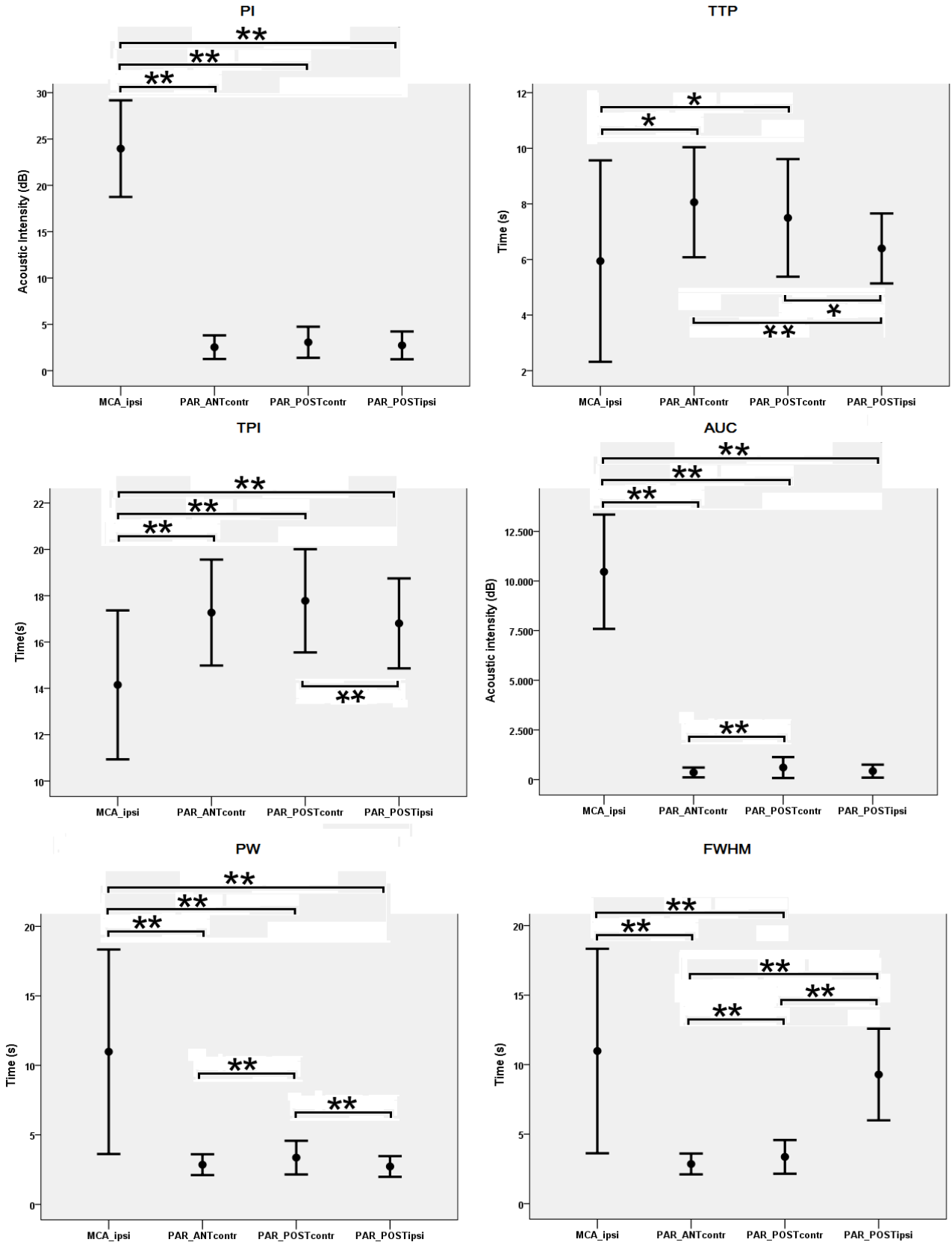

Figure 11: Parameter values (mean ±SD) in the $ROI_{MCAipsi}$ (MCA_ipsi) and the parenchyma regions $ROI_{ANTcontr}$ (PAR_ANTcontr), $ROI_{POSTcontr}$ (PAR_POSTcontr) and $ROI_{POSTipsi}$ (PAR_POSTipsi), with *significance of $p < 0.05$ and **significance of $p < 0.01$.

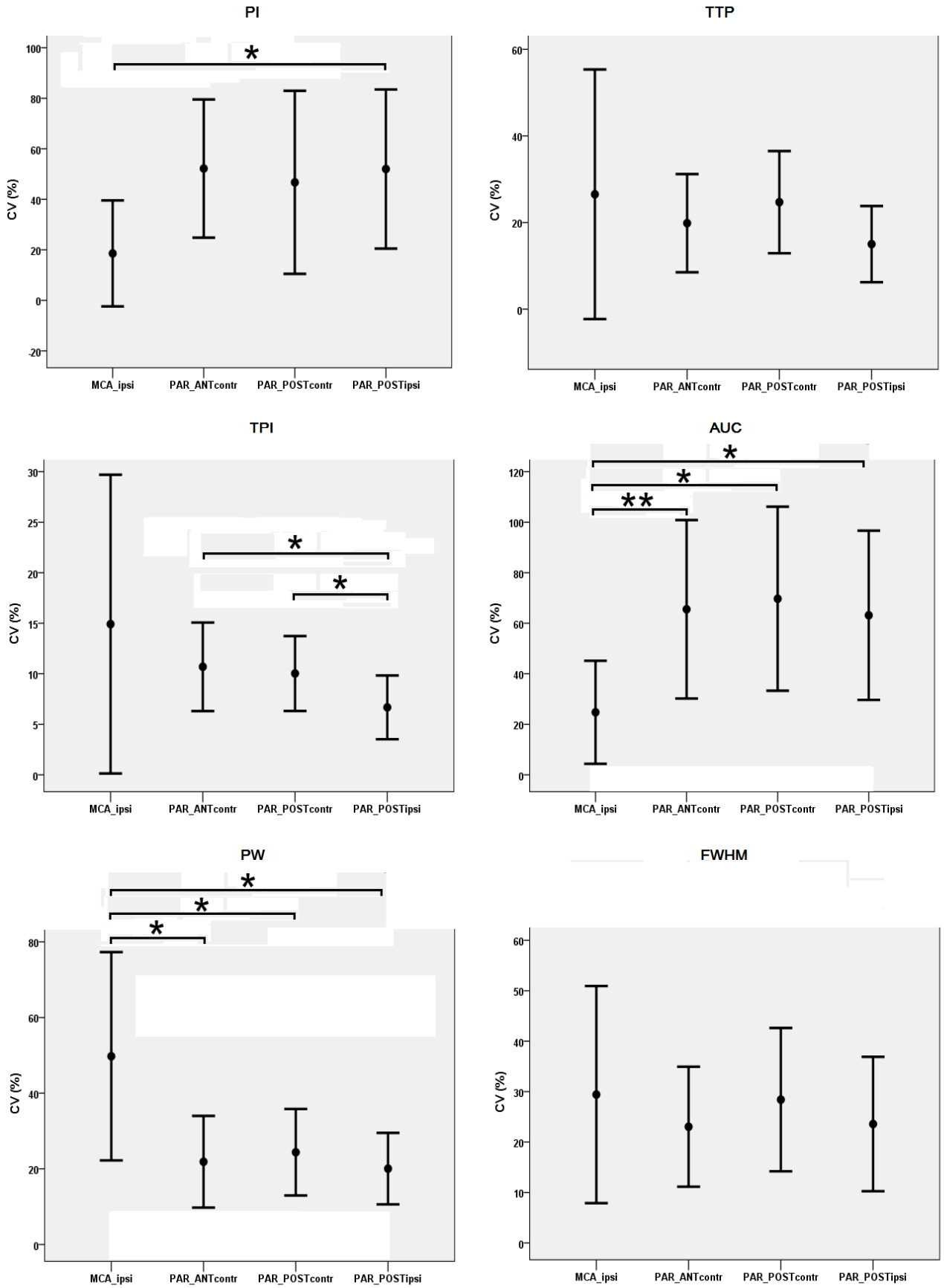

Figure 12: CV of the CEUS Parameters (mean ±SD) in the $ROI_{MCAipsi}$ (MCA_ipsi) and the parenchyma regions $ROI_{ANTcontr}$ (PAR_ANTcontr), $ROI_{POSTcontr}$ (PAR_POSTcontr) and $ROI_{POSTipsi}$ (PAR_POSTipsi), with *significance of $p < 0.05$ and **significance of $p < 0.01$.

7.3 Correlation between CBFV and the CEUS parameters

7.3.1 Hyperventilation

In Table 5 the duplex parameter values are shown during the baseline measurement before and after hyperventilation. In Table 6 the corresponding end-tidal CO_2 values are shown measured during baseline and at the start and end of the contrast measurement during hyperventilation.
As shown in Figure 13 and Figure 14, the end-tidal CO_2 decreased significantly during hyperventilation, resulting in a significant decrease in PSV and $CBFV_{mean}$. An average decrease of 21.2% of the baseline end-tidal CO_2 during mild hyperventilation resulted in an average decrease of 10,9% of the PSV and 16,7% of the $CBFV_{mean}$.

Table 5: Duplex parameters PSV and $CBFV_{mean}$ during hyperventilation and during the baseline measurement before hyperventilation.

Duplex measurement				
Subject	Parameter	Baseline	Hyperventilation	Change (%)
1	PSV	116	104	-10,3
	$CBFV_{mean}$	70	54	-22,9
2	PSV	102	91,2	-10,6
	$CBFV_{mean}$	59	54	-8,5
3	PSV	106	80,8	-23,8
	$CBFV_{mean}$	62	50	-19,4
4	PSV	119	106	-10,9
	$CBFV_{mean}$	70	52	-25,7
5	PSV	81,8	81,8	0,0
	$CBFV_{mean}$	47	50	6,4
6	PSV	107	87,4	-18,3
	$CBFV_{mean}$	58	51	-12,1
7	PSV	104	93	-10,6
	$CBFV_{mean}$	64	48	-25,0
8	PSV	95,9	93,1	-2,9
	$CBFV_{mean}$	59	45	-23,7
9	PSV	82,7	74	-10,5
	$CBFV_{mean}$	56	45	-19,6
Mean	PSV	101,6	90,1	-10,9
	$CBFV_{mean}$	60,6	49,9	-16,7

Table 6: The measured end-tidal CO2 at the baseline measurement, at the start and at the end of the CEUS measurement. In the column 'Change at start' the % change of the end-tidal CO2 at the start of the contrast measurement regarding the baseline measurement is shown.

End-tidal CO2				
Subject	Baseline	Start CEUS	End CEUS	Change at start (% of baseline)
1	5,8	4,5	3,8	-22,4
2	5,3	4,4	4,4	-17,0
3	5,7	4,7	4,2	-17,5
4	5,8	4,8	4	-17,2
5	5,4	4,4	4,3	-18,5
6	4,8	3,8	3,7	-20,8
7	5,4	4,5	3,8	-16,7
8	5,8	3,9	3,8	-32,8
9	5	3,6	3,1	-28,0
Mean	5,4	4,3	3,9	-21,2

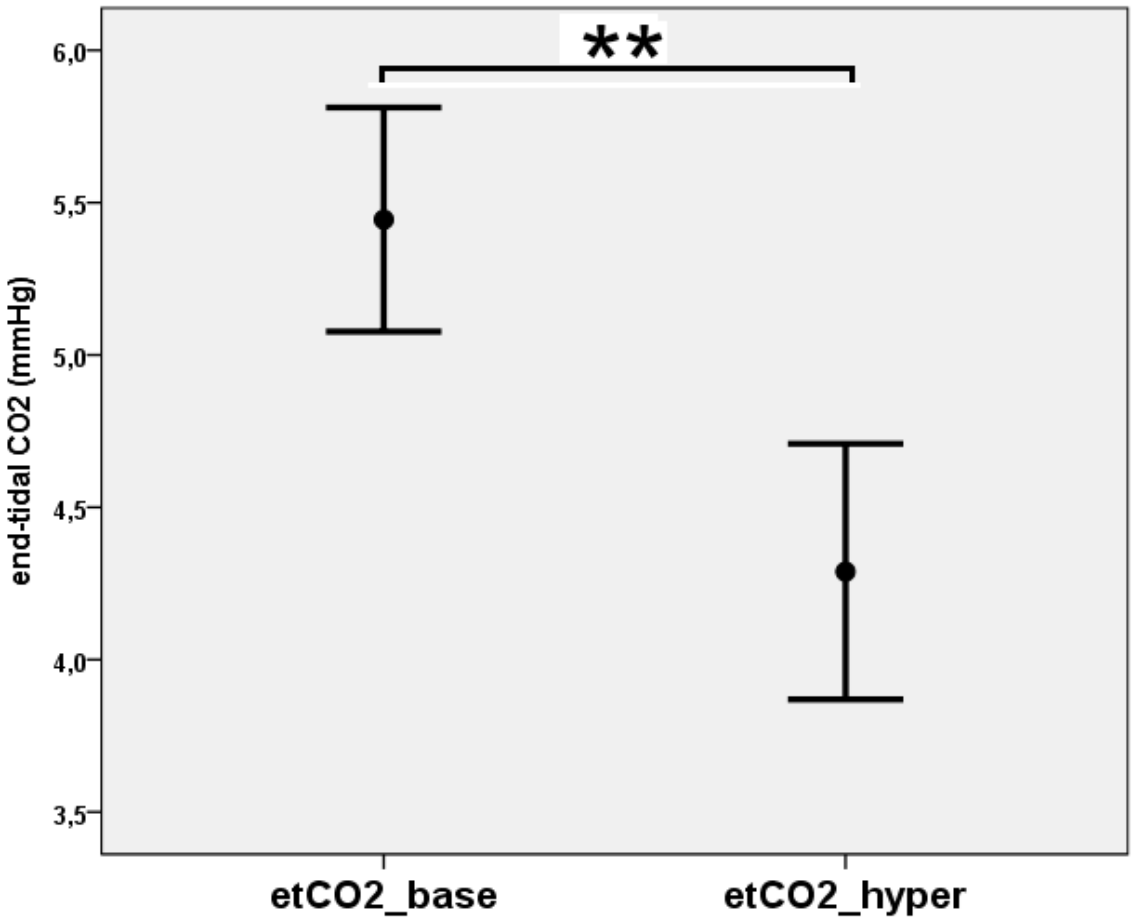

Figure 13: Values of the end-tidal CO2 (mean ±SD) during baseline (etCO2_base) and hyperventilation (etCO2_hyper), with *significance of p <0.05 and **significance of p <0.01.

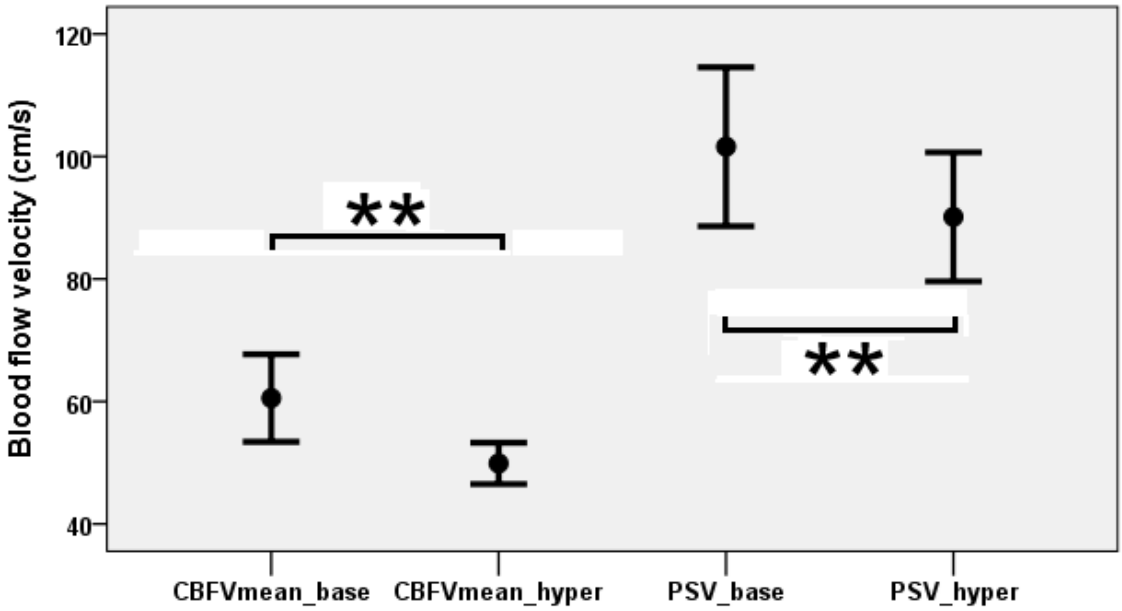

Figure 14: Values of the $CBFV_{mean}$ and PSV (mean ±SD) during baseline (CBFVmean_base, PSV_base) and during hyperventilation (CBFVmean_hyper, PSV_hyper), with *significance of p <0.05 and **significance of p <0.01.

In Figure 15 and Figure 16 the mean and standard deviation of the baseline $CBFV_{mean}$ and PSV measurements are shown with the corresponding hyperventilation value.

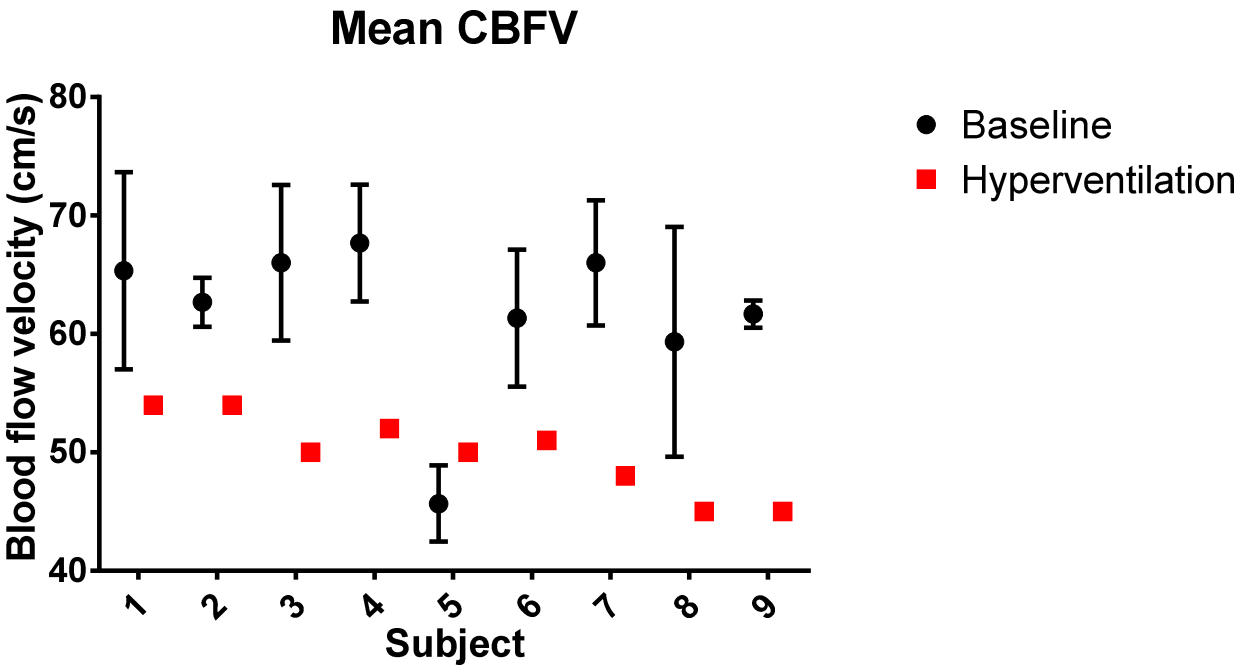

Figure 15: $CBFV_{mean}$ (cm/s) values during baseline and hyperventilation (mean ±SD)..

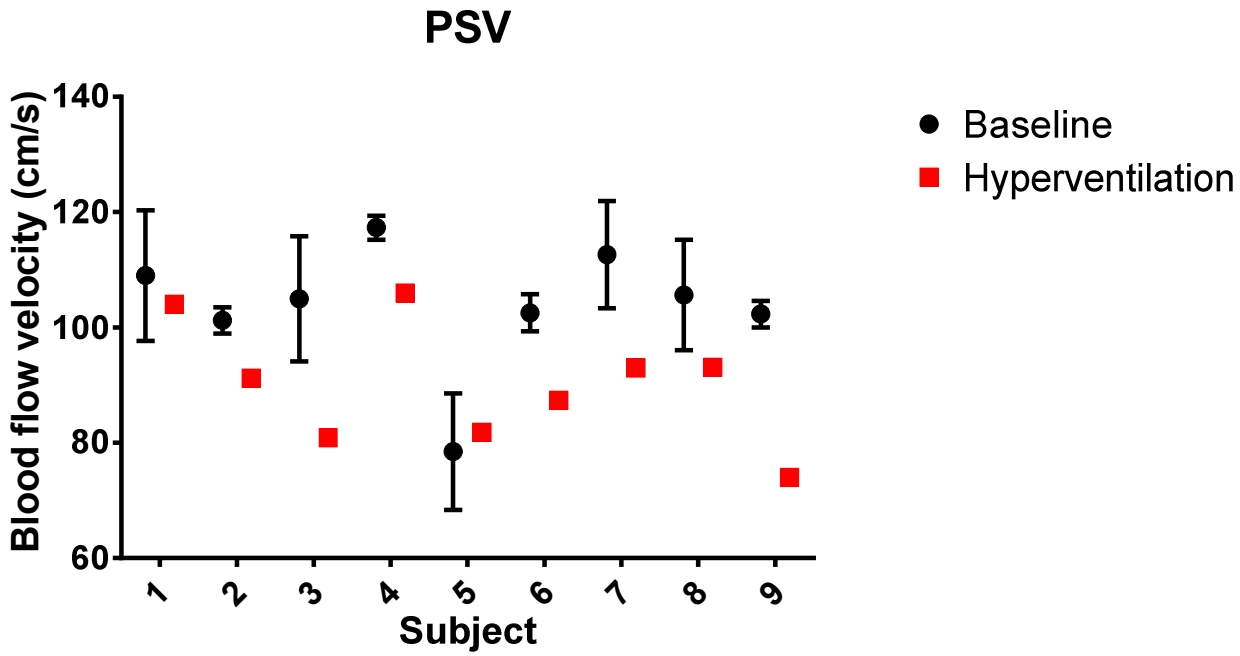

Figure 16: PSV (cm/s) values during baseline and hyperventilation (mean ±SD).

7.3.2 Effect of hyperventilation on the CEUS parameters

In Table 4 the mean parameter value of during hyperventilation as a percentage of the mean baseline value is shown. In Figure 17 to Figure 22 the mean and SD of perfusion parameters PI, TTP and PW during the baseline measurements in $ROI_{MCAipsi}$ and $ROI_{ANTcontr}$ are shown with the corresponding hyperventilation value. These figures illustrate the effect of the hyperventilation on these parameters as also shown in Table 4.

Parameter values during hyperventilation were mostly close or within the mean ±SD of the baseline measurements. However looking at the values that lie outside the mean ±SD and looking at the mean effect of the hyperventilation on the parameters as shown in Table 3, it seems that: PI decreased in all the four ROIs, TTP increased in the MCA region but decreases in the parenchyma regions, TPI remained unchanged in the MCA region but decreased in the parenchyma regions. All other parameters decreased in all regions during hyperventilation.

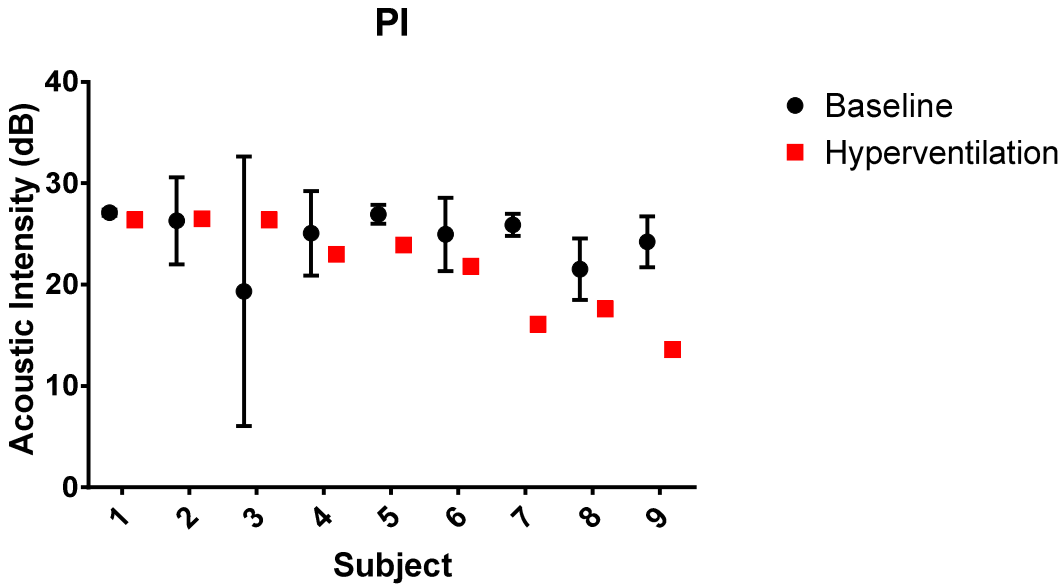

Figure 17: Parameter PI values (mean ±SD) during baseline CEUS measurements and the corresponding value during hyperventilation, in $ROI_{MCAipsi}$.

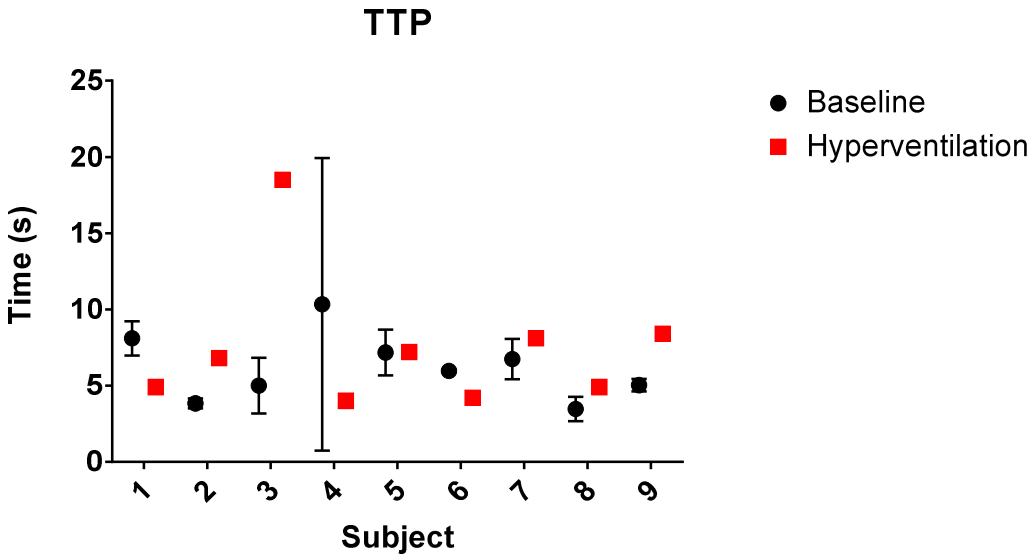

Figure 18: Parameter TTP values (mean ±SD) during baseline CEUS measurements and the corresponding value during hyperventilation, in $ROI_{MCAipsi}$.

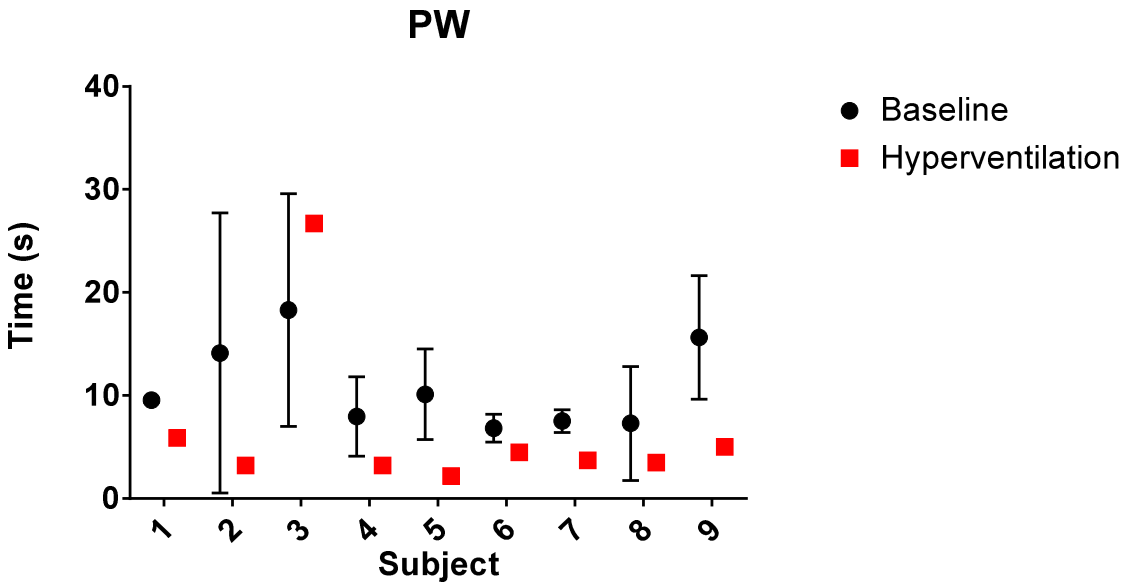

Figure 19: Parameter PW values (mean ±SD) during baseline CEUS measurements and the corresponding value during hyperventilation, in $ROI_{MCAipsi}$.

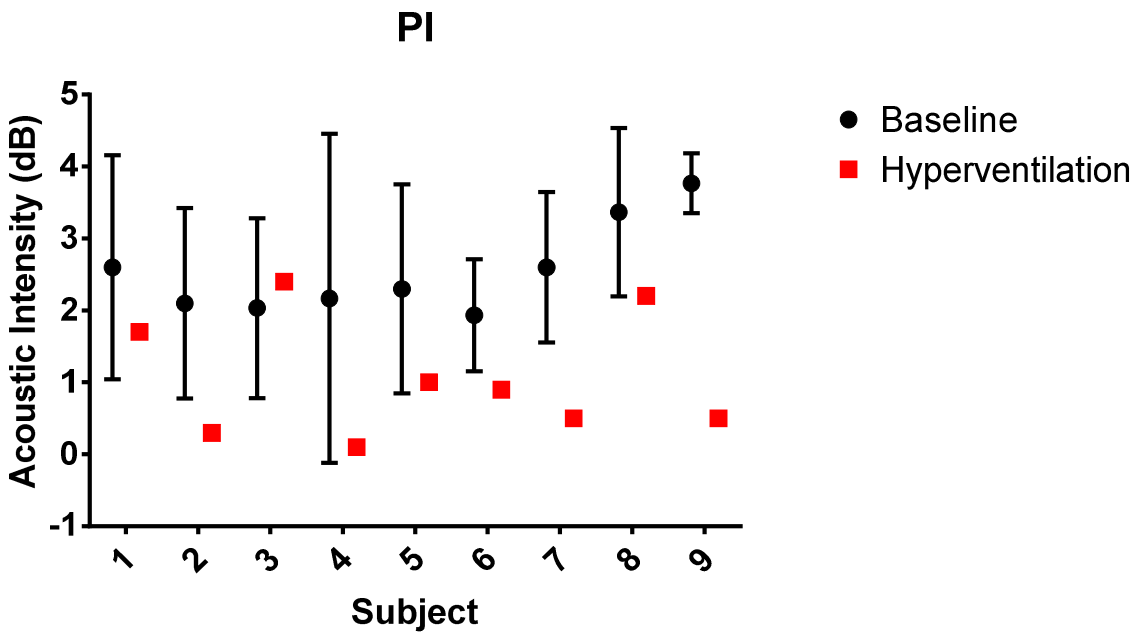

Figure 20: Parameter PI values (mean ±SD) during baseline CEUS measurements and the corresponding value during hyperventilation, in $ROI_{ANTcontr}$.

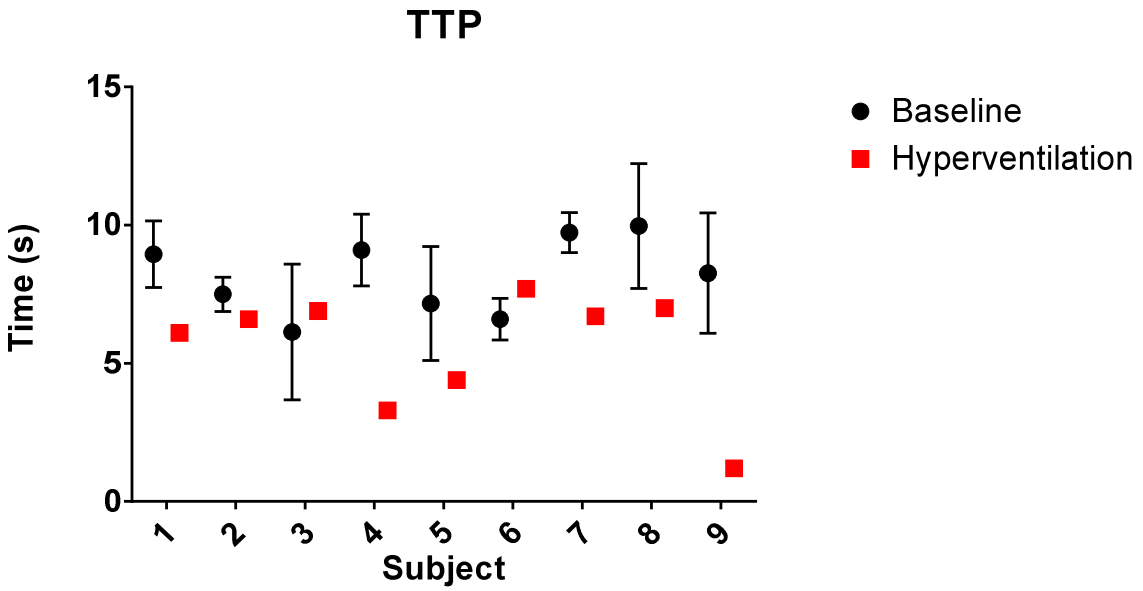

Figure 21: Parameter TTP values (mean ±SD) during baseline CEUS measurements and the corresponding value during hyperventilation, in $ROI_{ANTcontr}$.

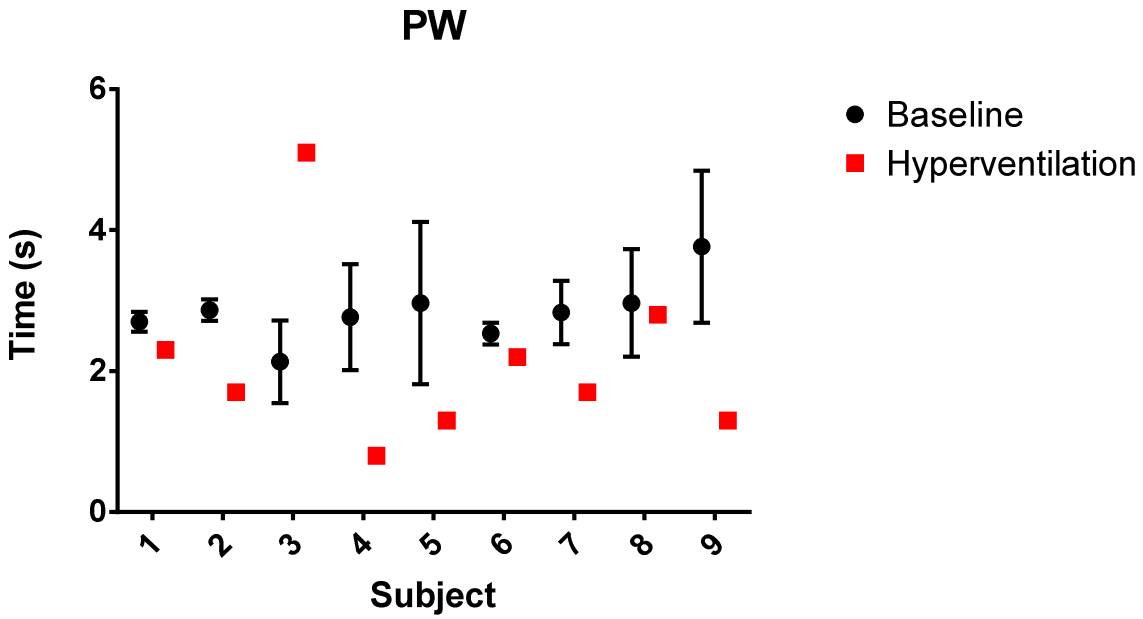

Figure 22: Parameter PW values (mean ±SD) during baseline CEUS measurements and the corresponding value during hyperventilation, in $ROI_{ANTcontr}$.

7.3.3 Correlation

In Table 7 to Table 10 the Pearson's correlation coefficients of the CEUS parameters compared to the $CBFV_{mean}$ in the four ROIs are shown. In Appendix III the Pearson's correlation coefficients of the CEUS parameters compared to the PSV in the four ROIs is shown in Table 16 to Table 19. The correlation of each of the CEUS parameters compared to the PSV or $CBFV_{mean,}$ was significant a maximum of two subjects.

Table 7: Pearson's correlation coefficient of the $CBFV_{mean}$ and the CEUS parameters in the $ROI_{MCAipsi}$.

$ROI_{MCAipsi}$		PI	TTP	TPI	AUC	PW	FWHM
Subject 2 CBFVmean	Pearson Correlation	-,323	-,953*	-,845	,573	,226	,734
	Sig. (2-tailed)	,677	,047	,155	,427	,774	,266
Subject 3 CBFV mean	Pearson Correlation	-,207	-,937	-,932	-,402	-,712	-,429
	Sig. (2-tailed)	,793	,063	,068	,598	,288	,571
Subject 4 CBFVmean	Pearson Correlation	,566	,102	,260	,625	,513	,586
	Sig. (2-tailed)	,434	,898	,740	,375	,487	,414
Subject 5 CBFV mean	Pearson Correlation	,994**	-,266	,498	,912	,612	,866
	Sig. (2-tailed)	,006	,734	,502	,088	,388	,134
Subject 6 CBFV mean	Pearson Correlation	,660	,915	,868	,815	,919	,878
	Sig. (2-tailed)	,340	,085	,132	,185	,081	,122
Subject 7 CBFV mean	Pearson Correlation	,916	-,755	,362	,935	,801	,877
	Sig. (2-tailed)	,084	,245	,638	,065	,199	,123
Subject 8 CBFVmean	Pearson Correlation	,356	-,645	,691	,104	,058	,094
	Sig. (2-tailed)	,644	,355	,309	,896	,942	,906
Subject 9 CBFVmean	Pearson Correlation	,937	-,962*	-,982*	,973*	,597	,943
	Sig. (2-tailed)	,063	,038	,018	,027	,403	,057

*. Correlation is significant at the 0.05 level (2-tailed); **. Correlation is significant at the 0.01 level (2-tailed).

Table 8: Pearson's correlation coefficient of the $CBFV_{mean}$ and the CEUS parameters in $ROI_{ANTcontr}$.

$ROI_{ANTcontr}$		PI	TTP	TPI	AUC	PW	FWHM
Subject 2 CBFVmean	Pearson Correlation	,316	,848	,275	,316	,834	,779
	Sig. (2-tailed)	,684	,152	,725	,684	,166	,221
Subject 3 CBFVmean	Pearson Correlation	-,259	-,527	-,950	-,864	-,976*	-,949
	Sig. (2-tailed)	,741	,473	,050	,136	,024	,051
Subject 4 CBFVmean	Pearson Correlation	,342	,751	,592	,289	,646	,602
	Sig. (2-tailed)	,658	,249	,408	,711	,354	,398
Subject 5 CBFVmean	Pearson Correlation	,204	,370	,564	,272	,416	,386
	Sig. (2-tailed)	,796	,630	,436	,728	,584	,614
Subject 6 CBFVmean	Pearson Correlation	,836	-,351	,189	,952*	,757	,723
	Sig. (2-tailed)	,164	,649	,811	,048	,243	,277
Subject 7 CBFVmean	Pearson Correlation	,548	,737	,713	,430	,593	,641
	Sig. (2-tailed)	,452	,263	,287	,570	,407	,359
Subject 8 CBFVmean	Pearson Correlation	,310	,317	,565	,050	-,199	-,387
	Sig. (2-tailed)	,690	,683	,435	,950	,801	,613
Subject 9 CBFVmean	Pearson Correlation	,974*	,683	-,302	,865	,591	,486
	Sig. (2-tailed)	,026	,317	,698	,135	,409	,514

*. Correlation is significant at the 0.05 level (2-tailed); **. Correlation is significant at the 0.01 level (2-tailed).

Table 9: Pearson's correlation coefficient of the $CBFV_{mean}$ and the CEUS parameters in the $ROI_{POSTcontr}$.

$ROI_{POSTcontr}$		PI	TTP	TPI	AUC	PW	FWHM
Subject 2 CBFVmean	Pearson Correlation	,315	,769	,768	,279	,712	,473
	Sig. (2-tailed)	,685	,231	,232	,721	,288	,527
Subject 3 CBFVmean	Pearson Correlation	-,407	-,864	-,965*	-,784	-,974*	-,983*
	Sig. (2-tailed)	,593	,136	,035	,216	,026	,017
Subject 4 CBFVmean	Pearson Correlation	,912	,494	,589	,653	,545	,565
	Sig. (2-tailed)	,088	,506	,411	,347	,455	,435
Subject 5 CBFVmean	Pearson Correlation	,392	,659	,698	,305	,494	,405
	Sig. (2-tailed)	,608	,341	,302	,695	,506	,595
Subject 6 CBFVmean	Pearson Correlation	,351	,761	,760	,255	,030	-,291
	Sig. (2-tailed)	,649	,239	,240	,745	,970	,709
Subject 7 CBFVmean	Pearson Correlation	,933	,266	,545	,934	,777	,898
	Sig. (2-tailed)	,067	,734	,455	,066	,223	,102
Subject 8 CBFVmean	Pearson Correlation	,292	-,980*	,043	,134	-,860	-,702
	Sig. (2-tailed)	,708	,020	,957	,866	,140	,298
Subject 9 CBFVmean	Pearson Correlation	,823	-,997**	-,998**	,755	,248	,574
	Sig. (2-tailed)	,177	,003	,002	,245	,752	,426

*. Correlation is significant at the 0.05 level (2-tailed); **. Correlation is significant at the 0.01 level (2-tailed).

Table 10: Pearson's correlation coefficient of the $CBFV_{mean}$ and the CEUS parameters in the $ROI_{POSTipsi}$.

$ROI_{POSTipsi}$		PI	TTP	TPI	AUC	PW	FWHM
Subject 2 CBFVmean	Pearson Correlation	,201	,105	,645	,225	,321	,259
	Sig. (2-tailed)	,799	,895	,355	,775	,679	,741
Subject 3 CBFVmean	Pearson Correlation	,632	-,988*	-,988*	,124	-,972*	-,841
	Sig. (2-tailed)	,368	,012	,012	,876	,028	,159
Subject 4 CBFVmean	Pearson Correlation	,457	,822	,711	,450	,815	,733
	Sig. (2-tailed)	,543	,178	,289	,550	,185	,267
Subject 5 CBFVmean	Pearson Correlation	,255	,926	,874	,234	,261	-,044
	Sig. (2-tailed)	,745	,074	,126	,766	,739	,956
Subject 6 CBFVmean	Pearson Correlation	-,159	,461	,991**	-,439	-,230	-,669
	Sig. (2-tailed)	,841	,539	,009	,561	,770	,331
Subject 7 CBFVmean	Pearson Correlation	,883	,116	,302	,785	,700	,701
	Sig. (2-tailed)	,117	,884	,698	,215	,300	,299
Subject 8 CBFVmean	Pearson Correlation	,471	-,517	,628	,445	-,261	-,173
	Sig. (2-tailed)	,529	,483	,372	,555	,739	,827
Subject 9 CBFVmean	Pearson Correlation	,525	,766	-,426	,409	,605	,438
	Sig. (2-tailed)	,475	,234	,574	,591	,395	,562

*. Correlation is significant at the 0.05 level (2-tailed); **. Correlation is significant at the 0.01 level (2-tailed).

8 Discussion

8.1 CEUS repeatability

In general, repeatability of CEUS for the quantification of CBF was low. Repeatability of all parameters was insufficient for quantification of flow in the MCA, with the lowest CV of 13.7% for the T_{PI}. For the parenchyma T_{PI} had an adequate repeatability, with a CV of 6.1% in the $ROI_{POSTipsi}$ and 9.7% in the contralateral parenchyma regions. All other parameters in the parenchyma had poor repeatability.

T_{PI}: parameter with the lowest variance?

T_{PI} showed the best repeatability. This may be explained by the first 10 seconds of the measurement included in the T_{PI}, in which no microbubbles arrive and therefore variation. The variation only takes place in the TTP period of the bolus curve. Due to the fact that the CV is calculated by dividing the variance by the mean value, the CV of T_{PI} is lower than the TTP because of the additional 10 seconds. Because the variation of interest takes place during the TTP period of the bolus curve, we conclude that the CV of the TTP is more representative for the variation of the arrival time than the T_{PI}. The only additional information the T_{PI} gives with respect to the TTP, is the time between the start of the measurement and the arrival of the microbubbles. Because measurements are started manually this results in additional variation in TPI. This variation is expected to be small in proportion with the total T_{PI} value. To compare the repeatability of the TTP and T_{PI}, the SD should be used instead of the CV to prevent misinterpretation.

Comparison of the CV in the MCA and parenchyma

The CV of the PI was significantly lower in the MCA than in the $ROI_{POSTipsi}$. In the MCA the blood may be close to microbubble saturation, which could explain the significantly lower CV in the MCA compared to the parenchyma regions. The microbubble saturation may reduce the variation induced by movement artefacts, variation in microbubble dose, scattering and skull artefacts. Microbubble saturation might also explain the significantly lower CV of the AUC in the MCA compared to the parenchyma regions. With microbubble saturation the PI of all the baseline measurements are comparable. Therefore it is expected that with comparable recirculation values the CV of the AUC is lower than in the parenchyma. The CV of the TTP and TPI in the MCA was not significantly different than in the parenchyma regions. This may be explained by their independence of microbubble concentration. The TTP and T_{PI} are expected not to be influenced by variation in microbubble dose, which has also been concluded by Meves et al.[72] The CV of the PW in the MCA was significantly higher than all parenchyma regions. It is expected that this is due to variation in the effect of recirculation on the bolus curve. Looking at the bolus curve fitting of this study, the PW depends on the course of the TIC in the first 10 seconds after the maximum peak is reached. Because in some measurements the recirculation influenced the TIC within 10 seconds after the maximum peak, the PW was larger.

In literature it was suggested that due to large variations in blood pressure, the variation of the CEUS outcome in large arteries would be larger than in the parenchyma. This due to the effects of the blood pressure on the size, the resonant frequency of the bubbles and the strength of the backscattered signal from the microbubbles.[39] However in this study this variation expressed in CV seems to be mostly comparable or lower than the CV of the parenchyma. This could suggest that the influence of the blood pressure on the behaviour of the microbubbles is less than expected or that the effect is the same in both the large arteries and the parenchyma.

Comparision of the CV in parenchyma regions

The CV values of all parameters of the parenchyma regions were not significantly different from each other except for the T_{PI}. We do not have an explanation of the significant differences in T_{PI} between the parenchyma regions. However the comparable CV values of the other parameters may suggest that skull artefacts and scattering do not increase the CV. An increased CV was expected in the anterior contralateral parenchyma region, due to more influences of shadowing or skull artefacts in the ipsilateral hemisphere. Due to different probe positions and therefore different scattering and skull artefacts

present, it was expected that the CV in the region contralateral to the MCA was higher than in other parenchyma regions.

Comparison of CEUS parameter values in MCA and parenchyma
The PI was significantly higher in the MCA region than in the parenchyma regions, due to high microbubble concentration in the MCA in comparison with the parenchyma. Furthermore the TTP was lower in the MCA then in the parenchyma. This can be explained by the higher CBFV in the MCA compared to the microcirculation in the parenchyma. The fact that the AUC, PW and FWHM was also significantly higher in the MCA compared to the parenchyma is explained by the differences in the course of the fitted bolus curve in the MCA region and in the parenchyma region. In contrast to the parenchyma regions, the bolus curves in the MCA region do not reach zero within the first minute after microbubble injection. This is reflected in higher AUC, PW and FWHM values.

Comparison of CEUS parameter values in parenchyma regions
The parameter values in the parenchyma regions differed significantly in all parameter except for the PI. The comparable PI in the parenchyma regions may indicate a comparable microbubble concentration and therefore a comparable blood volume. However the other parameters show significant differences between the parenchyma. We have no explanation for the specific significant differences for each parameter. Overall the differences indicate that there are significant differences in the bolus curves, even though the PI in the regions is nog significantly different. This may be explained by sources of variation affecting the TIC, such as movement artefacts and scattering from nearby tissue. However CBF differences between the parenchyma regions may also be present.

8.2 CBFV manipulation and correlations

In this study a significant decrease of 21.2% of the baseline end-tidal CO_2 during mild hyperventilation, resulted in a significant decrease of 10,9% of the PSV and 16,7% of the $CBFV_{mean}$ in the MCA. This corresponds to the findings of Bisschops et al. in which an increase of minute ventilation by 20% in patients after cardiac arrest decreased the mean CBFV in the MCA by 15% .[69]

It was expected that the PI would decrease due to a decrease of CBFV during hyperventilation and therefore an expected decrease of CBF. In percentage of the baseline values, the PI decreased less in the MCA during the hyperventilation than in the parenchyma regions. The decrease in PI in the parenchyma was much stronger than in the MCA region due to the higher baseline PI value. The TTP in the MCA increased during hyperventilation, whereas in the parenchyma the TTP decreases. Translating this TTP into CBFV this could mean that the CBFV in the MCA decreases, as expected, however in the microcirculation this CBFV increases. This may suggest a compensatory mechanism in the parenchyma which aims to keep the CBF constant.

The correlation of each of the CEUS parameters compared to the PSV or $CBFV_{mean,}$ was significant in only a maximum of two subjects. No pattern was visible in the Pearson's coefficients of the CEUS parameters that indicate a certain relation between the parameter and the CBFV. Also no pattern was seen in the Pearson's coefficients of the CEUS parameters in the different ROIs, for example different correlation coefficients in different ROIs. The lack of significance in the correlation was explained by the poor repeatability of the CEUS parameters. In case there is a significant correlation between certain CEUS parameters and CBFV, more measurements during CBF manipulation or a larger change in CBF are necessary to establish this correlation.

8.3 Quantification of the CBF

High variation in CEUS parameters has been described in literature as a difficult problem concerning the quantification of the CBF. In this study the repeatability of the bolus kinetic technique was investigated for the first time and the results confirm the high variability issues. Furthermore the study suggests that TTP and TPI are the most robust parameters in the parenchyma regions with the lowest and the most constant CV in different ROIs. Concerning the quantification of the CBF we believe that the poor repeatability within the same individual may be the most important limitation of this technique.

In case the CBFV is linearly related to the TTP, then a CV of ~20-25% for the TTP could still only detect large CBFV changes.

8.4 Study limitations

8.4.1 Determination of the repeatability

There are several limitations regarding the determination of the repeatability in this study. A limitation for example is the fact that the CEUS measurements were performed in intervals of at least 15 minutes, due to the time that was needed to ensure wash-out of the microbubbles. Assessment of repeatability requires a stable baseline CBF. We cannot exclude that the CBF could have changed between the different baseline measurements. PSV and $CBFV_{mean}$ showed adequate repeatability, suggesting no large changes in macrocirculatory CBF in time. . In addition, vital parameters such as blood pressure were kept stable over time, thus minimising spontaneous changes in the CBF. However, no information on the stability of the flow in the microcirculation was available. Taken together, a constant CBF during the experiment is uncertain.
Another limitation of the determination of the repeatability is the definition of adequate repeatability. A healthy CBF variability with a CV of 5–10% has been reported.[73] With a healthy CV of 5–10% of the CBF, the repeatability norm of a CV <10% may be too strict.

8.4.2 Determining of the correlation between CBFV and the CEUS parameters

One of the limitations of determining the correlation between the CBFV measured with the duplex and the CEUS parameters in this study is the restriction of only one hyperventilation measurement per subject. More hyperventilation measurements per subject would provide more insight in the effect of hyperventilation (and therefore a lower CBFV) on the CEUS parameters.

8.4.3 Microbubble administration

The main concern regarding our study protocol is the administration of the microbubbles. Just after preparation of the SonoVue solution the syringe was connected to the infusion. First duplex measurements were performed before administration of the microbubbles. These duplex measurements required approximately one minute. In this time, sedimentation of the microbubbles was visible in the syringe. We expect that there is a high limitation in CEUS measurements because it seems to be impossible to administer an equal microbubble dose in the measurements. Furthermore we experienced that the wash-out period of the SonoVue was frequently longer than 20 minutes. This variation may be due to inter-subject variation of clearance of microbubbles or due to microbubbles which initially remained in the infusion tube. We tried to facilitate the wash-out of the microbubbles by performing an extra 10 ml flush after the bolus measurement. After the extra flush was added to the protocol, no wash-out periods >20 minutes occurred.
Different amounts of sedimentation in the syringe, needle and/or infusion tube, result in different microbubble doses. We believe this is one of the main causes of the poor repeatability of the CEUS parameters, especially the intensity dependent parameters.

8.4.4 Insonation plane

Stability of the insonation plane probe during the CEUS measurements was adequate. Clear visualization of the MCA was present in almost all the measurements and due to the fact that the reflection of the contrast remained present after bolus arrival the probe position could be kept constant by focussing on the position of the MCA. Furthermore, after the CEUS measurements we checked the position of the probe by performing another duplex, which in all measurements confirmed a stable probe position. Still, subtle changes in probe position due to movement of the subject or the examinator is possible, especially during hyperventilation.. Small movement artefacts were supported by the observation of irregularities in the TICs during the data analysis.

8.4.5 Curve fitting

Due to the recirculation of the microbubbles, the acoustic intensity remained high in the MCA during the measurement. By fitting the bolus curve as defined in this study the decay of the acoustic intensity was larger than in the TIC of the MCA region. The fitted curve seemed to follow the TIC of the MCA accurately until just after the peak. This is also the reason that we have restricted the length of the TIC that we used to fit the bolus curves. Adjustment of the curve fitting analysis for the MCA, may result in more reliable parameters. On the other hand comparison of those specific parameters with the bolus parameters from the parenchyma would then be more difficult.

We believe that restricting the data analysis to only the first minute of the CEUS measurement does not affect the curve fitting any further, because the curves are only fitted based on the TIC of the first 40 seconds or shorter to eliminate the recirculation effect on the TIC in the MCA region as described above.

8.4.6 ROI selection and data analysis

Manual selection of the ROIs makes the data analysis approach observer dependent. To prevent selecting a parenchyma regions with artefacts, bad fits or large arteries, parameter images of the PI are used for the ROI selection. In these parameter images the maximum backscattered intensity is visible of each pixel, therefore some artefacts and large arteries are visible. After the ROI selection bad fits within the selected regions are eliminated from the TIC calculation. We believe that both the ROI selection in the PI parameter images and the elimination of bad fits improves the TIC of the regions. With our region selection and analysis methods we created an ideal situation, rather than a random selection. However, due to the explorative character of this study we think it is appropriate to first analyse the optimized TICs, in order to investigate whether with these optimized TICs quantification would be feasible in the future. When this is the case it would be important to further evaluate data analysis steps in such a way that the TICs are representable for its corresponding regions. A pre-processing step that could be considered is filtering of the pixelwise TICs in such a way that the TIC of each pixel also is influenced by the TICs of the near pixels

8.4.7 Microbubble interaction with the body

Passage of the microbubbles through the lung changes both the microbubble concentration and size, and therefore could introduce variations in quantification. Trapping of large microbubbles, diffusion of gases into the microbubbles and phagocytoses are expected to cause these variations. In this study, repeating the same SonoVue dosage after disappearance of the signal enhancement did not show a higher PI as mentioned by Skrok et al.[40] Skrok et al. showed an increase of 5 ± 1.5 dB in the second injections in the aorta and liver. In this study this effect was not seen. But this increase may have resulted from the high variation in the CEUS parameters as shown in this study.
Regarding the hyperventilation measurements performed in this study, the influence of lung filtration and diffusion may have created a larger variability with respect to the baseline measurements. This due to the changes blood gas and minute ventilation.

9 Conclusion

To enable CBF monitoring, quantification of CBF is essential and therefore the repeatability of the CEUS technique and the correlation between changes in CBF and the CEUS parameters were investigated in this study.

We conclude that the CEUS parameters have poor repeatability, except for the T_{PI} in the parenchyma regions. However the CV of the TTP is more representative for the variation of the arrival time than the T_{PI}. The poor repeatability corresponds with the high variation in CEUS outcome already described in literature. Furthermore no significant correlations were found between the CEUS parameters and the CBFV measured with duplex. For the quantification of the CBF we believe that the poor repeatability within the same individual is the most important limitation of this technique.

10 Future perspective

CEUS offers many significant advantages in the perfusion imaging of the brain over existing imaging modalities such as CT and MRI. Especially the application bedside and no radiation exposure. However, the clinical value of this technique is compromised by the relatively large variation in the imaging and quantification results. Quantification of the CBF with CEUS using the bolus kinetic technique is still far out of reach according this study and previous studies.

With the growth of our understanding of the microbubble behaviour and the development of microbubbles that are uniform in size and coating, in combination with developments in the areas of ultrasound systems, transducer design and signal processing, we believe that quantification of the CBF will be possible in the future. However, for the ultimate application at the ICU there are essential additional steps that need to be made.

11 Recommendations

We suggest that before quantification efforts are made in vivo with a certain microbubble, investigation of the microbubble reconstruction and the administration is performed. The prominent difficulty that we experienced in this study was to keep the SonoVue microbubbles from depositing. With all the expected sources of variability of the microbubble behaviour in vivo, it is crucial that in the reconstruction and the administration the variation is as low as possible. We expect that ultimately the microbubble reconstruction and administration must be done automatically instead of manually in order to effectively reduce variability.

Next to development of more suitable microbubbles as described in the previous chapter, also many steps can be taken regarding the imaging technique itself and the data analysis. Possible first steps following this project would be evaluation of different post processing steps regarding the curve fitting and perhaps the curve fit function itself. Furthermore in this study we have chosen for an insonation plane pointing towards the MCA. For a more reliable investigation of the parenchyma CEUS results it is recommended to avoid large arteries in the brain. This approach is probably better suited for the investigation of the microbubble behaviour or the perfusion in the parenchyma.

Regarding the development of a CBF monitoring technique in the ICU, the CEUS is not ready for use in clinical practice. We believe that the limitations of the technique due to the calcification of the acoustic window in older patients may be the most difficult limitation to overcome. When keeping in mind that the quantification of blood flow with CEUS will be possible in the future it is recommended to enhance the ultrasound technique and probe design in such a way that ultrasonography of the brain in is possible in every patient.

12 Bibliography

1. Dunn IF, Ellegala B, Fox JF, Dong HK. Principles of Cerebral Oxygenation and Blood Flow in the Neurological Critical Care Unit. *Neurocrit. Care* 2006;4:77-82. doi:10.1385/Neurocrit.

2. Dagal A, Lam AM. Cerebral blood flow and the injured brain: how should we monitor and manipulate it? *Curr. Opin. Anaesthesiol.* 2011;24(2):131-7. doi:10.1097/ACO.0b013e3283445898.

3. Zadoks J, Gijzen R. *Zorgstandaard Traumatisch Hersenletsel*.; 2014.

4. Limburg M, Voogdt H. *Zorgstandaard CVA/TIA*.; 2012.

5. Zhang H, Zhang B, Li S, Liang C, Xu K, Li S. Whole brain CT perfusion combined with CT angiography in patients with subarachnoid hemorrhage and cerebral vasospasm. *Clin. Neurol. Neurosurg.* 2013;115(12):2496-501. doi:10.1016/j.clineuro.2013.10.004.

6. Peerdeman SM, Girbes ARJ, Vandertop WP. Changes in cerebral glycolytic activity during transport of critically ill neurotrauma patients measured with microdialysis. *J. Neurol.* 2002;249(6):676-679.

7. Willie CK, Tzeng Y-C, Fisher J a, Ainslie PN. Integrative regulation of human brain blood flow. *J. Physiol.* 2014;592(Pt 5):841-59. doi:10.1113/jphysiol.2013.268953.

8. Freeman WD, Dawson SB, Flemming KD. The ABC ' s of Stroke Complications. *Semin. Neurol.* 2010;30(5):501-510.

9. Rowland MJ, Hadjipavlou G, Kelly M, Westbrook J, Pattinson KTS. Delayed cerebral ischaemia after subarachnoid haemorrhage : looking beyond vasospasm. *Br. J. Anaesth.* 2012;109(3):315-329. doi:10.1093/bja/aes264.

10. Badruddin A, Taqi MA, Abraham MG, Dani D, Zaidat OO. Neurocritical Care of a Reperfused Brain. *Curr neurol neurosci Rep* 2011;11:104-110. doi:10.1007/s11910-010-0156-9.

11. Donkin JJ, Vink R. Mechanisms of cerebral edema in traumatic brain injury: therapeutic developments. *Curr. Opin. Neurol.* 2010;23(3):293-9. doi:10.1097/WCO.0b013e328337f451.

12. Steiner L a., Czosnyka M. Should we measure cerebral blood flow in head-injured patients? *Br. J. Neurosurg.* 2002;16(5):429-439. doi:10.1080/0268869021000030221.

13. Kulik T, Kusano Y, Aronhime S, Sandler AL, Winn R. Regulation of cerebral vasculature in normal and ischemic brain. *Neuropharmacology* 2008;55(3):281-288. doi:10.1016/j.neuropharm.2008.04.017.Regulation.

14. Steiner L a, Andrews PJD. Monitoring the injured brain: ICP and CBF. *Br. J. Anaesth.* 2006;97(1):26-38. doi:10.1093/bja/ael110.

15. Helmy a, Vizcaychipi M, Gupta a K. Traumatic brain injury: intensive care management. *Br. J. Anaesth.* 2007;99(1):32-42. doi:10.1093/bja/aem139.

16. Levine J a. Measurement of energy expenditure. *Public Health Nutr.* 2007;8(7a):1123-1132. doi:10.1079/PHN2005800.

17. Le Roux P, Menon DK, Citerio G, et al. Consensus summary statement of the International Multidisciplinary Consensus Conference on Multimodality Monitoring in Neurocritical Care : A statement for healthcare professionals from the Neurocritical Care Society and the European Society of Intensive. *Intensive Care Med.* 2014;21:1-26. doi:10.1007/s00134-014-3369-6.

18. Robertson CS, Gopinath SP, Goodman JC, Contant CF, Valadka AB, Narayan RAJK. SjvO2 Monitoring in Head-Injured Patients. *J. Neurotrauma* 1995;12(5):891-896.

19. Frontera J, Ziai W, O'Phelan K, et al. Regional Brain Monitoring in the Neurocritical Care Unit. *Neurocrit. Care* 2015:348-359. doi:10.1007/s12028-015-0133-x.

20. Aaslid R, Huber P, Nornes H. Evaluation of cerebrovascular spasm with transcranial Doppler ultrasound. *J. Neurosurg.* 1984;60(1):37-41. doi:10.3171/jns.1984.60.1.0037.

21. White H, Venkatesh B. Applications of transcranial Doppler in the ICU: a review. *Intensive Care Med.* 2006;32(7):981-94. doi:10.1007/s00134-006-0173-y.

22. Loch Macdonald R. Management of cerebral vasospasm. *Neurosurg. Rev.* 2006;29(3):179-93. doi:10.1007/s10143-005-0013-5.

23. Quaia E. *Contrast Media in Ultrasonogrpahy: Basic Principles and Clinical Applications*.; 2005.

24. Cosgrove D, Lassau N. Imaging of perfusion using ultrasound. *Eur. J. Nucl. Med. Mol. Imaging* 2010;37 Suppl 1(July):S65-85. doi:10.1007/s00259-010-1537-7.

25. Seidel G, Meyer-Wiethe K. Ultrasound Perfusion Imaging in Acute Ischemic Stroke. In: Schaller B, ed. *State-of-the-Art Imaging in Stroke Volume 1*.; 2007:1-31.

26. Powers J, Averkiou M, Bruce M. Principles of cerebral ultrasound contrast imaging. *Cerebrovasc. Dis.* 2009;27 Suppl 2(suppl 2):14-24. doi:10.1159/000203123.

27. Claudon M, Dietrich CF, Choi B., Cosgrove DO, Kudo M. Guidelines and Good Clinical Practice Recommendations for Contrast Enhanced Ultrasound (CEUS) in the Liver – Update 2012. *Ultraschall Med* 2013;34:11-29.

28. Piscaglia F, Nolsøe C, Dietrich CF, et al. The EFSUMB Guidelines and Recommendations on the Clinical Practice of Contrast Enhanced Ultrasound (CEUS): update 2011 on non-hepatic applications. *Ultraschall Med.* 2011;33(1):33-59. doi:10.1055/s-0031-1281676.

29. Ter Haar G. Safety and bio-effects of ultrasound contrast agents. *Med. Biol. Eng. Comput.* 2009;47(8):893-900. doi:10.1007/s11517-009-0507-3.

30. Meairs S, Alonso A. Ultrasound, microbubbles and the blood-brain barrier. *Prog. Biophys. Mol. Biol.* 2007;93(1-3):354-62. doi:10.1016/j.pbiomolbio.2006.07.019.

31. Jungehulsing GJ, Brunecker P, Nolte CH, et al. Diagnostic transcranial ultrasound perfusion-imaging at 2.5 MHz does not affect the blood-brain barrier. *Ultrasound Med. Biol.* 2008;34(1):147-50. doi:10.1016/j.ultrasmedbio.2007.07.006.

32. Postert T, Hoppe P, Federlein J, et al. Contrast agent specific imaging modes for the ultrasonic assessment of parenchymal cerebral echo contrast enhancement. *J. Cereb. Blood Flow Metab.* 2000;20(12):1709-16. doi:10.1097/00004647-200012000-00010.

33. Wei K, Jayaweera a. R, Firoozan S, Linka a., Skyba DM, Kaul S. Quantification of Myocardial Blood Flow With Ultrasound-Induced Destruction of Microbubbles Administered as a Constant Venous Infusion. *Circulation* 1998;97(5):473-483. doi:10.1161/01.CIR.97.5.473.

34. Hudson JM, Karshafian R, Burns PN. Quantification of flow using ultrasound and microbubbles: a disruption replenishment model based on physical principles. *Ultrasound Med. Biol.* 2009;35(12):2007-20. doi:10.1016/j.ultrasmedbio.2009.06.1102.

35. Mahoney M, Sorace A, Warram J, Samuel S, Hoyt K. Volumetric contrast-enhanced ultrasound imaging of renal perfusion. *J Ultrasound Med* 2014;33(8):1427-1437. doi:10.7863/ultra.33.8.1427.Volumetric.

36. Veltmann C, Lohmaier S, Schlosser T, et al. On the design of a capillary flow phantom for the evaluation of ultrasound contrast agents at very low flow velocities. *Ultrasound Med Biol.* 2002;28(5):625-634.

37. Lassau N, Chebil M, Chami L, Bidault S, Girard E, Roche A. Dynamic contrast-enhanced ultrasonography (DCE-US): A new tool for the early evaluation of antiangiogenic treatment. *Target. Oncol.* 2010;5(1):53-58. doi:10.1007/s11523-010-0136-7.

38. Dietrich CF, Averkiou MA, Correas JM, Lassau N, Leen E, Piscaglia F. An EFSUMB Introduction into Dynamic Contrast- Enhanced Ultrasound (DCE-US) for Quantification of Tumour Perfusion. *Ultraschall Med* 2012;33:344-351.

39. Tang M, Mulvana H, Gauthier T, Lim AKP. Quantitative contrast-enhanced ultrasound imaging : a review of sources of variability. *Interface Focus* 2011;(May):520-539.

40. Skrok J. Markedly increased signal enhancement after the second injection of SonoVue compared to the first – a quantitative normal volunteer study. In: *12th European Symp. on Ultrasound Contrast Imaging, January 25-26th, 2007*. Rotterdam, The Netherlands; 2007.

41. Gupta I. Investigating the Influence of the Physiological Environment on Quantitative Contrast-enhanced Ultrasound Imaging. *J. Med. Ultrasound* 2014;22(1):9-17. doi:10.1016/j.jmu.2013.10.009.

42. Eyding J, Wilkening W, Krogias C, Przuntek H, Meves S, Postert T. Validation of the Depletion Kinetic in Semiquantitative Ultrasonographic Cerebral Perfusion Imaging Using 2 Different Techniques of Data Acquisition. 2004:1035-1040.

43. Berg D, Godau J, Walter U. Transcranial sonography in movement disorders. *Lancet Neurol.* 2008;7:1044-55. doi:10.1016/S1474-4422(08)70239-4.

44. Postert T, Muhs a., Meves S, Federlein J, Przuntek H, Buttner T. Transient Response Harmonic Imaging : An Ultrasound Technique Related to Brain Perfusion. *Stroke* 1998;29(9):1901-1907. doi:10.1161/01.STR.29.9.1901.

45. Seidel G, Albers T, Meyer K, Wiesmann M. Perfusion harmonic imaging in acute middle cerebral artery infarction. *Ultrasound Med. Biol.* 2003;29(9):1245-1251. doi:10.1016/S0301-5629(03)01016-0.

46. Bartels E, Bittermann H-J. Transcranial Contrast Imaging of Cerebral Perfusion in Stroke Patients Following Decompressive Craniectomy. *Ultraschall Med* 2004;25:206-213.

47. Federlein J, Postert T, Meves S, Weber S, Przuntek H, Büttner T. Ultrasonic evaluation of pathological brain perfusion in acute stroke using second harmonic imaging. *J. Neurol. Neurosurg. Psychiatry* 2000;69(5):616-22. Available at: http://www.pubmedcentral.nih.gov/articlerender.fcgi?artid=1763382&tool=pmcentrez&rendertype=abstract.

48. Stolz E, Allendörfer J, Jauss M, Traupe H, Kaps M. Sonographic harmonic grey scale imaging of brain perfusion: scope of a new method demonstrated in selected cases. *Ultraschall Med.* 2002;23(5):320-4. doi:10.1055/s-2002-35058.

49. Eyding J, Krogias C, Wilkening W, Postert T. Detection of cerebral perfusion abnormalities in acute stroke using phase inversion harmonic imaging (PIHI): preliminary results. *J. Neurol. Neurosurg. Psychiatry* 2004;75(6):926-929. doi:10.1136/jnnp.2003.026195.

50. Kern R, Perren F, Schoeneberger K, Gass A, Hennerici M, Meairs S. Ultrasound microbubble destruction imaging in acute middle cerebral artery stroke. *Stroke* 2004;35:1665-16670.

51. Seidel G, Meyer-Wiethe K, Berdien G, Hollstein D, Toth D, Aach T. Ultrasound perfusion imaging in acute middle cerebral artery infarction predicts outcome. *Stroke.* 2004;35(5):1107-11. doi:10.1161/01.STR.0000124125.19773.40.

52. Wiesmann M, Meyer K, Albers T, Seidel G. Parametric perfusion imaging with contrast-enhanced ultrasound in acute ischemic stroke. *Stroke.* 2004;35(2):508-13. doi:10.1161/01.STR.0000114877.58809.3D.

53. Bartels E. Evaluation of Cerebral perfusion deficit in stroke patients using new transcranial contrast imaging CPS technology. *Ultraschall Med* 2005;26:478-486.

54. Caruso G, Salvaggio G, Ragusa P, Brancatelli G, Lagalla R. Ultrasonic evaluation with second harmonic imaging and SonoVue in the assessment of cerebral perfusion in diabetic patients: a case-control study. *Eur. Radiol.* 2005;15(4):823-8. doi:10.1007/s00330-004-2474-2.

55. Krogias C, Postert T, Meves S, Wilkening W, Przuntek H, Eyding J. Semiquantitative analysis of ultrasonic cerebral perfusion imaging. *Ultrasound Med. Biol.* 2005;31(8):1007-12. doi:10.1016/j.ultrasmedbio.2005.01.001.

56. Bartels E, Bittermann H-J. Transcranial Contrast Imaging of Cerebral Perfusion in Patients With Space-Occupying Intracranial Lesions. *J Ultrasound Med* 2006;25:499-507.

57. Eyding J, Krogias C, Schöllhammer M, et al. Contrast-enhanced ultrasonic parametric perfusion imaging detects dysfunctional tissue at risk in acute MCA stroke. *J. Cereb. Blood Flow Metab.* 2006;26(4):576-82. doi:10.1038/sj.jcbfm.9600216.

58. Seidel G, Cangür H, Meyer-Wiethe K, et al. On the ability of ultrasound parametric perfusion imaging to predict the area of infarction in acute ischemic stroke. *Ultraschall Med.* 2006;27(6):543-8. doi:10.1055/s-2006-927023.

59. Vicenzini E, Delfini R, Magri F, et al. Semiquantitative human cerebral perfusion assessment with ultrasound in brain space-occupying lesions: preliminary data. *J. Ultrasound Med.* 2008;27(5):685-92. Available at: http://www.ncbi.nlm.nih.gov/pubmed/18424642.

60. Seidel G, Algermissen C, Christoph a., Claassen L, Vidal-Langwasser M, Katzer T. Harmonic Imaging of the Human Brain : Visualization of Brain Perfusion With Ultrasound. *Stroke* 2000;31(1):151-154. doi:10.1161/01.STR.31.1.151.

61. Meyer K, Seidel G. Transcranial contrast diminution imaging of the human brain: a pilot study in healthy volunteers. *Ultrasound Med. Biol.* 2002;28(02):1433-1437.

62. Seidel G, Meyer K, Metzler V, Toth D, Vida-Langwasser M, Aach T. Human cerebral perfusion analysis with ultrasound contrast agent constant infusion: a pilot study on healthy volunteers. *Ultrasound Med. Biol.* 2002;28(2):183-189.

63. Eyding J, Wilkening W, Reckhardt M, et al. Contrast Burst Depletion Imaging (CODIM): A New Imaging Procedure and Analysis Method for Semiquantitative Ultrasonic Perfusion Imaging. *Stroke* 2003;34(1):77-83. doi:10.1161/01.STR.0000046455.51363.E2.

64. Eyding J, Wilkening W, Reckhardt M, Meves S, Postert T. Reliability of Semiquantitative Ultrasonic Perfusion Imaging of the Brain. *J. Neuroimaging* 2004;14(2):143-149. doi:10.1177/1051228404263273.

65. Seidel G, Kaps M. Harmonic Imaging of the Vertebrobasilar System. *Stroke* 1997;28(8):1610-1613. doi:10.1161/01.STR.28.8.1610.

66. Hölscher T, Postert T, Meves S, Thies T, Ermert H. Assessment of brain perfusion with echo contrast specific imaging modes and Optison. *Acad Radiol* 2002;9:386-388.

67. Eyding J, Krogias C, Wilkening W, Meves S, Ermert H, Postert T. Parameters of cerebral perfusion in phase-inversion harmonic imaging (PIHI) ultrasound examinations. *Ultrasound Med. Biol.* 2003;29(10):1379-1385. doi:10.1016/S0301-5629(03)01035-4.

68. Bolognese M, Artemis D, Alonso A, Hennerici MG, Meairs S, Kern R. Real-time ultrasound perfusion imaging in acute stroke: assessment of cerebral perfusion deficits related to arterial recanalization. *Ultrasound Med. Biol.* 2013;39(5):745-52. doi:10.1016/j.ultrasmedbio.2012.11.022.

69. Bisschops LLA, Hoeven JG Van Der, Hoedemaekers CWE. Preserved metabolic coupling and cerebrovascular reactivity during mild hypothermia after cardiac arrest*. *Crit. Care Med.* 2010;38(7):1542-1547. doi:10.1097/CCM.0b013e3181e2cc1e.

70. Krogias C, Henneböhl C, Geier B, et al. Transcranial ultrasound perfusion imaging and perfusion-MRI--a pilot study on the evaluation of cerebral perfusion in severe carotid artery stenosis. *Ultrasound Med. Biol.* 2010;36(12):1973-80. doi:10.1016/j.ultrasmedbio.2010.08.017.

71. Eyding J, Nolte-Martin A, Krogias C, Postert T. Changes of contrast-specific ultrasonic cerebral perfusion patterns in the course of stroke; reliability of region-wise and parametric imaging analysis. *Ultrasound Med. Biol.* 2007;33(3):329-34. doi:10.1016/j.ultrasmedbio.2006.08.013.

72. Meves SH, Wilkening W, Thies T, et al. Comparison between echo contrast agent-specific imaging modes and perfusion-weighted magnetic resonance imaging for the assessment of brain perfusion. *Stroke* 2002;33:2433-2437.

73. Panerai RB. Complexity of the human cerebral circulation. *Philos. Trans. A. Math. Phys. Eng. Sci.* 2009;367(1892):1319-36. doi:10.1098/rsta.2008.0264.

Appendix I
Abbreviations

ICU	Intensive care unit
A	Plateau intensity parameter of the refill intensity curve
AUC	Area under the curve (of the bolus TIC)
BBB	Blood brain barrier
CBF	Cerebral blood flow
CBFV	Cerebral blood flow velocity
$CBFV_{mean}$	Duplex parameter, the mean CBFV calculated in the duplex mode
CBI	Contrast burst imaging
CBV	Cerebral blood volume
CEUS	Contrast enhanced ultrasound
CPP	Cerebral perfusion pressure
CPS	Contrast pulse sequencing
CTA	Computed tomography angiography
CVR	Cerebrovascular resistance
DCI	Delayed cerebral ischemia
DSA	Digital subtraction angiography
FWHM	Full width at half of the peak intensity increase (of the bolus TIC)
HI	Harmonic imaging
ICM	intracerebral microdialysis
ICP	Intracranial pressure
LDF	Laser Doppler fowmetry
MAP	Mean arterial pressure
MCA	Middle cerebral artery
MI	Mechanical index
NIRS	Near-infrared spectroscopy
P_{aO2}	Carbon dioxide partial pressure
$PbtO_2$	Brain parenchymal oxygen tension
PCT	Perfusion computed tomography
PG	Positive gradient (of the bolus TIC)
PI	Pulse inversion
PI	Peak intensity (of the bolus TIC)
PIHI	Pulse inversion harmonic imaging
PM	Power modulation
PMPI	Power modulated PIHI
PSV	Duplex parameter, the peak systolic velocity calculated in the duplex mode
PW	Peak width (of the bolus TIC)
RMSE	Root mean square error

$ROI_{ANTcontr}$	ROI selected in the parenchyma of the contralateral hemisphere at the anterior side
$ROI_{MCAipsi}$	ROI selected in the ipsilateral MCA
$ROI_{POSTcontr}$	ROI selected in the parenchyma of the contralateral hemisphere at the posteror side
$ROI_{POSTipsi}$	ROI selected in the parenchyma of the ipsilateral hemisphere at the posterior side
SAH	Subarachnoid hemorrhage
$SjvO_2$	Jugular bulb oxygen saturation
SSE	Sum of squared error
TBI	Traumatic brain injury
TCD	Transcranial Doppler
TDF	Thermal diffusion flowmetry
TIC	Time intensity curve
T_{PI}	Time-to-peak intensity (of the bolus TIC)
TTP	Time-to-peak (of the bolus TIC)
TVI	Time variance imaging
UCA	Ultrasound contrast agent
β	Rise rate parameter of the refill intensity curve

Appendix II

Study Protocol

SUMMARY

Rationale: The primary goal of neurocritical care is the prevention and management of secondary cerebral damage. Cerebral ischemia is considered as a common final pathway in secondary brain injury and generally occurs when the balance between delivery and consumption of oxygen and nutrients in the brain is disturbed. Monitoring the cerebral blood flow (CBF) is essential in patients with acute brain injury, however, no bedside technique is available for use in critically ill patients. Contrast enhanced ultrasound (CEUS) is an established technique that allows real-time assessment of focal lesions in the brain and for assessment of neurovascular lesion in patients with sroke. Ultrasound is an attractive technique because it is non-invasive, has a high temporal resolution and can be used at the bedside. With the use of ultrasound contrast agents (UCAs) the low level of acoustic intensity due to the ultrasound absorption of the skull can be overcome, thus improving the signal-to-noise ratio. No quantitative technique has been developed yet in the CEUS technology.

Objective: This protocol is a first pilot study to determine both feasibility and reproducibility of CEUS in the quantification of CBF. Aim of the current study is to determine the reproducibility of CEUS in quantification of cerebral blood flow, compared to transcranial Doppler at normal and impaired CBF. In addition, differences in quantification using a bolus technique and the refill kinetics will be studied.

Study design: Observational study

Study population: Healthy human volunteers, 18 - 35 yr old

Intervention (if applicable): Not applicable

Main study parameters/endpoints: Main study parameter is the reproducibility of the CEUS bolus kinetics and the flash-replenishment method. A difference between the measurements of more than 10% is considered to imply poor reproducibility. As a control, the reproducibility of measurement of the flow velocity in the ipsilateral middle cerebral artery will be assessed. Secondary study parameters are 1) Correlation between the bolus kinetics approach and the flash-replenishment method and 2) Comparison of the CEUS bolus technique with transcranial Doppler (at 2 different levels of cerebral blood flow. 3) determination of the attenuation of the signal by the skull bone.

Nature and extent of the burden and risks associated with participation, benefit and group relatedness:

The burden of acute brain injury is enormous, both from a clinical and economical perspective. Since adequate supply of blood containing oxygen and glucose is crucial for the recovery and survival of brain tissue, monitoring the cerebral blood flow (CBF) is an essential part of neurocritical care. However, easy, non-invasive and reliable direct bedside monitoring of the CBF is not feasible at this moment in the ICU. Development of such a method is very likely to improve the quality of care in patients with acute brain injury since early detection of reduced cerebral blood flow provides the opportunity of intervention to prevent ischemia. In addition, the effect of therapeutic intervention to improve cerebral blood flow can be assessed with adaption of the intervention if necessary.

The burden of the study procedures consists of the time investment related to the screening procedure and 1 visit to the hospital, with a total time of hospitalisation of approximately 4 hours. All subjects will visit the hospital for a screening visit in which a medical interview, physical examination, ECG recording and transcranial Doppler will be performed. For the bloodflow measurements, transcranial ultrasound and Doppler will be performed, which is not painful and does not induce any discomfort. In addition, an ultrasound of the left or right kidney will be performed that is also not painful and does not induce any discomfort. All subjects will receive a standard venous canula (18G) in the left or right fossa cubiti. Mild hyperventilation is performed by the subject itself, and is generally well tolerated in previous experiments in our department.

The use of ultrasound, Doppler and transcranial Doppler for the measurement of flow is without any risk. The ultrasound contrast agent SonoVue is used in general clinical practice (mainly by cardiologists and oncologists) and has an excellent safety profile. Mild, temporary side effects have been reported, such as nausea, flushing,

pruritus and backache. The risk of serious adverse events caused by the use of SonoVue is estimated at 0.0086%, of which none were fatal. Possible adverse effects associated with mild hyperventilation are easily managed by cessation of hyperventilation.
Our research population consists of young male and female volunteers that are from a young age group (18-35 years) and in general good health. We chose to select this young and healthy population to avoid the risks of SonoVue even further.
Privacy of the volunteers is guarded by handling and storing the research data using the guidelines of good clinical practice (GCP) as recorded in our data management plan. There is no risk of social stigmatization. There is no risk for exclusion from health insurance.
In light of the abovementioned potential issues of concern, we assess the possible damage for our volunteers in the present study to be `light`. We assess the possibility that this will occur as `small`. Therefore, in line with the guidelines provided by the NFU (Dutch Federation of University Medical Centres), the risk classification for this study is `negligible risk`.

1. INTRODUCTION AND RATIONALE

The primary goal of neurocritical care is the prevention and management of secondary cerebral damage[1,2]. This series of pathological events occur in the early phase following primary brain injury and result in an increase in cerebral damage with an associated increased risk of poor outcome. A large number of mechanisms are implicated in the pathophysiology of secondary cerebral damage. Cerebral ischemia is considered as a common final pathway in secondary brain injury and generally occurs when the balance between delivery and consumption of oxygen and nutrients in the brain is disturbed. Since adequate supply of blood containing oxygen and glucose is crucial for the recovery and survival of brain tissue, monitoring the cerebral blood flow (CBF) is an essential part of neurocritical care[3]. However, easy, non-invasive and reliable direct bedside monitoring of the CBF is not feasible at this moment in the ICU. Current techniques of CBF monitoring have important limitations. Perfusion MRI, perfusion CT or SPECT scanning are not routinely available, use radiation or radioactive tracers and are generally not available at the bedside. Currently used bedside CBF monitors such as a thermal diffusion probe are invasive and estimate only regional CBF. Other techniques such as jugular venous oxygen saturation or brain tissue oxygen pressure are surrogate markers and do not represent actual cerebral blood flow. Transcranial Doppler (TCD) is frequently used in the ICU for measurement of cerebral blood flow velocity in the larger cerebral arteries. As the diameter of the insonated vessel in transcranial Doppler is unknown, cerebral blood flow cannot be determined by this technique. Another major limitation of conventional Doppler ultrasound for the imaging of CBF in acute brain injury is that it is not sensitive enough to detect the blood flow in small vessels where the major part of the hemodynamic response occurs.
Contrast enhanced ultrasound (CEUS) is an established technique that allows real-time assessment of focal lesions in the brain[4]. Ultrasound is an attractive technique because it is non-invasive, has a high temporal resolution and can be used at the bedside. With the use of ultrasound contrast agents (UCAs) the low level of acoustic intensity due to the ultrasound absorption of the skull can be overcome, thus improving the signal-to-noise ratio. So far, CEUS has mainly been applied for the qualitative monitoring of the brain parenchyma, for instance in neuro-oncologic surgery. More recently a (semi)quantitative approach is developed for patients with neurovascular pathology such as acute stroke[5].
Several CEUS methods have been developed to measure the CBF. The main approaches to measure the blood flow in the microcirculation with UCAs are the bolus kinetics, depletion kinetics and refill kinetics. In addition several contrast specific imaging modes have been used to quantify CBF.
The different methods of quantification of CBF have advantages and disadvantages and have not yet been directly compared within one patient. In addition, the reproducibility of the technique is not well studied. Although CEUS is a promising technique for bedside monitoring of CBF in ICU patients with acute brain injury, more research is necessary before this technique can be used in clinical practice. Development of the quantification method, optimisation of the contrast administration and imaging technique and ultimately, validation studies, are required before this technique can be applied in general patient care. This protocol is a first pilot study to determine both feasibility and reproducibility of CEUS in the quantification of CBF.

Aim of the current study is to determine the reproducibility of CEUS in quantification of cerebral blood flow, compared to transcranial Doppler at normal and impaired CBF. In addition, differences in quantification using a bolus technique and the refill kinetics will be studied.

2. OBJECTIVES

Primary Objective:
Determine the reproducibility of CEUS for measurement of CBF.

Secondary Objective(s):

- Correlation between flow measurements using the bolus kinetics approach with the flash-replenishment method.
- Correlation between flow measurements using the CEUS bolus technique with transcranial Doppler
- Determination of the effect of attenuation of the skull on the flow measurements by determining the correlation between measurement of renal artery blood flow with Doppler and renal blood flow measurements using the CEUS bolus technique.

3. STUDY DESIGN

We will perform an observational study in healthy volunteers.

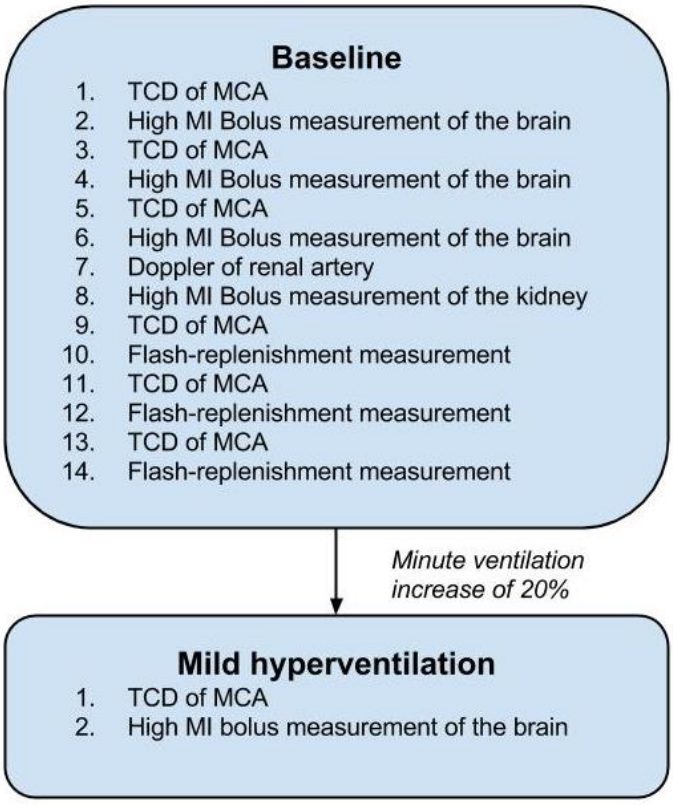

Figure 1: overview of the experiments

Study protocol

Cerebral CEUS

Cerebral CEUS will be performed unilaterally, at the side with the most optimal temporal window. First the the bolus kinetics method using a high mechanical index (MI) will be performed, followed by the flash-replenishment technique. Each test is performed 3 times, separated by a 15 minute break to allow the ultrasound contrast agent (UCA) to wash-out from the blood stream. After mild hyperventilation, only the bolus technique will be used in a single measurement. All measurements will be performed after assessment of the CBF velocity in the middle cerebral artery using TCD.

Renal CEUS

The skull bone is a major source of bias in the calculation of the cerebral blood flow from the CEUS data. The thickness of the temporal acoustic window is expected to be heterogeneous within and between patients. Therefore the acoustic window increases the inhomogeneity of the acoustic power distribution in the brain. This results in an even greater variance in perfusion parameters in different regions of interest. In order to analyse the differences in acoustic power distribution in a patient with and without the skull bone, CEUS of the kidney will be performed. A single measurement of the flow velocities of the left or right renal artery will be performed using Doppler, followed by a single measurement of the renal blood flow using the bolus kinetic CEUS technique.

Bolus kinetics method brain

Flow velocities in the middle cerebral artery will be measured by TCD ipsilaterally to the CEUS measurements. An intravenous injection of 2.5 ml the UCA SonoVue (Bracco Imaging Europe BV, Amsterdam, 8 µL/ml) will be given as a bolus. Simultaneously high mechanical imaging will be performed for 2 minutes (MI>1).

Bolus kinetics method kidney

Flow velocities in the left or right renal artery will be estimated by Doppler, ipsilateral to the renal CEUS measurements. A single intravenous injection of 2.5 ml the UCA SonoVue (Bracco Imaging Europe BV, Amsterdam, 8 µL/ml) will be given as a bolus. Simultaneously high mechanical imaging of the ipsilateral kidney will be performed for 2 minutes (MI>0.5).

Flash-replenishment technique brain

Flow velocities in the middle cerebral artery will be measured by TCD ipsilaterally to the CEUS measurements. The contrast agent SonoVue (Bracco Imaging Europe BV, Amsterdam) will be infused intravenously at a concentration of 8 µL/ml with a speed of 1 ml/min through an intravenous access in the left or right fossa cubiti. Five minutes after the start of UCA infusion a flash-replenishment measurement will be performed by applying (~8) high MI flashes of MI>1, followed by switching to low MI imaging with an MI of 0.17 for ~10 seconds.

$PaCO_2$ manipulation

Mild changes in $PaCO_2$ will be induced in order to induce small changes in cerebral blood flow. After obtaining baseline measurements volunteers will be asked to increase the minute ventilation by 20% (as measured by end-tidal CO_2 measurement). Patients will be asked to breath normally through a short oral tube using noseclips to prevent air leakage through the nose. The end-tidal CO2 pressure is measured at the end of the tube and continuously displayed on the monitor. After baseline ultrasound values have been obtained, volunteers will be asked to increase the minute ventilation by 20% to decrease cerebral blood flow. Previously, we have shown that an increase of minute ventilation by 20% in patients after cardiac arrest is safe and changes CBF velocity by 15% [6]. Volunteers will be asked to keep end-tidal CO2 pressure stable at 20% above the baseline end-tidal CO2 pressure by visual guidance of the value on the monitor.

4. STUDY POPULATION

4.1 Population (base)

The population consists of a total of 10 young healthy volunteers, between 18-35 years old. Before inclusion, subjects must meet all inclusion criteria and none of the exclusion criteria. Recruitment of healthy volunteers will take place by placement of posters in the medical faculty and several other faculties and locations on the campus of the Radboud University Nijmegen. This method of recruitment has been used in previous studies in our department and has resulted in more than adequate numbers of subjects willing to participate.

4.2 Inclusion criteria

- Healthy men or women of 18-35 years old

4.3 Exclusion criteria

- Hypersensitivity to the active substance(s) or to any of the excipients in SonoVue
- Right-to-left shunt cardiac shunt
- Severe pulmonary hypertension (pulmonary artery pressure >90 mmHg)
- Uncontrolled systemic hypertension
- Pregnancy
- Lactation
- Participation in another clinical trial within 3 months prior to the experimental day.
- History, signs, or symptoms of cardiovascular disease or pulmonary disease
- History, signs or symptoms of neurological disease
- History, signs or symptoms of renal disease
- History of hyperventilation

4.4 Sample size calculation

In this first pilot study we plan to include 10 volunteers. Since this study has an explorative nature, a power calculation is not provided.

5. TREATMENT OF SUBJECTS

Study specific measurements (Figure 1)

Study protocol

CEUS of the brain will be performed unilaterally, at the side with the most optimal temporal window. First the the bolus kinetics method using a high mechanical index (MI) will be performed, followed by a single CEUS bolus measurement of the kidney. Then the flash-replenishment technique of the brain will be performed. Each of the CEUS measurements of the brain is performed 3 times, separated by a 15 minute break to allow the ultrasound contrast agent (UCA) to wash-out from the blood stream. After mild hyperventilation, only the CEUS bolus technique of the brain will be used in a single measurement. All the brain measurements will be performed after assessment of the CBF velocity in the middle cerebral artery using TCD. The single kidney measurement will be performed after assessment of the blood flow velocity in the renal artery using Doppler.

Measurement technique

Bolus kinetics method brain

Flow velocities in the middle cerebral artery will be measured by TCD ipsilaterally to the CEUS measurements. An intravenous injection of 2.5 ml the UCA SonoVue (Bracco Imaging Europe BV, Amsterdam, 8 µL/ml) will be given as a bolus. Simultaneously high mechanical imaging will be performed for 2 minutes (MI>1).

Bolus kinetics method kidney

Flow velocities in the left or right renal artery will be estimated by Doppler, ipsilateral to the renal CEUS measurements. A single intravenous injection of 2.5 ml the UCA SonoVue (Bracco Imaging Europe BV, Amsterdam, 8 µL/ml) will be given as a bolus. Simultaneously high mechanical imaging of the ipsilateral kidney will be performed for 2 minutes (MI>0.5).

Flash-replenishment technique brain

Flow velocities in the middle cerebral artery will be measured by TCD ipsilaterally to the CEUS measurements. The contrast agent SonoVue (Bracco Imaging Europe BV, Amsterdam) will be infused intravenously at a concentration of 8 µL/ml with a speed of 1 ml/min through an intravenous access in the left or right fossa cubiti. Five minutes after the start of UCA infusion a flash-replenishment measurement will be performed by applying (~8) high MI flashes of MI>1, followed by switching to low MI imaging with an MI of 0.17 for ~10 seconds.

$PaCO_2$ manipulation

Mild changes in $PaCO_2$ will be induced in order to induce small changes in cerebral blood flow. After obtaining baseline measurements volunteers will be asked to increase the minute ventilation by 20% (as measured by end-tidal CO_2 measurement). Patients will be asked to breath normally through a short oral tube using noseclips to prevent air leakage through the nose. The end-tidal CO_2 pressure is measured at the end of the tube and continuously displayed on the monitor. After baseline ultrasound values have been obtained, volunteers will be asked to increase the minute ventilation by 20% to decrease cerebral blood flow. Previously, we have shown that an increase of minute ventilation by 20% in patients after cardiac arrest is safe and changes CBF velocity by 15% [6]. Volunteers will be asked to keep end-tidal CO_2 pressure stable at 20% above the baseline end-tidal CO2 pressure by visual guidance of the value on the monitor.

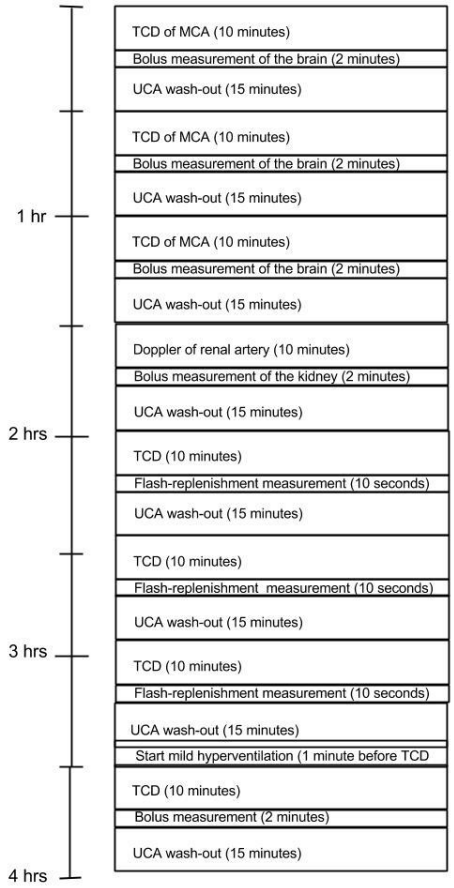

Figure 2: schematic representation of the experiments in time

6. METHODS

6.1 Study parameters/endpoints

6.1.1 Main study parameter/endpoint

Main study parameter is the reproducibility of the CEUS bolus kinetics and the flash-replenishment method. Tests will be performed at baseline by a single investigator, the differences between the subsequent measurements at baseline will be compared (all measurements performed within 90 minutes). A difference between the measurements of more than 10% is considered to imply poor reproducibility. As a control, the reproducibility of measurement of the flow velocity in the ipsilateral middle cerebral artery will be assessed. The investigator performing the test is blinded for the results, as determination of flow is only possible after off-line analysis.

6.1.2 Secondary study parameters/endpoints (if applicable)

Secondary study parameters are

- Correlation between the bolus kinetics approach and the flash-replenishment method of the brain. All measurements will be performed by a single investigator.
- Flow measurements performed with the CEUS bolus of the brain technique will be correlated with transcranial Doppler (at 2 different levels of cerebral blood flow).
- Flow measurements performed with the CEUS bolus technique of the kidney will be correlated with Doppler.

6.2 Randomisation, blinding and treatment allocation

Not applicable

6.3 Study procedures

A schematic overview of the procedure is presented in Figure 2

Procedures

Screening

Subjects will be recruited by posters in the university area. Before inclusion in the study, all procedures will be explained to the subjects, informed consent will be obtained after a minimum of 24 hours.

After inclusion in the study, volunteers will be subjected to a medical examination during the screening visit, which will take place within 4 weeks of the experiment day. A medical history will be obtained including prior engagement in studies, allergic and other adverse reactions during hospital admissions. A physical examination including measurement of blood pressure, heart rate, auscultation of heart and lungs and examination of the abdomen will be performed. In addition, a neurological examination will be performed and the quality of the temporal bone window for insonation will be assessed. Also a 12-lead ECG will be recorded. Subjects are eligible for the study if all tests are normal, if they meet all inclusion and none of the exclusion criteria and if the temporal bone window is accessible for ultrasound.

Experiments

At the day of the measurements, first a standard venous catheter (18 G venflon) will be placed in the left or right fossa cubiti. Subjects will be placed on a bed in a horizontal position with the head in midline and elevated at 30 degrees. Measurements will be performed as depicted in Figure 1.

The first series of measurements are performed while the subject is at baseline under normoventilation.

CEUS measurements

First a transcranial Doppler will be performed and the left or right temporal window will be chosen for insonation (both for the transcranial Doppler and for the CEUS). Next, mean flow velocities of the middle cerebral artery at 50 mm from the temporal bone window will be assessed and documented. Next, an intravenous injection of 2.5 ml the UCA SonoVue (Bracco Imaging Europe BV, Amsterdam, 8 µL/ml) will be given as a bolus. Simultaneously high mechanical imaging will be performed for 2 minutes (MI>1). After a wash-out of 15 minutes the entire procedure is repeated (please see figure 2) for a total of 3 measurements. Then the flow velocities in the left or right renal artery will be estimated by Doppler, ipsilateral to the renal CEUS measurements. A single intravenous injection of 2.5 ml the UCA SonoVue (Bracco Imaging Europe BV, Amsterdam, 8 µL/ml) will be given as a bolus. Simultaneously high mechanical imaging of the ipsilateral kidney will be performed for 2 minutes (MI>0.5).

After this single renal CEUS measurement, the new set of experiments using the flash-replenishment method will be started after a 15 minute wash-out period.

Mean flow velocities of the middle cerebral artery at 50 mm from the temporal bone window will be assessed and documented. The contrast agent SonoVue (Bracco Imaging Europe BV, Amsterdam) will be infused intravenously at a concentration of 8 µL/ml with a speed of 1 ml/min through an intravenous access in the left or right fossa cubiti. Five minutes after the start of UCA infusion a flash-replenishment measurement will be performed by applying (~8) high MI flashes of MI>1, followed by switching to low MI imaging with an MI of 0.17 for ~10 seconds. The intravenous infusion will be stopped immediately after the recording period of 10 seconds. After a wash-out of 15 minutes the entire procedure is repeated (please see figure 2) for a total of 3 measurements.

After the final flash-replenishment method a 15 minute wash-out period will follow.

$PaCO_2$ manipulation

After obtaining all baseline measurements volunteers will be asked to increase the minute ventilation by 20% (as measured by end-tidal CO_2 measurement). Patients will be asked to breath normally through a short oral tube using noseclips to prevent air leakage trough the nose. The end-tidal CO_2 pressure is measured at the end of the tube and continuously displayed on the monitor. After baseline ultrasound values have been obtained, volunteers will be asked to increase the minute ventilation by 20% to decrease cerebral blood flow. Previously, we have shown that an increase of minute ventilation by 20% in patients after cardiac arrest is safe and changes CBF velocity by 15% [6]. Volunteers will be asked to keep end-tidal CO_2 pressure stable at 20% above the baseline end-tidal CO2 pressure by visual guidance of the value on the monitor.

Mean flow velocities of the middle cerebral artery at 50 mm from the temporal bone window will be assessed and documented. Next, an intravenous injection of 2.5 ml the UCA SonoVue (Bracco Imaging Europe BV, Amsterdam, 8 µL/ml) will be given as a bolus. Simultaneously high mechanical imaging will be performed for 2 minutes (MI>1). The measurements will end after a single transcranial Doppler and a single CEUS bolus kinetics measurement.

6.4 Withdrawal of individual subjects

Subjects can leave the study at any time for any reason if they wish to do so without any consequences. The investigator can decide to withdraw a subject from the study for urgent medical reasons.

6.4.1 Specific criteria for withdrawal (if applicable)

Not applicable

6.5 Replacement of individual subjects after withdrawal

After withdrawal or exclusion of a subject, the subject will be replaced in order to maintain an adequate sample size of the study. A maximum of 5 subjects will be replaced.

6.6 Follow-up of subjects withdrawn from treatment

After withdrawal or exclusion of a subject, subjects are monitored medically if necessary for the time of the study. For all subjects who are prematurely withdrawn, the reason will be documented carefully.

6.7 Premature termination of the study

The coordinating investigator has the right to discontinue the clinical study at any time for medical or procedural reasons.

7. STATISTICAL ANALYSIS

7.1 Primary study parameter(s)

Each bolus measurement results in one time-intensity curve with the perfusion parameters TTP, PI, FWHM, and AUC. The reproducibility of bolus kinetics parameters TTP, PI, FWHM, and AUC will be determined by calculation of the % change from the mean of the 3 individual measurements. A change of > 10% will be considered to indicate poor reproducibility.

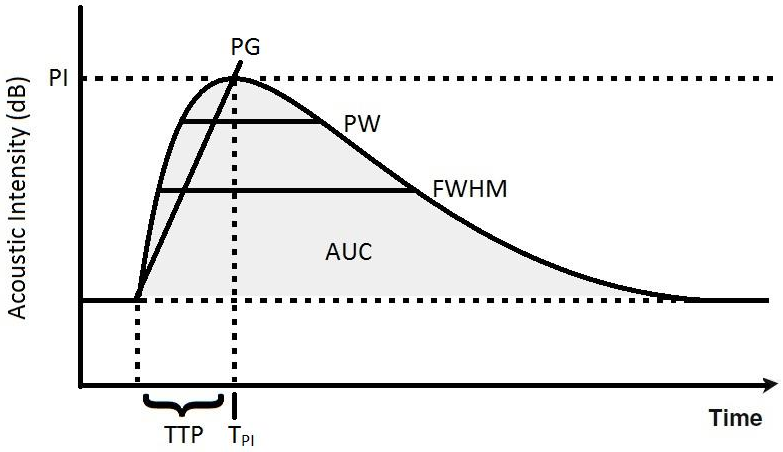

Figure 3: Time intensity curve of the bolus kinetic CEUS approach, with time-to-peak (TTP), time-to-peak intensity (T_{PI}), peak intensity (PI), peak width (PW, full width at 90% of the maximum intensity), full width at half of the maximum intensity increase (FWHM), area under the curve (AUC) and positive gradient (PG, slope of the wash-in phase).

The flash-replenishment perfusion parameters (A, β and A×β) are determined from the time-intensity-curves (TIC) retrieved from continuous measurement of the intensity response of the ultrasound. Each flash-replenishment measurement therefore results in one TIC with one responding A, β and A×β value. The reproducibility of the flash-replenishment perfusion parameters A, β and A×β will be determined by determination of the % change from the mean of the 3 individual measurements. A change of > 10% will be considered to indicate poor reproducibility.

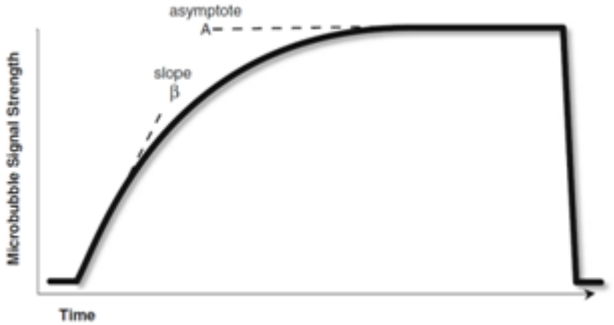

Figure 4: Time intensity curve flash-replenishment perfusion. Intensity curve of the refill kinetics, resulting from high MI pulses followed by low MI pulses.

The TCD and Doppler recordings will generate a quantitative variable for the blood flow velocity. Similar to the CEUS, a mean flow velocity from the 3 measurements will be determined and the percentage change from the mean value will be calculated.

7.2 Secondary study parameter(s)

- The correlation between the high MI bolus perfusion parameters (TTP, PI, FWHM, AUC) of the brain and the flash-replenishment perfusion parameters (A, β and A×β). will be determined by linear regression analysis with the calculation of the Pearson's correlation coefficient. The correlation will be calculated using the data obtained during baseline and hyperventilation. A p value < 0.05 is considered to indicate statistical significance.
- The correlation between the high MI bolus perfusion parameters (TTP, PI, FWHM, AUC) of the brain and the mean flow velocity in the middle cerebral artery will be determined by linear regression analysis with the calculation of the Pearson's correlation coefficient. The correlation will be calculated using the data obtained during baseline and hyperventilation. A p value < 0.05 is considered to indicate statistical significance.
- The correlation between the high MI bolus perfusion parameters (TTP, PI, FWHM, AUC) of the kidney and the mean flow velocity in the renal artery will be determined by linear regression analysis with the calculation of the Pearson's correlation coefficient. The correlation will be calculated using the data obtained during baseline and hyperventilation. A p value < 0.05 is considered to indicate statistical significance.

REFERENCES

1. Bouzat P, Sala N, Payen JF, Oddo M. Beyond intracranial pressure: optimization of cerebral blood flow, oxygen, and substrate delivery after traumatic brain injury. Annals of intensive care 2013;3:23.
2. Maas AI, Stocchetti N, Bullock R. Moderate and severe traumatic brain injury in adults. The Lancet Neurology 2008;7:728-41.
3. Dagal A, Lam AM. Cerebral blood flow and the injured brain: how should we monitor and manipulate it? Current opinion in anaesthesiology 2011;24:131-7.
4. Kang ST, Yeh CK. Ultrasound microbubble contrast agents for diagnostic and therapeutic applications: current status and future design. Chang Gung medical journal 2012;35:125-39.
5. Eyding J, Krogias C, Meves S, Przuntek H, Postert T. Quantitative ultrasonographic evaluation of cerebral perfusion in acute stroke is possible. Stroke; a journal of cerebral circulation 2004;35:2432-3; author reply 3.
6. Bisschops LL, Hoedemaekers CW, Simons KS, van der Hoeven JG. Preserved metabolic coupling and cerebrovascular reactivity during mild hypothermia after cardiac arrest. Critical care medicine 2010;38:1542-7.
7. World Medical A. World Medical Association Declaration of Helsinki: ethical principles for medical research involving human subjects. Jama 2013;310:2191-4.
8. Piscaglia F, Bolondi L, Italian Society for Ultrasound in M, Biology Study Group on Ultrasound Contrast A. The safety of Sonovue in abdominal applications: retrospective analysis of 23188 investigations. Ultrasound in medicine & biology 2006;32:1369-75.
9. de Goeij M, van Eijk LT, Vanelderen P, et al. Systemic inflammation decreases pain threshold in humans in vivo. PloS one 2013;8:e84159.
10. Kox M, Ramakers BP, Pompe JC, van der Hoeven JG, Hoedemaekers CW, Pickkers P. Interplay between the acute inflammatory response and heart rate variability in healthy human volunteers. Shock 2011;36:115-20.
11. Kox M, van Eijk LT, Zwaag J, et al. Voluntary activation of the sympathetic nervous system and attenuation of the innate immune response in humans. Proceedings of the National Academy of Sciences of the United States of America 2014;111:7379-84.
12. Kox M, Stoffels M, Smeekens SP, et al. The influence of concentration/meditation on autonomic nervous system activity and the innate immune response: a case study. Psychosomatic medicine 2012;74:489-94.
13. Kox M, Vrouwenvelder MQ, Pompe JC, van der Hoeven JG, Pickkers P, Hoedemaekers CW. The effects of brain injury on heart rate variability and the innate immune response in critically ill patients. Journal of neurotrauma 2012;29:747-55.

Appendix III:

Additional results

Table 11: PSV and CBFVmean values of the individual duplex measurements with the corresponding mean, standard deviation (SD), coefficient of the variation (CV) and the parameters during hyperventilation expressed in percentage of the mean baseline.

Subject 1	**PSV**	**$CBFV_{mean}$**	**Subject 1**	**PSV**	**$CBFV_{mean}$**
Baseline 1	119,0	72	Mean Baseline	112,3	65,3
Baseline 2	117,0	68,0	SD Baseline	9,9	8,3
Baseline 3	101,0	56,0	CV (% of mean)	8,8	0,1
Hyperventilation	104,0	54,0	hyper (% of mean baseline)	92,6	82,7
Subject 2	**PSV**	**$CBFV_{mean}$**	**Subject 2**	**PSV**	**$CBFV_{mean}$**
Baseline 1	103,0	65,0	Mean Baseline	101,2	62,7
Baseline 2	98,7	61,0	SD Baseline	2,3	2,1
Baseline 3	102,0	62,0	CV (% of mean)	2,2	3,3
Hyperventilation	91,2	54,0	hyper (% of mean baseline)	90,1	86,2
Subject 3	**PSV**	**$CBFV_{mean}$**	**Subject 3**	**PSV**	**$CBFV_{mean}$**
Baseline 1	95,9	60,0	Mean Baseline	105,0	66,0
Baseline 2	117,0	73,0	SD Baseline	10,9	6,6
Baseline 3	102,0	65,0	CV (% of mean)	10,3	9,9
Hyperventilation	80,9	50,0	hyper (% of mean baseline)	77,1	75,8
Subject 4	**PSV**	**$CBFV_{mean}$**	**Subject 4**	**PSV**	**$CBFV_{mean}$**
Baseline 1	115,0	62,0	Mean Baseline	117,3	67,7
Baseline 2	119,0	71,0	SD Baseline	2,1	4,9
Baseline 3	118,0	70,0	CV (% of mean)	1,8	7,3
Hyperventilation	106,0	52,0	hyper (% of mean baseline)	90,3	76,8
Subject 5	**PSV**	**$CBFV_{mean}$**	**Subject 5**	**PSV**	**$CBFV_{mean}$**
Baseline 1	81,8	47,0	Mean Baseline	78,5	45,7
Baseline 2	67,1	42,0	SD Baseline	10,1	3,2
Baseline 3	86,5	48,0	CV (% of mean)	12,9	7,0
Hyperventilation	81,8	50,0	hyper (% of mean baseline)	104,2	109,5
Subject 6	**PSV**	**$CBFV_{mean}$**	**Subject 6**	**PSV**	**$CBFV_{mean}$**
Baseline 1	99,6	58,0	Mean Baseline	102,5	61,3
Baseline 2	102,0	58,0	SD Baseline	3,2	5,8
Baseline 3	106,0	68,0	CV (% of mean)	3,2	9,4
Hyperventilation	87,4	51,0	hyper (% of mean baseline)	85,2	83,2
Subject 7	**PSV**	**$CBFV_{mean}$**	**Subject 7**	**PSV**	**$CBFV_{mean}$**
Baseline 1	119,0	70,0	Mean Baseline	112,7	66,0
Baseline 2	102,0	60,0	SD Baseline	9,3	5,3
Baseline 3	117,0	68,0	CV (% of mean)	8,2	8,0
Hyperventilation	93,0	48,0	hyper (% of mean baseline)	82,5	72,7
Subject 8	**PSV**	**$CBFV_{mean}$**	**Subject 8**	**PSV**	**$CBFV_{mean}$**
Baseline 1	115,0	70,0	Mean Baseline	105,6	59,3
Baseline 2	106,0	51,0	SD Baseline	9,6	9,7
Baseline 3	95,9	57,0	CV (% of mean)	9,0	16,4
Hyperventilation	93,1	45,0	hyper (% of mean baseline)	88,1	75,8
Subject 9	**PSV**	**$CBFV_{mean}$**	**Subject 9**	**PSV**	**$CBFV_{mean}$**
Baseline 1	105,0	61,0	Mean Baseline	102,3	61,7
Baseline 2	101,0	61,0	SD Baseline	2,3	1,2
Baseline 3	101,0	63,0	CV (% of mean)	2,3	1,9
Hyperventilation	74,0	45,0	hyper (% of mean baseline)	72,3	73,0
			Total	**PSV**	**$CBFV_{mean}$**
			Mean Baseline	104,2	61,7
			SD Baseline	4,0	2,8
			CV (% of mean)	6,5	7,0
			hyper (% of mean baseline)	87,0	81,7

Table 12: CEUS parameter values in the $ROI_{MCAipsi}$. The mean, standard deviation and the coefficient of variation (CV) as percentage of the mean are shown. Furthermore the parameters values of the hyperventilation measurements are expressed in percentage of the mean baseline.

Subject 1	**PI**	**TTP**	**TPI**	**AUC**	**PW**	**FWHM**
Mean Baseline	27,1	8,1	17,1	11477,9	9,5	45,6
SD Baseline	0,3	1,2	0,8	320,4	0,2	2,2
CV (% of mean)	0,9	14,6	4,5	2,8	1,9	4,8
hyper (% of mean baseline)	97,4	60,8	40,4	86,4	62,0	63,4
Subject 2	**PI**	**TTP**	**TPI**	**AUC**	**PW**	**FWHM**
Mean Baseline	26,3	3,8	12,4	11018,3	14,1	39,3
SD Baseline	4,3	0,3	0,4	3328,4	13,6	16,4
CV (% of mean)	16,3	8,3	3,4	30,2	96,2	41,9
hyper (% of mean baseline)	100,9	179,6	106,5	40,4	22,4	27,8
Subject 3	**PI**	**TTP**	**TPI**	**AUC**	**PW**	**FWHM**
Mean Baseline	19,3	5,0	12,6	12955,7	18,3	44,3
SD Baseline	13,3	1,8	3,6	2522,8	11,3	8,8
CV (% of mean)	68,9	36,9	28,5	19,5	61,8	19,8
hyper (% of mean baseline)	136,4	371,7	224,2	101,8	145,7	102,2
Subject 4	**PI**	**TTP**	**TPI**	**AUC**	**PW**	**FWHM**
Mean Baseline	25,1	10,4	17,6	9092,7	8,0	32,0
SD Baseline	4,2	9,6	7,9	4522,6	3,9	17,0
CV (% of mean)	16,8	92,5	45,2	49,7	48,6	53,2
hyper (% of mean baseline)	91,6	38,6	53,6	53,8	39,7	42,2
Subject 5	**PI**	**TTP**	**TPI**	**AUC**	**PW**	**FWHM**
Mean Baseline	26,9	7,1	14,4	11617,1	10,1	40,6
SD Baseline	0,9	1,5	2,3	1151,2	4,4	6,1
CV (% of mean)	3,4	21,0	15,8	9,9	43,0	15,1
hyper (% of mean baseline)	88,7	100,4	78,2	16,5	21,4	15,8
Subject 6	**PI**	**TTP**	**TPI**	**AUC**	**PW**	**FWHM**
Mean Baseline	25,0	6,0	14,3	9436,5	6,8	33,3
SD Baseline	3,6	0,1	0,5	2257,1	1,3	8,4
CV (% of mean)	14,5	1,6	3,6	23,9	19,6	25,2
hyper (% of mean baseline)	87,3	69,8	91,3	69,4	66,1	64,6
Subject 7	**PI**	**TTP**	**TPI**	**AUC**	**PW**	**FWHM**
Mean Baseline	25,9	6,7	15,5	10060,9	7,6	36,2
SD Baseline	1,1	1,4	1,5	83,7	1,1	5,3
CV (% of mean)	4,2	20,2	9,6	0,8	14,6	14,6
hyper (% of mean baseline)	62,4	120,2	89,4	29,9	48,5	33,6
Subject 8	**PI**	**TTP**	**TPI**	**AUC**	**PW**	**FWHM**
Mean Baseline	21,5	3,4	12,3	7719,1	7,3	30,7
SD Baseline	3,0	0,8	0,8	4460,1	5,5	19,7
CV (% of mean)	14,1	23,0	6,4	57,8	75,9	64,1
hyper (% of mean baseline)	81,6	142,7	83,5	53,0	47,9	48,3
Subject 9	**PI**	**TTP**	**TPI**	**AUC**	**PW**	**FWHM**
Mean Baseline	24,2	5,0	14,0	11827,2	15,6	48,8
SD Baseline	2,5	0,4	0,9	731,6	6,0	0,7
CV (% of mean)	10,4	8,7	6,8	6,2	38,4	1,4
hyper (% of mean baseline)	56,0	168,3	135,4	31,3	32,0	38,4
Total	**PI**	**TTP**	**TPI**	**AUC**	**PW**	**FWHM**
Mean Baseline	24,6	6,2	14,5	10578,4	10,8	39,0
SD Baseline	3,9	2,9	2,4	1700,4	4,6	6,8
CV (% of mean)	16,6	25,2	13,7	22,3	44,4	26,7
hyper (% of mean baseline)	89,2	139,1	100,3	53,6	54,0	48,5

Table 13: CEUS parameter values in the $ROI_{ANTcontr}$. The mean, standard deviation and the coefficient of variation (CV) as percentage of the mean are shown. Furthermore the parameters values of the hyperventilation measurements are expressed in percentage of the mean baseline.

Subject 1	**PI**	**TTP**	**TPI**	**AUC**	**PW**	**FWHM**
Mean Baseline	2,6	8,9	20,4	296,0	2,7	8,0
SD Baseline	1,6	1,2	0,3	180,8	0,2	0,3
CV (% of mean)	59,6	13,2	1,4	61,1	6,5	3,7
hyper (% of mean baseline)	65,5	68,2	53,6	60,9	86,2	93,3
Subject 2	**PI**	**TTP**	**TPI**	**AUC**	**PW**	**FWHM**
Mean Baseline	2,1	7,5	16,9	299,0	2,9	9,2
SD Baseline	1,3	0,6	0,7	204,7	0,2	0,9
CV (% of mean)	62,7	8,7	4,2	68,5	6,1	9,6
hyper (% of mean baseline)	16,0	88,1	99,3	6,7	58,3	51,8
Subject 3	**PI**	**TTP**	**TPI**	**AUC**	**PW**	**FWHM**
Mean Baseline	2,0	6,1	13,7	218,3	2,1	6,8
SD Baseline	1,2	2,4	2,4	172,2	0,6	1,7
CV (% of mean)	62,1	39,6	17,2	78,9	26,9	25,2
hyper (% of mean baseline)	119,3	112,7	136,0	318,4	240,8	314,8
Subject 4	**PI**	**TTP**	**TPI**	**AUC**	**PW**	**FWHM**
Mean Baseline	2,2	9,1	18,6	305,3	2,8	8,2
SD Baseline	2,3	1,3	2,5	387,8	0,8	2,6
CV (% of mean)	104,2	14,3	13,7	127,0	27,3	31,2
hyper (% of mean baseline)	5,9	35,8	65,4	1,2	30,3	32,7
Subject 5	**PI**	**TTP**	**TPI**	**AUC**	**PW**	**FWHM**
Mean Baseline	2,3	7,2	17,0	390,6	2,9	9,6
SD Baseline	1,5	2,1	2,5	351,1	1,2	4,1
CV (% of mean)	62,0	28,6	14,4	89,9	39,7	43,1
hyper (% of mean baseline)	44,1	61,6	72,1	13,1	42,5	41,7
Subject 6	**PI**	**TTP**	**TPI**	**AUC**	**PW**	**FWHM**
Mean Baseline	2,0	6,6	16,7	222,9	2,5	7,9
SD Baseline	0,8	0,8	1,3	65,4	0,1	0,6
CV (% of mean)	39,3	11,4	7,7	29,4	5,0	7,4
hyper (% of mean baseline)	44,4	116,0	100,7	33,8	85,7	78,9
Subject 7	**PI**	**TTP**	**TPI**	**AUC**	**PW**	**FWHM**
Mean Baseline	2,6	9,7	19,4	311,5	2,8	8,3
SD Baseline	1,1	0,7	1,3	179,5	0,4	1,3
CV (% of mean)	40,3	7,2	6,5	57,6	14,7	15,1
hyper (% of mean baseline)	20,9	68,6	77,6	10,1	58,8	56,2
Subject 8	**PI**	**TTP**	**TPI**	**AUC**	**PW**	**FWHM**
Mean Baseline	3,3	9,9	17,6	426,4	2,9	8,7
SD Baseline	1,2	2,3	1,8	256,1	0,8	2,1
CV (% of mean)	34,9	23,1	10,4	60,1	26,2	24,6
hyper (% of mean baseline)	66,3	70,4	74,9	67,7	97,1	102,9
Subject 9	**PI**	**TTP**	**TPI**	**AUC**	**PW**	**FWHM**
Mean Baseline	3,8	8,3	18,0	690,8	3,8	12,6
SD Baseline	0,4	2,1	2,1	88,1	1,1	3,5
CV (% of mean)	11,9	25,9	11,4	12,8	29,1	28,1
hyper (% of mean baseline)	14,3	14,1	99,5	8,6	33,3	52,3
Total	**PI**	**TTP**	**TPI**	**AUC**	**PW**	**FWHM**
Mean Baseline	2,5	8,1	17,6	351,2	2,8	8,8
SD Baseline	0,5	0,7	0,8	107,6	0,4	1,3
CV (% of mean)	53,0	19,1	9,7	65,0	20,2	20,9
hyper (% of mean baseline)	44,1	70,6	86,6	57,8	81,4	91,6

Table 14: CEUS parameter values in the $ROI_{POSTcontr}$. The mean, standard deviation and the coefficient of variation (CV) as percentage of the mean are shown. Furthermore the parameters values of the hyperventilation measurements are expressed in percentage of the mean baseline.

Subject 1	**PI**	**TTP**	**TPI**	**AUC**	**PW**	**FWHM**
Mean Baseline	1,5	11,0	23,2	230,1	3,4	10,2
SD Baseline	0,7	3,1	1,6	156,6	0,9	2,5
CV (% of mean)	47,6	27,9	7,1	68,0	26,2	24,8
hyper (% of mean baseline)	153,3	71,2	46,0	62,4	61,7	58,0
Subject 2	**PI**	**TTP**	**TPI**	**AUC**	**PW**	**FWHM**
Mean Baseline	3,0	7,9	17,7	599,8	3,6	13,1
SD Baseline	2,0	2,2	2,1	456,2	0,6	4,9
CV (% of mean)	66,8	27,4	11,8	76,1	16,6	37,8
hyper (% of mean baseline)	13,4	70,3	89,0	4,9	48,1	39,6
Subject 3	**PI**	**TTP**	**TPI**	**AUC**	**PW**	**FWHM**
Mean Baseline	2,0	5,9	13,9	249,7	2,3	7,6
SD Baseline	1,1	2,3	2,3	194,2	0,7	2,3
CV (% of mean)	52,5	39,7	16,3	77,8	31,1	29,5
hyper (% of mean baseline)	115,0	160,6	139,2	189,9	175,0	177,8
Subject 4	**PI**	**TTP**	**TPI**	**AUC**	**PW**	**FWHM**
Mean Baseline	3,5	6,5	18,1	618,9	3,3	11,6
SD Baseline	0,1	2,6	2,5	202,4	1,2	3,9
CV (% of mean)	2,1	40,3	13,8	32,7	35,6	33,4
hyper (% of mean baseline)	7,6	19,1	65,3	1,6	17,9	22,2
Subject 5	**PI**	**TTP**	**TPI**	**AUC**	**PW**	**FWHM**
Mean Baseline	3,9	10,6	19,9	1018,8	4,7	16,3
SD Baseline	2,8	2,3	1,9	1046,7	1,7	8,1
CV (% of mean)	72,7	22,0	9,6	102,7	35,5	49,9
hyper (% of mean baseline)	10,2	41,5	67,3	3,4	37,3	36,3
Subject 6	**PI**	**TTP**	**TPI**	**AUC**	**PW**	**FWHM**
Mean Baseline	1,2	7,3	18,3	150,9	2,3	7,2
SD Baseline	1,3	2,2	1,5	194,3	0,8	2,2
CV (% of mean)	108,2	30,2	8,1	128,8	34,1	31,1
hyper (% of mean baseline)	98,7	73,3	91,3	121,5	117,9	139,0
Subject 7	**PI**	**TTP**	**TPI**	**AUC**	**PW**	**FWHM**
Mean Baseline	2,3	7,1	18,6	264,6	2,6	7,9
SD Baseline	0,3	0,8	1,4	38,0	0,2	0,3
CV (% of mean)	11,9	11,2	7,4	14,3	6,8	4,2
hyper (% of mean baseline)	11,6	88,2	84,2	5,7	71,7	66,1
Subject 8	**PI**	**TTP**	**TPI**	**AUC**	**PW**	**FWHM**
Mean Baseline	4,0	6,8	17,8	721,5	3,3	11,2
SD Baseline	1,9	1,1	0,9	413,1	0,8	3,2
CV (% of mean)	45,9	16,8	5,0	57,3	23,5	28,6
hyper (% of mean baseline)	41,8	156,1	96,7	48,9	135,9	127,0
Subject 9	**PI**	**TTP**	**TPI**	**AUC**	**PW**	**FWHM**
Mean Baseline	4,6	7,7	17,8	1225,5	4,8	18,6
SD Baseline	0,6	0,8	1,5	255,5	0,6	2,4
CV (% of mean)	13,6	10,0	8,2	20,8	11,9	12,8
hyper (% of mean baseline)	7,4	154,3	132,4	5,1	86,2	68,6
Total	**PI**	**TTP**	**TPI**	**AUC**	**PW**	**FWHM**
Mean Baseline	2,9	7,9	18,4	564,4	3,4	11,5
SD Baseline	0,9	0,8	0,5	298,0	0,4	2,2
CV (% of mean)	46,8	25,0	9,7	64,3	24,6	28,0
hyper (% of mean baseline)	51,0	92,7	90,2	49,3	83,5	81,6

Table 15: CEUS parameter values in the $ROI_{POSTipsi}$. The mean, standard deviation and the coefficient of variation (CV) as percentage of the mean are shown. Furthermore the parameters values of the hyperventilation measurements are expressed in percentage of the mean baseline.

Subject 1	**PI**	**TTP**	**TPI**	**AUC**	**PW**	**FWHM**
Mean Baseline	3,4	11,0	23,2	230,1	3,4	10,2
SD Baseline	1,8	3,1	1,6	156,6	0,9	2,5
CV (% of mean)	54,7	27,9	7,1	68,0	26,2	24,8
hyper (% of mean baseline)	34,8	71,2	46,0	62,4	61,7	58,0
Subject 2	**PI**	**TTP**	**TPI**	**AUC**	**PW**	**FWHM**
Mean Baseline	2,6	7,9	17,7	599,8	3,6	13,1
SD Baseline	1,8	2,2	2,1	456,2	0,6	4,9
CV (% of mean)	68,1	27,4	11,8	76,1	16,6	37,8
hyper (% of mean baseline)	29,4	70,3	89,0	4,9	48,1	39,6
Subject 3	**PI**	**TTP**	**TPI**	**AUC**	**PW**	**FWHM**
Mean Baseline	4,3	5,9	13,9	249,7	2,3	7,6
SD Baseline	0,7	2,3	2,3	194,2	0,7	2,3
CV (% of mean)	17,2	39,7	16,3	77,8	31,1	29,5
hyper (% of mean baseline)	85,1	160,6	139,2	189,9	175,0	177,8
Subject 4	**PI**	**TTP**	**TPI**	**AUC**	**PW**	**FWHM**
Mean Baseline	2,6	6,5	18,1	618,9	3,3	11,6
SD Baseline	0,8	2,6	2,5	202,4	1,2	3,9
CV (% of mean)	31,6	40,3	13,8	32,7	35,6	33,4
hyper (% of mean baseline)	50,4	19,1	65,3	1,6	17,9	22,2
Subject 5	**PI**	**TTP**	**TPI**	**AUC**	**PW**	**FWHM**
Mean Baseline	2,6	10,6	19,9	1018,8	4,7	16,3
SD Baseline	3,0	2,3	1,9	1046,7	1,7	8,1
CV (% of mean)	118,4	22,0	9,6	102,7	35,5	49,9
hyper (% of mean baseline)	8,2	41,5	67,3	3,4	37,3	36,3
Subject 6	**PI**	**TTP**	**TPI**	**AUC**	**PW**	**FWHM**
Mean Baseline	1,6	7,3	18,3	150,9	2,3	7,2
SD Baseline	0,9	2,2	1,5	194,3	0,8	2,2
CV (% of mean)	57,6	30,2	8,1	128,8	34,1	31,1
hyper (% of mean baseline)	155,3	73,3	91,3	121,5	117,9	139,0
Subject 7	**PI**	**TTP**	**TPI**	**AUC**	**PW**	**FWHM**
Mean Baseline	3,4	7,1	18,6	264,6	2,6	7,9
SD Baseline	1,1	0,8	1,4	38,0	0,2	0,3
CV (% of mean)	32,4	11,2	7,4	14,3	6,8	4,2
hyper (% of mean baseline)	9,6	88,2	84,2	5,7	71,7	66,1
Subject 8	**PI**	**TTP**	**TPI**	**AUC**	**PW**	**FWHM**
Mean Baseline	1,8	6,8	17,8	721,5	3,3	11,2
SD Baseline	0,6	1,1	0,9	413,1	0,8	3,2
CV (% of mean)	36,9	16,8	5,0	57,3	23,5	28,6
hyper (% of mean baseline)	31,7	156,1	96,7	48,9	135,9	127,0
Subject 9	**PI**	**TTP**	**TPI**	**AUC**	**PW**	**FWHM**
Mean Baseline	3,0	7,7	17,8	1225,5	4,8	18,6
SD Baseline	1,6	0,8	1,5	255,5	0,6	2,4
CV (% of mean)	53,7	10,0	8,2	20,8	11,9	12,8
hyper (% of mean baseline)	11,4	154,3	132,4	5,1	86,2	68,6
Total	**PI**	**TTP**	**TPI**	**AUC**	**PW**	**FWHM**
Mean Baseline	2,8	7,9	18,4	564,4	3,4	11,5
SD Baseline	0,8	0,8	0,5	298,0	0,4	2,2
CV (% of mean)	52,3	25,0	9,7	64,3	24,6	28,0
hyper (% of mean baseline)	46,2	92,7	90,2	49,3	83,5	81,6

Table 16: Pearson's correlation coefficient of the PSV and the CEUS parameters in the $ROI_{MCAipsi}$.

$ROI_{MCAipsi}$		PI	TTP	TPI	AUC	PW	FWHM
Subject 2 PSV	Pearson Correlation	-,150	-,980*	-,928	,515	,130	,601
	Sig. (2-tailed)	,850	,020	,072	,485	,870	,399
Subject 3 PSV	Pearson Correlation	-,401	-,901	-,868	,515	-,677	-,346
	Sig. (2-tailed)	,599	,099	,132	,485	,323	,654
Subject 4 PSV	Pearson Correlation	,602	,038	,211	,734	,677	,729
	Sig. (2-tailed)	,398	,962	,789	,266	,323	,271
Subject 5 PSV	Pearson Correlation	,956*	-,076	,659	,956*	,754	,930
	Sig. (2-tailed)	,044	,924	,341	,044	,246	,070
Subject 6 PSV	Pearson Correlation	,739	,944	,948	,850	,907	,858
	Sig. (2-tailed)	,261	,056	,052	,150	,093	,142
Subject 7 PSV	Pearson Correlation	,891	-,616	,529	,945	,894	,948
	Sig. (2-tailed)	,109	,384	,471	,055	,106	,052
Subject 8 PSV	Pearson Correlation	,316	-,535	,808	,122	,050	,131
	Sig. (2-tailed)	,684	,465	,192	,878	,950	,869
Subject 9 PSV	Pearson Correlation	,988*	-,986*	-,998**	,976*	,502	,950
	Sig. (2-tailed)	,012	,014	,002	,024	,498	,050

*. Correlation is significant at the 0.05 level (2-tailed); **. Correlation is significant at the 0.01 level (2-tailed).

Table 17: Pearson's correlation coefficient of the PSV and the CEUS parameters in the $ROI_{ANTcontr}$.

$ROI_{ANTcontr}$		PI	TTP	TPI	AUC	PW	FWHM
Subject 2 PSV	Pearson Correlation	,388	,879	,418	,377	,855	,799
	Sig. (2-tailed)	,612	,121	,582	,623	,145	,201
Subject 3 PSV	Pearson Correlation	-,419	-,421	-,878	-,948	-,999**	-,980*
	Sig. (2-tailed)	,581	,579	,122	,052	,001	,020
Subject 4 PSV	Pearson Correlation	,525	,798	,609	,476	,750	,724
	Sig. (2-tailed)	,475	,202	,391	,524	,250	,276
Subject 5 PSV	Pearson Correlation	,367	,512	,699	,444	,560	,534
	Sig. (2-tailed)	,633	,488	,301	,556	,440	,466
Subject 6 PSV	Pearson Correlation	,718	-,390	,293	,874	,874	,832
	Sig. (2-tailed)	,282	,610	,707	,126	,126	,168
Subject 7 PSV	Pearson Correlation	,514	,784	,793	,400	,605	,657
	Sig. (2-tailed)	,486	,216	,207	,600	,395	,343
Subject 8 PSV	Pearson Correlation	,218	,329	,606	-,025	-,214	-,404
	Sig. (2-tailed)	,782	,671	,394	,975	,786	,596
Subject 9 PSV	Pearson Correlation	,989*	,687	-,299	,846	,565	,440
	Sig. (2-tailed)	,011	,313	,701	,154	,435	,560

*. Correlation is significant at the 0.05 level (2-tailed); **. Correlation is significant at the 0.01 level (2-tailed).

Table 18: Pearson's correlation coefficient of the PSV and the CEUS parameters in the $ROI_{POSTcontr}$.

$ROI_{POSTcontr}$		PI	TTP	TPI	AUC	PW	FWHM
Subject 2 PSV	Pearson Correlation	,439	,805	,745	,325	,682	-,212
	Sig. (2-tailed)	,561	,195	,255	,675	,318	,788
Subject 3 PSV	Pearson Correlation	-,463	-,750	-,898	-,823	-,920	,418
	Sig. (2-tailed)	,537	,250	,102	,177	,080	,582
Subject 4 PSV	Pearson Correlation	,921	,539	,647	,723	,614	-,957*
	Sig. (2-tailed)	,079	,461	,353	,277	,386	,043
Subject 5 PSV	Pearson Correlation	,555	,628	,765	,484	,624	,651
	Sig. (2-tailed)	,445	,372	,235	,516	,376	,349
Subject 6 PSV	Pearson Correlation	,224	,714	,800	,128	-,096	,565
	Sig. (2-tailed)	,776	,286	,200	,872	,904	,435
Subject 7 PSV	Pearson Correlation	,903	,211	,651	,892	,734	-,412
	Sig. (2-tailed)	,097	,789	,349	,108	,266	,588
Subject 8 PSV	Pearson Correlation	,335	-,993**	,183	,239	-,743	,869
	Sig. (2-tailed)	,665	,007	,817	,761	,257	,131
Subject 9 PSV	Pearson Correlation	,829	-,975*	-,989*	,777	,351	,654
	Sig. (2-tailed)	,171	,025	,011	,223	,649	,346

*. Correlation is significant at the 0.05 level (2-tailed); **. Correlation is significant at the 0.01 level (2-tailed).

Table 19: Pearson's correlation coefficient of the CBFVmean and the CEUS parameters in the $ROI_{POSTipsi}$.

$ROI_{POSTipsi}$		PI	TTP	PW	AUC	PW	FWHM
Subject 2 PSV	Pearson Correlation	,805	,805	,745	,325	,682	,418
	Sig. (2-tailed)	,195	,195	,255	,675	,318	,582
Subject 3 PSV	Pearson Correlation	-,750	-,750	-,898	-,823	-,920	-,957*
	Sig. (2-tailed)	,250	,250	,102	,177	,080	,043
Subject 4 PSV	Pearson Correlation	,539	,539	,647	,723	,614	,651
	Sig. (2-tailed)	,461	,461	,353	,277	,386	,349
Subject 5 PSV	Pearson Correlation	,628	,628	,765	,484	,624	,565
	Sig. (2-tailed)	,372	,372	,235	,516	,376	,435
Subject 6 PSV	Pearson Correlation	,714	,714	,800	,128	-,096	-,412
	Sig. (2-tailed)	,286	,286	,200	,872	,904	,588
Subject 7 PSV	Pearson Correlation	,211	,211	,651	,892	,734	,869
	Sig. (2-tailed)	,789	,789	,349	,108	,266	,131
Subject 8 PSV	Pearson Correlation	-,993**	-,993**	,183	,239	-,743	-,546
	Sig. (2-tailed)	,007	,007	,817	,761	,257	,454
Subject 9 PSV	Pearson Correlation	-,975*	-,975*	-,989*	,777	,351	,654
	Sig. (2-tailed)	,025	,025	,011	,223	,649	,346

*. Correlation is significant at the 0.05 level (2-tailed); **. Correlation is significant at the 0.01 level (2-tailed).

Appendix IV

Systematic Review

The potential of contrast enhanced ultrasound as a bedside monitoring technique of the cerebral blood flow at the intensive care unit

[1,2]E.J. Vinke, [2]C.H. Slump, [3]C.L. de Korte and [1]C.W.E. Hoedemaekers

[1]Department of Intensive Care, Radboud University Medical Centre, Nijmegen, The Netherlands

[2]Department of Technical Medicine, University of Twente, Enschede, The Netherlands

[3]Medical Ultrasound Imaging Center, Department of Radiology, Radboud University Medical Center, Nijmegen, The Netherlands

Abstract:
Neurocritical care is focused on the prevention and the minimization of secondary brain damage and the facilitation of neurological recovery. Since adequate supply of blood containing oxygen and glucose is crucial for the recovery and survival of brain tissue, monitoring the cerebral blood flow (CBF) is an essential part of neurocritical care. However, easy, non-invasive and reliable direct bedside monitoring of the CBF is not feasible at this moment in the ICU. This review focussed on the potential of contrast enhanced ultrasound techniques being a monitoring technique of the CBF at the ICU. The flash-replenishment contrast ultrasound method using the refill kinetics has the highest potential for becoming a CBF monitoring technique at the ICU. This because of its high temporal resolution, short acquisition time (~10 seconds after optimal positioning of the transducer) and the use of low MI, which avoids the shadowing effect and movement artefacts. Furthermore this technique uses an UCA infusion, which decreases the needed pause between subsequent measurements. However, a comparison study between the different methods must be performed to reassure the flash-replenishment method is as promising as expected.

Introduction:

Clinical relevance

Acute brain injury (ABI) has a high mortality and morbidity.[8] ABI is caused by stroke or traumatic brain injury (TBI). The extend of the brain damage depends on both the primary brain damage following the injury and the secondary brain damage. Brain ischemia is the major common pathway of secondary brain damage, but hyperperfusion also leads to brain damage.[7] Neurocritical care is focused on the prevention and the minimization of secondary brain damage and the facilitation of neurological recovery.[7] Since adequate supply of blood containing oxygen and nutrients is crucial for the recovery and survival of brain tissue, monitoring the cerebral blood flow (CBF) is an essential part of neurocritical care. However, easy, non-invasive, reliable and bedside monitoring of the CBF is not feasible in the ICU at this moment.

In order to limit the risk of secondary brain damage in patients with ABI, changes in the brain perfusion must be detected before irreversible damage has occurred. Furthermore, the effects of the interventions must be monitored in order to adjust therapy. Therefore, monitoring of the CBF is essential. Currently direct and bedside measurement of the overall CBF is not available for clinical use. CBF can only be directly measured using PET, perfusion weighted MRI, Xenon CT, SPECT and CT perfusion.[7] A non-invasive bedside monitoring device which is able to monitor CBF continuously would be ideal.

Cerebral contrast enhanced ultrasound (CEUS) has been suggested as a promising method to measure CBF in patients with acute brain injury at the ICU. Ultrasound is an attractive technique because it is non-invasive, has a high temporal resolution and can be used at the bedside. Ultrasound contrast agents (UCAs) have been used for visualization of the cerebral arteries to overcome the low level of acoustic intensity due to the ultrasound absorption of the skull leading to a poor signal-to-noise ratio.

Ultrasound contrast agents

UCAs consist of microbubbles, which are gas-filled particles of 1-10 µm diameter. Because of their small size, they are able to pass through the microcirculation and when they are dissolved the gas is removed from the blood via exhalation. Microbubbles increase the reflectivity of blood due to its very low acoustic impedance with respect to blood. Furthermore, microbubbles demonstrate a non-linear behaviour in response to ultrasound. In the frequency domain this results in harmonics. Since tissue is less non-linear, these harmonics can be used to distinguish the microbubble echoes from tissue echoes.[6] When microbubbles are expanded with a strong negative pressure, the shell stabilizing the bubble can break. The mechanical index (MI) gives an indication of the likelihood of bubble disruption, defined as: $= \frac{P-}{\sqrt{f}}$, where *P-* is the negative pressure and *f* the ultrasound frequency. A high MI indicates an higher probability of microbubble disruption. The threshold between a low MI and high MI is not clearly defined. In extracranial organs, ultrasound intensities with a MI of > 0.5 are referred to as high MI imaging. In transcranial imaging a MI of > 1.0 is needed for the destruction of the microbubbles to compensate for the ultrasound absorption of the skull.[45] With a MI of about 0.1 or less in extracranial imaging, the microbubbles examined are not significantly destroyed, but give a good harmonic contrast signal. In transcranial imaging, an MI up to 0.2 is used to compensate for skull attenuation.[37]

Ultrasound contrast agent detection

One of the methods to distinguish microbubbles from tissue is by using its harmonic behaviour. Examples of these methods are harmonic B-mode imaging (HI) and multi-pulse imaging techniques such as power modulation (PM), pulse inversion (PI) and contrast pulse sequencing (CPS) or combination of these techniques. Next to this non-linear imaging, also linear scattering and bubble destruction can be used for imaging of contrast agents. Techniques using these characteristics are power Doppler, contrast burst imaging (CBI) and time variance imaging (TVI).

From microbubble to perfusion measurement

In CEUS three different approaches are used to measure the CBF. These approaches are based on the bolus, refill (replenishment) and depletion kinetics.

Bolus kinetics

After a bolus injection, microbubbles enter the insonation field and the acoustic intensity in this plane increases. The acoustic intensity over time can be represented by a time intensity curve (TIC) as shown in Figure 1. Microbubbles entering the insonation field are destroyed by ultrasound energy. To allow inflow into the parenchyma, a frame rate of 0.25-1 Hz must be used. Different parameters of the TIC can be extracted, such as: time-to-peak (TTP), time-to-peak intensity (T_{PI}), peak intensity (PI), peak width (PW, full width at 90% of the

maximum intensity), full width at half of the maximum intensity increase (FWHM), area under the curve (AUC) and positive gradient (PG, slope of the wash-in phase).

Refill kinetics

The refill kinetics approach is based on the reappearance of UCA after complete destruction of the microbubbles, when a constant UCA infusion is given. By destroying the UCA within the scanning plane using a high MI flash image, a negative bolus of contrast agent is created locally and new microbubbles enter the plane. The refill intensity curve can be achieved using two methods. Figure 2 shows the refill intensity curve of the flash-replenishment method using low MI ultrasound imaging to monitor replenishment kinetics in real-time after UCA destruction. The second method, called the increasing intervals method, detects the intensity gain between destructive ultrasound frames at increasing pulsing intervals, from 50 ms to 8000 ms.[45] After bubble destruction, microbubble tissue replenishment can be described as an exponential curve with the corresponding equation: $y = A(1 - e^{-\beta t})$, where y is the acoustic intensity in decibel (dB), *t* represents time (flash-replenishment imaging) or pulsing interval (increasing intervals method), β represents the rise rate of the acoustic intensity over time and A is the plateau of acoustic intensity, reflecting the microvascular cross-sectional area. β is said to be directly related to the blood flow velocity and A to the blood volume. Therefore, the product of both (A×β) is correlated with the blood flow.[49]

Depletion kinetics

Depletion kinetics is based on the destruction of contrast agent at a constant frame rate with a high MI. The TIC decreases to a new equilibrium, determined by a balance between destruction and reperfusion of the UCA. Three mathematical models have been applied for analysing the depletion curve: an exponential decay model, a complex exponential model which separates the curve into destruction and reperfusion phases providing a perfusion and destruction coefficient, and a simple linear model (Figure 3). Because of the short sampling time needed (1- 10 seconds), depletion kinetics can be analysed using either bolus injection or infusion.[45]

Aim of this study

A CEUS method which measures CBF quantitatively has not yet been found. Only qualitative and semi-quantitative parameters were measured. Furthermore, the different CEUS methods have their own limitations and measure different parameters related to CBF. The aim of this review is to establish which CEUS technique has the highest potential for becoming a bedside monitoring technique of the CBF.

Materials and Methods/Case Material:

The requirements of a bedside monitoring technique at the ICU are considered regarding the execution and the data analysis.

Requirements regarding CEUS execution

1. *Bedside Applicability at the ICU:* A lot of equipment is connected to the patients at the ICU and they are continuously monitored. Transport of these patients is not practical, time consuming and has its risks. The study of Peerdeman et al. in 2002 indicates possible deleterious effect of transportation in critically ill, mechanically ventilated, head-injured patients. Therefore transportation of these patients should be avoided if possible.[33]
2. *Repeatable measurement:* Optimizing therapy is an ongoing process at the ICU. To know the effect of therapy on the CBF and to be able to detect changes in the CBF over time, it is not sufficient to have a single measurement of the CBF. The measurement must be repeatable at least every few hours and comparable, therefore a low inter observer variability and a low operator dependency is preferred.
3. *Safe measurement:* Inherent to the previous point, the measurement has to be safe and without side effects for the patients.

Requirements regarding data analysis

1. *Semi-quantitative or quantitative outcome:* the goal of the CBF measurement is early detection of alteration of the CBF before irreversible (secondary) damage occurs. Furthermore the CBF measurements can help monitoring the effects of interventions in order to adjust therapy. Therefore, it is important that relative changes over time can be measured in an individual patient.
2. *Suitable measurement characteristics:* The technique should have sufficient temporal resolution, spatial resolution and accuracy.

These requirements were the guidance to the ultrasound technique with the highest potential for being a monitoring technique of the CBF at the ICU.

In order to compare all different ultrasound techniques on the requirements, the studies are categorized according to the ultrasound detection kinetic principle that was used: bolus kinetics, refill kinetics and depletion kinetics. From each category the execution and data analyses characteristics are compared, as described below:

Execution characteristics: Executors, study population, UCA type, UCA dosage, side-effects after UCA administration, duration, insonation approach.
Data analysis: Reference method, ultrasound method, acquisition time, temporal and spatial resolution, outcome parameters.

Search strategy

To retrieve the articles of interest for this review, an online literature search (PubMed) was conducted on October the 23rd 2014. The search terms included are listed in Table 1. Inclusion criteria were a human study published in English between 1994 and 2014, which used transcranial CEUS in order to measure CBF or related parameters. Reviews and general discussion papers, not presenting original data were excluded. Two authors (EV,CH) independently assessed the eligibility by reading abstracts and, if necessary, whole articles. The snowball method was used to manually select relevant references from the reference list of included articles.

Results:

Two hundred and forty eight publications met the search criteria and were evaluated. In Figure 4 a flowchart of the literature review process is shown. Two hundred and thirteen publications were excluded because the studies were performed in animals, the publications were not available in English or because no transcranial CEUS was used to measure CBF or related parameters. By means of the snowball method, 2 articles were added to the article selection. Hence, thirty eight publications were eligible for review (Table 1).

In the ongoing development of CEUS, studies had different objectives regarding the quantification of the cerebral perfusion. Some studies investigated the potential of the CEUS techniques for cerebral perfusion measurement. The potential was studied by evaluating whether there was accurate contrast in different cerebral structures[1,36,38] or whether it was possible to visualize cerebral perfusion deficits[2,3,5,9,11,16,25,28,40,44,46,48,50]. Furthermore, the three different CEUS methods (bolus, depletion, refill) were evaluated by looking at the dependence of the measured parameters on dose or infusion rate, UCA, frame rate and insonation depth.[14,15,31,39,43] Next to the three different kinetics, different contrast-specific imaging modes were used in the different studies. Some studies compared different contrast-specific imaging modes.[3,10,13,19,35,41]

Demographic data
Table 2 shows the included studies and the study population. Fifteen studies (39%) were performed on healthy volunteers and 17 studies (45%) were performed on patients. The remaining 6 studies (16%) were performed on patients and controls. In total 296 healthy volunteers and 347 patients were included in the studies. Mostly ischemic stroke patients were included in the studies. Other diseases in which the perfusion was analysed was hemispheric syndrome, brain tumor, intracerebral haemorrhage, Moya-moya syndrome, severe ICA stenosis, TBI, intracranial space-occupying lesions and diabetes type II (Table 3).

Exclusion criteria were the contraindications for the UCA as in the operators instruction of the UCA, such as right-left shunt, severe pulmonary hypertension, ARDS and pregnant and lactating women. Furthermore the additional exclusion criteria were added in case a reference method was used, such as MRI or CT.

Ultrasound Contrast Agents
Until 2003 the UCAs Levovist (Sehering) and Optison (Amersham Health) were mainly used. Later SonoVue (Bracco) was mainly used. In 15 publications (39%) the toleration of the UCAs was not mentioned. In four studies (11%) mild side effects (mild transient headache after investigation, mild burning sensation in right upper abdominal quadrant) and local side effects of Optison were described. In nineteen studies (50%) no side effects owing to the UCAs were observed. 23 studies mentioned usage of a saline flush after the UCA administration. 16 studies used a saline flush of 10 ml, 4 studies used 5 ml and 2 studies used 3 ml. Table 4 provides an overview of the study population and mentioned side effects of each UCA.

Insonation approach
In 34 studies the CEUS were performed via the transtemporal approach (Table 5). In 23 of these studies, a sufficient acoustic transtemporal bone window was one of the inclusion criteria of the subjects. Three different transtemporal approaches were used. Onesided transtemporal insonation is insonation through the acoustic window at one side, imaging only the hemisphere of that side. Transtemporal twosided insonation is insonation of both acoustic windows one after another, imaging both corresponding hemispheres. Onesided bilateral insonation is insonation through one acoustic window, but imaging both hemispheres.
14 studies used the twosided transtemporal approach. 20 studies used the onesided transtemporal approach, which was performed on the side of the pathologic hemisphere. 6 studies used the onesided bilateral approach. In 4 studies, patients with decompressive craniectomy and patients undergoing craniotomy were included.

Duration
The total duration of the ultrasound examination was defined as the sum of the time necessary for search of the correct plane of insonation, the time between the UCA injection and the start of the acquisition and the acquisition time itself. Correct placement of the transducer is the most time consuming in an examination and depends on the executor's experience and patient characteristics. Furthermore the time between the UCA injection and the start of the acquisition and the acquisition time itself depends on the imaging method, which is described for each technique in section 4.3.

Another influence on the duration of a measurement is the time needed to ensure the contrast has been removed from the circulation. In the studies in which different UCAs, UCA concentrations, insonation planes, different sides or different imaging techniques were compared in the same patient a pause was used to ensure removal of

the UCA. This pause was mentioned in nineteen studies, in which the pause varied from 5 to 30 minutes (Table 6). In the depletion kinetic studies which mentioned this pause, it lasted 10 minutes. In the refill kinetic studies which mentioned this pause, it lasted 10 or 15 minutes. In the bolus kinetic studies mentioning this pause, it lasted 5-10, 10, 20 or 30 minutes.

Temporal and spatial resolution
The temporal resolution of the techniques depends on the frame rate, which depends on the ultrasound method. In section 4.3 the frame rate of each ultrasound method is described. The spatial resolution depends on the transducer frequency, where an increasing frequency results in an improved spatial resolution. However increasing the transducer frequency decreases the penetration depth. The used transducer frequency and the frame rate of the different studies can be found in Tables 7 a)-d), Table 8 and Table 9.

Executor dependence and inter observer variability
In most studies the executor, or the experience of the executor were not mentioned. Overall, executors mentioned in the studies were medical doctors with experience in the ultrasound measurements. Furthermore, comparability between brain perfusion assessment was studied by Hölscher et al in 2005.[20] Hölscher et al. concluded that contrast burst imaging achieves comparable results in different centers using the same scanning protocol.

Data analysis
Additional information about the measurement characteristics and the perfusion parameter characteristics are described in this section for the bolus, refill and depletion kinetics approach.

Reference method
28 studies used a reference method to validate the CEUS measurements. Several studies used MRI or CT as a reference for the localization of the perfusion deficits in order to define the regions of interest (ROIs) and/or to evaluate the perfusion parameter results in these regions.[1–4,9,12,16,21,25,38,40,44,48,50] In some studies also the correlation between measured perfusion parameters of the ultrasound measurement and comparable perfusion MRI or CT parameters were determined in order to validate the CEUS data.[15,23,27,30,32] The perfusion state was mostly performed by the analysis of local time intensity curves in pre-specified ROI (region-wise imaging) or by the visual interpretation of pixel-wise parametric images.[9,44,50,51] In 2007 Eyding et al. compared these two analysis methods and concluded that parameter imaging was less accurate than the region-wise analysis.[12]

Bolus kinetics
The cerebral blood flow was assessed with the bolus kinetic approach in twenty seven studies (71%) to analyse the cerebral perfusion. In Tables 7 a), b), c) and d) present an overview of the characteristics of these bolus kinetic studies.

Ultrasound method
Harmonic imaging was the most commonly used ultrasound method, performed in thirteen of the twenty-seven bolus kinetics studies. From these thirteen studies using this technique, five studies used the integrated backscatter modus. In addition pulse inversion harmonic imaging was used in 6 studies. Other imaging methods used were contrast burst imaging, time variance imaging, power modulation imaging and contrast pulse sequencing.[19–21,30,35,46,48] Three studies used both the time variance imaging and the contrast burst imaging.[19,30,35]

Acquisition time
The acquisition time in the bolus kinetics approach depends on the frame rate and the number of images taken. Not all the studies described the frame rate, or number of images or the acquisition time. Two studies described none of these characteristics. Nine studies only described the frame rate and one study described only the number of frames. Nine studies described the frame rate and the acquisition time. The frame rates used were 0.5 Hz in 11 studies, 0.67 Hz in 3 studies, 1 Hz in 3 studies and 30 Hz in 1 study. In 6 studies used an ECG triggered pulsing interval of one frame every four cardiac cycles.
The number of images acquired was >36. The time needed for the acquisition described in the bolus approach studies was > 60 seconds. In all bolus approach studies, the acquisition started immediately after the UCA injection.

Perfusion parameters
The perfusion parameters that were determined using the bolus kinetic approach are: PI, AUC, TTP, TPI, mean transit time, PG, rise-time (time between 10% of the PI and 90% of the PI) and PW. PI and TTP were mostly analysed for defining perfusion deficits. Studies agree on the dose and depth dependence of PI and the depth-independent TTP, which makes TTP the most reliable parameter in the bolus kinetic.[30] However the translation

from this TTP towards quantitative CBF measurements remains difficult because TTP is believed to be correlated with the CBFV instead of CBF and because of to the inter- and intra-individual variability of TTP.

Seidel et al. defined hypoperfusion as a TTP delay of >3 seconds and a 50% lower intensity increase.[44] Bartels et al. used an intensity increase <15%, resulting from the contrast enhancement as a cut-off for hypoperfusion.[2] However, Krogias et al determined the intra-individual range of perfusion parameters to describe individual cut-off scores and concluded that TPI is the most robust parameter of the bolus parameters because of its depth independence and that a delay of 3-4 seconds would be the cut-off for hypoperfusion,[28] which was also confirmed by Meyer-Wiethe et al.[32] Eyding et al. expanded this 3 seconds TTP cut-off by defining 'no perfusion' when no bolus-like curve progression was visible and 'normal perfusion' when a bolus-like progression of the TIC and TPI within +/- 3 seconds of the intra-individual median of the ROIs of the nonaffected contralateral hemisphere was present.[9]

Depletion kinetics

6 studies (16%) used depletion kinetics to analyse the cerebral perfusion. Table 9 provides an overview of the characteristics of these studies using the depletion kinetics approach.

Ultrasound method

The ultrasound methods used in the depletion studies were Harmonic Imaging with integrated backscatter[31], Contrast Burst imaging[13–15], Pulse inversion harmonic imaging[13,24] and Power pulse inversion contrast harmonic imaging[25]. Eyding et al. concluded that PIHI was more reliable than CBI, in combination with second generation UCA.[13]

Acquisition time

The studies using the depletion kinetics approach described different acquisition times varying from a few seconds to 35 seconds. The acquisition time of only a few seconds are calculated from the amount of flashes times the frame rate. The amount of flashes needed to reach an equilibrium depends on the UCA dosage, which was investigated by Eyding et al.[14] They concluded that a frame rate of 1 Hz was optimal due to a higher signal-to-noise ratio than with a higher frame rate. Furthermore, the time between the start of the UCA injection and the start of the acquisition varies from 30 to 90 seconds. Kern et al. combined the depletion kinetic approach with the bolus kinetic approach, in which direct after the start of the infusion the TTP was measured and after that the depletion acquisition started.[24]

Perfusion parameters

The perfusion parameters measured with the depletion kinetic approach were: Intensity (I), PC, DC, T_{min}, ΔI, intensity before the depletion ($I(t_0)$), baseline intensity ($I(t_{baseline})$).

In 2002, Meyer and Seidel et al. investigated the depletion kinetics approach in healthy subjects using a rapid sequence harmonic imaging. Using this technique the time intensity curves could be collected within seconds. Contrast half-life and the baseline intensity were computed from selected ROIs for two different infusion rates. It was concluded that with higher UCA infusion the contrast half-life was more depth dependent, which could be explained by the shadowing effect.[31]

Eyding et al. investigated the diagnostic potential of the new contrast burst imaging method in healthy subjects in 2003.[15] They assumed there was a constant microbubble concentration at a specific time after the bolus and concluded that PC seemed to be independent of depth and independent of type of UCA. However DC showed high inter- and intra-individual variation.
In 2004 Eyding et al. investigated the influence of the frame rate and different UCAs on the perfusion coefficient (PC). They concluded that PC was independent of type of UCA and the frame rate.[14]
Kern et al. studied whether perfusion deficits could be detected with depletion kinetics using power pulse inversion contrast harmonic imaging (PPICHI), assuming a constant UCA concentration 30 seconds after the bolus. They used the perfusion parameters ΔI, $I(t_0)$ and $I(t_{baseline})$ to identify the perfusion deficits. Reduced microbubble destruction (lower ΔI) was shown in infarction regions, compared to the non-affected region.[25]

Refill kinetics

Five studies (13%) used refill kinetics to analyse the cerebral perfusion. From these studies, Bartels et al., Kern et al. and Bolognese et al., the bolus kinetics was additionally used in order to measure the real-time bolus kinetic parameter TTP.[3,4,23] Table 8 presents an overview of the characteristics of the CEUS studies using the refill kinetics approach.

Ultrasound method
The ultrasound methods used in the refill kinetic studies were harmonic imaging[43], contrast pulse sequencing[3,4,23] and power modulation imaging[18]. In 2002, Seidel et al. investigated the refill kinetics approach in humans using the pulsing interval method in healthy volunteers.[43] A high MI was used of 1.0-1.6 with different time intervals in order to receive the refill parameters. In 2005, Bartels et al. used the flash-replenishment refill method in order to evaluate cerebral perfusion deficit using CPS and concluded that CPS imaging was a suitable tool for the ultrasonographic evaluation of cerebral perfusion. However, Bartels et al. did not use the refill parameters, but the intensity increase and TTP in the perfusion evaluation.[3]

The first study in humans using real-time ultrasound perfusion imaging with a low MI (rt-UPI) to assess cerebral perfusion through the intact skull was done by Kern et al.[23] Kern et al. concluded that the performance of real-time refill kinetics is relatively simple as compared with previous ultrasound methods for the evaluation of brain tissue perfusion. Analysis of data is possible online and involves selection of one or multiple ROIs. Consequent calculation and display of refill kinetics are practically instantaneous, thus allowing immediate bedside interpretation of results. These features reflect important advantages over first-generation techniques of CEUS, which were limited by relatively difficult and operator dependent data acquisition, tedious data transfer, and off-line analysis. Furthermore this real-time refill approach avoids the shadowing effect, which is a significant problem associated with high MI imaging. The shadowing problem is eliminated with low MI imaging, because bubbles are not destroyed with such low acoustic pressure. The rt-UPI offers a far better temporal resolution than all the other modalities that have been described previously. This is due to the fact that this refill approach is not restricted to triggered image sequences of 1 Hz or less because of bubble destruction.[23]

Acquisition time
The acquisition time of the refill kinetic approach depends on the method used. Seidel et al., who used the time interval approach, did not mention a precise acquisition time.[43] However, summation of the used time intervals indicates that an acquisition time of several minutes. The flash-replenishment method on the other hand was described to have an acquisition time of ~10 seconds.[4,18,23]
Seidel et al. and Heppner et al. used an infusion in order to create a steady UCA concentration before the measurement. However Bartels et al. Kern et al. and Bolognese et al. used a (slow) bolus, assuming a steady state of UCA is reached after the highest peak intensity. Kern et al. and Bolognese et al. started the acquisition direct after the bolus injection in order to measure the TTP. After that (around 45 seconds after the injection) the flash replenishment method started.[4,23] Seidel et al. were using an contrast infusion and started the acquisition 90 seconds after the start of the infusion.[43]

Perfusion parameters
The perfusion parameters which were assessed using the refill kinetic approach were: A, β and A×β. Amplitude A is dependent on the insonation depth, which makes A×β also depth dependent. Theoretically, the parameter β on the other hand is depth independent. Parameter A, assessed by Bolognese et al., showed high standard deviation, just as has been shown by Kern et al.. They suggested this could be explained by the inter-individual differences of acoustic attenuation of the skull.

Kern et al and Bolognese et al. calculated the optimal cut-off for the additional bolus parameter TTP which was measured real time with low MI (rt-TTP), and the refill parameters.[4,23] Kern et al. concluded that the refill parameters β and A×β and the bolus parameter TTP had high sensitivity for discriminating ischemic from normal tissue in the ROC analysis. Optimal cut-off values of these parameters for identification of ischemic brain tissue were as follows: rt-TTP > 10.1 seconds, $\beta < 0.76$, $A < 1.89$ and $A\times\beta < 1.91$. Subsequently Bolognese et al. concluded that both rt-TTP of bolus kinetics and the slope factor β of refill kinetics measured with real-time ultrasound perfusion imaging are suitable parameters to assess the changes of cerebral perfusion in acute MCA stroke.[4]

Discussion:

CEUS is a non-invasive, safe and easy method to measure cerebral perfusion parameters. Therefore, CEUS has been suggested as a promising modality as bedside monitoring technique of the cerebral perfusion at the ICU. Several studies have performed different CEUS methods and measured corresponding perfusion parameters. The techniques have been performed in patients with different cerebral perfusion pathologies over the last 20 years and several perfusion parameters have been proven to be sensitive to detect these perfusion deficits. However due to high intra- and inter-individual variation of the perfusion parameters quantification of the CBF has not yet been performed.

Execution characteristics

Applicability at the ICU
An important requirement of the monitoring technique is the repeatability, therefore the execution of the technique and the duration must be feasible at the ICU. After probe positioning the cerebral perfusion parameters of the insonation plane can be measured in a few minutes or even seconds. However, the positioning time of the probe for each insonation plane depends on the executor's experience. Overall the medical doctors with experience in cerebral (contrast) ultrasonography performed the measurements. To be able to use this technique at the ICU, several insonation planes of both hemispheres ought to be measured regularly. Therefore, an experienced executor is necessary in order to shorten the probe positioning time for each insonation plane to ensure the repeatability of the technique at the ICU. Furthermore, the time between measuring different insonation planes may be shortened by choosing a contrast imaging technique that uses a UCA infusion, rather than a bolus.

Another requirement which was originally not defined in this review is that the monitoring technique should be feasible for all the ICU patients. Our main concern of the applicability of transtemporal CEUS at the ICU is the possible need for a sufficient transtemporal window for the execution. In the execution of TCD and transcranial color coded duplex (TCCD), patients regularly have an insufficient window (5-20%).[26] Furthermore, the sufficiency of the acoustic window decreases with age, due to progressive osseous calcification.[52] A majority of the ICU patients are > 60 years old, therefore a CEUS technique in which both temporal acoustic windows need to be sufficient does not meet the requirements at the ICU. However UCAs have been used to increase the sensitivity of TCD and TCCD in patients with an insufficient transtemporal window.[17,47]

Safety
Overall no severe adverse events have been documented in numerous volunteer studies using these contrast agents, which have included hundreds of patients.[42] In the studies reviewed, only 4 cases of mild local side effects on the UCA Optison were described on a total of 623 subjects undergoing the measurement. Theoretically the interaction between the ultrasound and the UCA could cause damage to the microvasculature.[34] Studies investigating the integrity of the blood brain barrier (BBB) in humans after using standard contrast-enhanced ultrasound perfusion imaging did not lead to MRI detectable BBB changes or focal brain damage.[22,29] These results are reassuring but not totally conclusive in terms of ultrasound safety, since hypothetically more subtle effects of ultrasound and microbubbles on the BBB might be missed by MRI.[29]

In order to minimize the possible adverse bioeffects, the EFSUMB Guidelines on the clinical practice of CEUS state that the operator should be mindful of the desirability of keeping the MI low and of avoiding long exposure times.[34]

Data analysis

Contrast detection method
Studies using the bolus kinetic approach and the depletion kinetic approach are based on using a high MI. This high MI results in a temporal resolution of ~1 second. Furthermore the high MI is accompanied with the shadowing effect. With the refill kinetics on the other hand, a better temporal resolution can be used, because after the bubble destruction at start, the MI is low and no microbubbles will be destructed during the replenishment, which also results in no shadowing effect. This high temporal resolution will also result in less movement artefacts due to movement of the probe or the patient. Therefore the refill kinetic approach seems to be the contrast imaging technique with the most potential for being a bedside monitoring technique of the cerebral perfusion.

An important question that remains unanswered is whether a high MI is needed to increase the signal-to-noise ratio. All the studies using the bolus kinetic approach used a high MI. Therefore, low MI CEUS (in for example low MI bolus kinetics or refill kinetics) might be more sensitive to artefacts. However, to date no study has compared the different CEUS techniques using low and high MI.

Outcome parameters
From the theoretical point of view, time dependent parameters like TTP (bolus kinetics), perfusion coefficient (depletion kinetics) or β (refill kinetics) are the most useful for the quantification of the cerebral perfusion. This because amplitude also depends on the insonation depth and therefore depends on the attenuation of the skull. In accordance with this theoretical point of view, studies that investigated the depth and ultrasound dosage dependence of the different perfusion parameters found higher dependence of these external factors in the amplitude parameters, rather than the time parameters. Studies agree on focusing on the time dependent parameters, which seem to be the most reliable perfusion parameters.

It remains unknown which of the time parameters is the most reliable for the estimation of the CBF. Bolognese et al. compared the time parameters of the low MI bolus and refill kinetics and concluded that rt-TTP and β were both sensitive parameters for the detection of perfusion changes in acute MCA stroke. Based on the outcome parameters, no superior technique can be indicated. For all methods the focus should be on the time dependent parameters.

The sensitivity of the CEUS perfusion parameters was studied using perfusion CT or diffusion or perfusion weighted MRI as reference method. However the gold standard for quantifying CBF is positron emission tomography (PET) with ^{15}O-labeled water. High cost and limited accessibility have restricted the widespread clinical use of PET. The approximation of the CBF using perfusion CT has been validated, but these approximations do not meet the true CBF as measured with the gold standard.

Limitations
The identification of the highest potential CEUS technique in this systematic review has limitations. Since no comparison studies between the different CEUS techniques have been performed it is difficult to conclude which technique has the highest potential. Moreover not all studies mentioned information about the executor of the measurements, total duration of the measurements, acquisition time, the UCA procedure and the data analysis.

Challenges
To assure repeatability of the measurement, a short duration of the measurement is ideal. Despite a variation in acquisition time between minutes and seconds is present between the bolus versus the depletion and refill method, the total time of the measurement mainly depends on the time needed to position the probe and the pause between subsequent measurements. In a few bolus kinetic studies, both hemispheres were assessed through one acoustic temporal window. This shortens the total measurement duration dramatically, because only one side has to be investigated. However, comparison between the two hemispheres might be difficult due to the insonation angle. On the other hand, measuring at two sides separately makes using one consistent insonation angle difficult. Therefore, the question is whether using one acoustic window side is preferable. Another consideration is the use of an infusion, as suggested by Bolognese et al. This way several insonation planes can be made during the same infusion.[4]

Focussing on the quantification of the CBF, the relation between CBF and the time parameter must be identified in order to quantitatively measure the CBF. Although, high variability of CBF between different subjects and variability of the CBF within the patient makes this quantification of the CBF even more difficult. However, this step is necessary to be able to monitor the cerebral perfusion. The perfusion parameters must not only be able to identify hypoperfusion or healthy perfusion, but ideally also hyperperfusion and the degree of the perfusion.

Conclusions:

CEUS is a non-invasive, safe and easy method to measure cerebral perfusion parameters. Therefore, CEUS has been suggested as a promising modality as bedside monitoring technique of the cerebral perfusion at the ICU. The flash-replenishment contrast ultrasound method using the refill kinetics and high MI flashes followed by low MI ultrasound has the highest potential to become a CBF monitoring technique at the intensive care unit. This because of its high temporal resolution, short acquisition time (~10 seconds after optimal positioning of the transducer) and the use of low MI, which avoids the shadowing effect and movement artefacts. Furthermore this technique uses an UCA infusion, which decreases the needed pause between subsequent measurements. However, a comparison study between the different methods must be performed to reassure the flash-replenishment method is indeed as promising as expected.

References

1. Bartels E, Bittermann H-J. Transcranial Contrast Imaging of Cerebral Perfusion in Stroke Patients Following Decompressive Craniectomy. Ultraschall Med 2004; 25:206–13.

2. Bartels E, Bittermann H-J. Transcranial Contrast Imaging of Cerebral Perfusion in Patients With Space-Occupying Intracranial Lesions. J Ultrasound Med 2006; 25:499–507.

3. Bartels E. Evaluation of Cerebral perfusion deficit in stroke patients using new transcranial contrast imaging CPS technology. Ultraschall Med 2005; 26:478–86.

4. Bolognese M, Artemis D, Alonso A, Hennerici MG, Meairs S, Kern R. Real-time ultrasound perfusion imaging in acute stroke: assessment of cerebral perfusion deficits related to arterial recanalization. Ultrasound Med Biol 2013; 39:745–52. Retrieved 30 September 2014 from http://www.ncbi.nlm.nih.gov/pubmed/23453375

5. Caruso G, Salvaggio G, Ragusa P, Brancatelli G, Lagalla R. Ultrasonic evaluation with second harmonic imaging and SonoVue in the assessment of cerebral perfusion in diabetic patients: a case-control study. Eur Radiol 2005; 15:823–8. Retrieved 30 September 2014 from http://www.ncbi.nlm.nih.gov/pubmed/15368073

6. Cosgrove D, Lassau N. Imaging of perfusion using ultrasound. Eur J Nucl Med Mol Imaging 2010; 37 Suppl 1:S65–85. Retrieved 28 August 2014 from http://www.ncbi.nlm.nih.gov/pubmed/20640418

7. Dagal A, Lam AM. Cerebral blood flow and the injured brain: how should we monitor and manipulate it? Curr Opin Anaesthesiol 2011; 24:131–7. Retrieved 9 September 2014 from http://www.ncbi.nlm.nih.gov/pubmed/21386665

8. Dunn IF, Ellegala B, Fox JF, Dong HK. Perspectives in Brain Physiology Principles of Cerebral Oxygenation and Blood Flow in the Neurological Critical Care Unit reprint request to : Neurocrit Care 2006; 4:77–82.

9. Eyding J, Krogias C, Schöllhammer M, Eyding D, Wilkening W, Meves S, et al. Contrast-enhanced ultrasonic parametric perfusion imaging detects dysfunctional tissue at risk in acute MCA stroke. J Cereb Blood Flow Metab 2006; 26:576–82. Retrieved 9 September 2014 from http://www.ncbi.nlm.nih.gov/pubmed/16121127

10. Eyding J, Krogias C, Wilkening W, Meves S, Ermert H, Postert T. Parameters of cerebral perfusion in phase-inversion harmonic imaging (PIHI) ultrasound examinations. Ultrasound Med Biol 2003; 29:1379–85. Retrieved 9 September 2014 from http://linkinghub.elsevier.com/retrieve/pii/S0301562903010354

11. Eyding J, Krogias C, Wilkening W, Postert T. Detection of cerebral perfusion abnormalities in acute stroke using phase inversion harmonic imaging (PIHI): preliminary results. J Neurol Neurosurg Psychiatry 2004; 75:926–9. Retrieved 30 September 2014 from http://jnnp.bmj.com/cgi/doi/10.1136/jnnp.2003.026195

12. Eyding J, Nolte-Martin A, Krogias C, Postert T. Changes of contrast-specific ultrasonic cerebral perfusion patterns in the course of stroke; reliability of region-wise and parametric imaging analysis. Ultrasound Med Biol 2007; 33:329–34. Retrieved 30 September 2014 from http://www.ncbi.nlm.nih.gov/pubmed/17207904

13. Eyding J, Wilkening W, Krogias C, Przuntek H, Meves S, Postert T. Validation of the Depletion Kinetic in Semiquantitative Ultrasonographic Cerebral Perfusion Imaging Using 2 Different Techniques of Data Acquisition. 2004; :1035–40.

14. Eyding J, Wilkening W, Reckhardt M, Meves S, Postert T. Reliability of Semiquantitative Ultrasonic Perfusion Imaging of the Brain. J Neuroimaging 2004; 14:143–9. Retrieved 31 October 2014 from http://jon.sagepub.com/cgi/doi/10.1177/1051228404263273

15. Eyding J, Wilkening W, Reckhardt M, Schmid G, Meves S, Ermert H, et al. Contrast Burst Depletion Imaging (CODIM): A New Imaging Procedure and Analysis Method for Semiquantitative Ultrasonic Perfusion Imaging. Stroke 2003; 34:77–83. Retrieved 9 September 2014 from http://stroke.ahajournals.org/cgi/doi/10.1161/01.STR.0000046455.51363.E2

16. Federlein J, Postert T, Meves S, Weber S, Przuntek H, Büttner T. Ultrasonic evaluation of pathological brain perfusion in acute stroke using second harmonic imaging. J Neurol Neurosurg Psychiatry 2000; 69:616–22. Retrieved from http://www.pubmedcentral.nih.gov/articlerender.fcgi?artid=1763382&tool=pmcentrez&rendertype=abstract

17. Gahn G, Gerber J, Hallmeyer S, Hahn G, Ackerman RH, Reichmann H. Contrast-Enhanced Transcranial Color-Coded Duplexsonography in Stroke Patients with Limited Bone Windows. Am J Neuroradiol 2000; 21:509–14.

18. Heppner P, Ellegala DB, Durieux M, Jane J a, Lindner JR. Contrast ultrasonographic assessment of cerebral perfusion in patients undergoing decompressive craniectomy for traumatic brain injury. J Neurosurg 2006; 104:738–45. Retrieved from http://www.ncbi.nlm.nih.gov/pubmed/16703878

19. Hölscher T, Postert T, Meves S, Thies T, Ermert H. Assessment of brain perfusion with echo contrast specific imaging modes and Optison. Acad Radiol 2002; 9:386–8.

20. Hölscher T, Wilkening W, Draganski B, Meves SH, Eyding J, Voit H, et al. Transcranial ultrasound brain perfusion assessment with a contrast agent-specific imaging mode: results of a two-center trial. Stroke 2005; 36:2283–5. Retrieved 30 September 2014 from http://www.ncbi.nlm.nih.gov/pubmed/16141430

21. Ickenstein GW, Valaikiene J, Koch H, Hau P, Erban P, Schlachetzki F. Ultrasonic contrast agents in transcranial perfusion sonography (TPS) for follow-up of patients with high grade gliomas. Ultrason Sonochem 2008; 15:510–6. Retrieved 30 September 2014 from http://www.ncbi.nlm.nih.gov/pubmed/18029220

22. Jungehulsing GJ, Brunecker P, Nolte CH, Fiebach JB, Kunze C, Doepp F, et al. Diagnostic transcranial ultrasound perfusion-imaging at 2.5 MHz does not affect the

blood-brain barrier. Ultrasound Med Biol 2008; 34:147–50. Retrieved 17 November 2014 from http://www.ncbi.nlm.nih.gov/pubmed/17854981

23. Kern R, Diels A, Pettenpohl J, Kablau M, Brade J, Hennerici MG, et al. Real-time ultrasound brain perfusion imaging with analysis of microbubble replenishment in acute MCA stroke. J Cereb Blood Flow Metab 2011; 31:1716–24. Retrieved 24 September 2014 from http://www.pubmedcentral.nih.gov/articlerender.fcgi?artid=3170938&tool=pmcentrez&rendertype=abstract

24. Kern R, Kablau M, Sallustio F, Fatar M, Stroick M, Hennerici MG, et al. Improved detection of intracerebral hemorrhage with transcranial ultrasound perfusion imaging. Cerebrovasc Dis 2008; 26:277–83. Retrieved 31 October 2014 from http://www.ncbi.nlm.nih.gov/pubmed/18648201

25. Kern R, Perren F, Schoeneberger K, Gass A, Hennerici M, Meairs S. Ultrasound microbubble destruction imaging in acute middle cerebral artery stroke. Stroke 2004; 35:1665–16670.

26. Krejza J, Swiat M, Pawlak M, Oszkinis G, Weigele J, Hurst R, et al. Suitability of temporal bone acoustic window: conventional TCD versus transcranial color-coded duplex sonography. J Neuroimaging 2007; 17:311–4.

27. Krogias C, Henneböhl C, Geier B, Hansen C, Hummel T, Meves S, et al. Transcranial ultrasound perfusion imaging and perfusion-MRI--a pilot study on the evaluation of cerebral perfusion in severe carotid artery stenosis. Ultrasound Med Biol 2010; 36:1973–80. Retrieved 11 September 2014 from http://www.ncbi.nlm.nih.gov/pubmed/20950933

28. Krogias C, Postert T, Meves S, Wilkening W, Przuntek H, Eyding J. Semiquantitative analysis of ultrasonic cerebral perfusion imaging. Ultrasound Med Biol 2005; 31:1007–12. Retrieved 30 September 2014 from http://www.ncbi.nlm.nih.gov/pubmed/16085090

29. Meairs S, Alonso A. Ultrasound, microbubbles and the blood-brain barrier. Prog Biophys Mol Biol 2007; 93:354–62. Retrieved 27 August 2014 from http://www.ncbi.nlm.nih.gov/pubmed/16959303

30. Meves SH, Wilkening W, Thies T, Eyding J, Hölscher T, Finger M, et al. Comparison between echo contrast agent-specific imaging modes and perfusion-weighted magnetic resonance imaging for the assessment of brain perfusion. Stroke 2002; 33:2433–7.

31. Meyer K, Seidel G. Transcranial contrast diminution imaging of the human brain: a pilot study in healthy volunteers. Ultrasound Med Biol 2002; 28:1433–7.

32. Meyer-Wiethe K, Cangür H, Schindler A, Koch C, Seidel G. Ultrasound perfusion imaging: determination of thresholds for the identification of critically disturbed perfusion in acute ischemic stroke--a pilot study. Ultrasound Med Biol 2007; 33:851–6. Retrieved 9 September 2014 from http://www.ncbi.nlm.nih.gov/pubmed/17445970

33. Peerdeman SM, Girbes ARJ, Vandertop WP. Changes in cerebral glycolytic activity during transport of critically ill neurotrauma patients measured with microdialysis. J Neurol 2002; 249:676–9.

34. Piscaglia F, Nolsøe C, Dietrich CF, Cosgrove DO, Gilja OH, Bachmann Nielsen M, et al. The EFSUMB Guidelines and Recommendations on the Clinical Practice of Contrast Enhanced Ultrasound (CEUS): update 2011 on non-hepatic applications. Ultraschall Med 2011; 33:33–59. Retrieved from http://www.ncbi.nlm.nih.gov/pubmed/21874631

35. Postert T, Hoppe P, Federlein J, Helbeck S, Ermert H, Przuntek H, et al. Contrast agent specific imaging modes for the ultrasonic assessment of parenchymal cerebral echo contrast enhancement. J Cereb Blood Flow Metab 2000; 20:1709–16. Retrieved from http://www.ncbi.nlm.nih.gov/pubmed/11129787

36. Postert T, Muhs a., Meves S, Federlein J, Przuntek H, Buttner T. Transient Response Harmonic Imaging : An Ultrasound Technique Related to Brain Perfusion. Stroke 1998; 29:1901–7. Retrieved 30 September 2014 from http://stroke.ahajournals.org/cgi/doi/10.1161/01.STR.29.9.1901

37. Powers J, Averkiou M, Bruce M. Principles of cerebral ultrasound contrast imaging. Cerebrovasc Dis 2009; 27 Suppl 2:14–24. Retrieved 9 September 2014 from http://www.ncbi.nlm.nih.gov/pubmed/19372657

38. Seidel G, Albers T, Meyer K, Wiesmann M. Perfusion harmonic imaging in acute middle cerebral artery infarction. Ultrasound Med Biol 2003; 29:1245–51. Retrieved 30 September 2014 from http://linkinghub.elsevier.com/retrieve/pii/S0301562903010160

39. Seidel G, Algermissen C, Christoph a., Claassen L, Vidal-Langwasser M, Katzer T. Harmonic Imaging of the Human Brain : Visualization of Brain Perfusion With Ultrasound. Stroke 2000; 31:151–4. Retrieved 30 September 2014 from http://stroke.ahajournals.org/cgi/doi/10.1161/01.STR.31.1.151

40. Seidel G, Cangür H, Meyer-Wiethe K, Renault G, Herment a, Schindler a, et al. On the ability of ultrasound parametric perfusion imaging to predict the area of infarction in acute ischemic stroke. Ultraschall Med 2006; 27:543–8. Retrieved 24 September 2014 from http://www.ncbi.nlm.nih.gov/pubmed/17146746

41. Seidel G, Kaps M. Harmonic Imaging of the Vertebrobasilar System. Stroke 1997; 28:1610–3. Retrieved from http://stroke.ahajournals.org/cgi/doi/10.1161/01.STR.28.8.1610

42. Seidel G, Meairs S. Ultrasound contrast agents in ischemic stroke. Cerebrovasc Dis 2009; 27 Suppl 2:25–39. Retrieved 31 October 2014 from http://www.ncbi.nlm.nih.gov/pubmed/19372658

43. Seidel G, Meyer K, Metzler V, Toth D, Vida-Langwasser M, Aach T. Human cerebral perfusion analysis with ultrasound contrast agent constant infusion: a pilot study on healthy volunteers. Ultrasound Med Biol 2002; 28:183–9.

44. Seidel G, Meyer-Wiethe K, Berdien G, Hollstein D, Toth D, Aach T. Ultrasound perfusion imaging in acute middle cerebral artery infarction predicts outcome. Stroke 2004; 35:1107–11. Retrieved 30 September 2014 from http://www.ncbi.nlm.nih.gov/pubmed/15031454

45. Seidel G, Meyer-Wiethe K. Ultrasound Perfusion Imaging in Acute Ischemic Stroke. In: Schaller B, ed. State-of-the-art Imaging in Stroke Volume 1. 2007:1–31.

46. Stolz E, Allendörfer J, Jauss M, Traupe H, Kaps M. Sonographic harmonic grey scale imaging of brain perfusion: scope of a new method demonstrated in selected cases. Ultraschall Med 2002; 23:320–4. Retrieved from http://www.ncbi.nlm.nih.gov/pubmed/12400023

47. Totaro R, Marini C, Sacco S, Baldassarre M, Carolei A. CONTRAST-ENHANCED TRANSCRANIAL DOPPLER SONOGRAPHY IN PATIENTS WITH ACUTE CEREBROVASCULAR DISEASES. Funct Neurol 2000; 16:11–6.

48. Vicenzini E, Delfini R, Magri F, Puccinelli F, Altieri M, Santoro A, et al. Semiquantitative human cerebral perfusion assessment with ultrasound in brain space-occupying lesions: preliminary data. J Ultrasound Med 2008; 27:685–92. Retrieved from http://www.ncbi.nlm.nih.gov/pubmed/18424642

49. Wei K, Jayaweera a. R, Firoozan S, Linka a., Skyba DM, Kaul S. Quantification of Myocardial Blood Flow With Ultrasound-Induced Destruction of Microbubbles Administered as a Constant Venous Infusion. Circulation 1998; 97:473–83. Retrieved 8 September 2014 from http://circ.ahajournals.org/cgi/doi/10.1161/01.CIR.97.5.473

50. Wiesmann M, Meyer K, Albers T, Seidel G. Parametric perfusion imaging with contrast-enhanced ultrasound in acute ischemic stroke. Stroke 2004; 35:508–13. Retrieved 30 September 2014 from http://www.ncbi.nlm.nih.gov/pubmed/14739406

51. Wiesmann M, Seidel G. Ultrasound Perfusion Imaging of the Human Brain. Stroke 2000; 31:2421–5. Retrieved 31 October 2014 from http://stroke.ahajournals.org/cgi/doi/10.1161/01.STR.31.10.2421

52. Wijnhoud AD, Franckena M, van der Lugt A, Koudstaal PJ, Dippel EDWJ. Inadequate acoustical temporal bone window in patients with a transient ischemic attack or minor stroke: role of skull thickness and bone density. Ultrasound Med Biol 2008; 34:923–9. Retrieved 28 December 2014 from http://www.ncbi.nlm.nih.gov/pubmed/18243493

Figures and Tables:

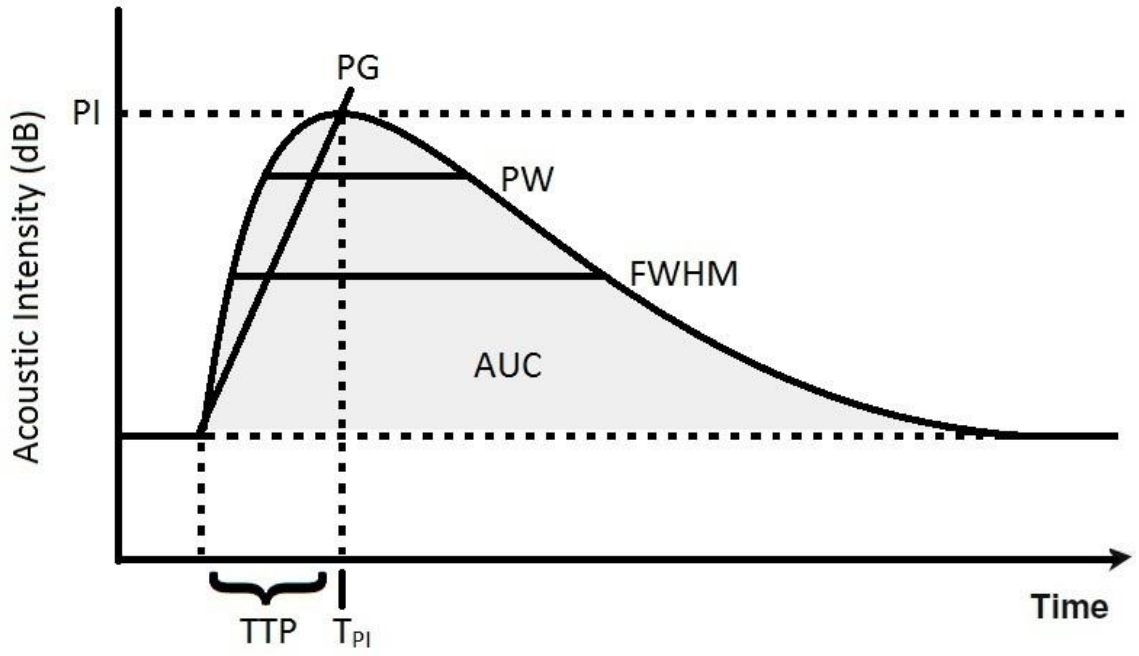

Figure 1: Time intensity curve of the bolus kinetic CEUS approach, with the perfusion parameters: area under the curve (AUC), full width at half of the maximum intensity increase (FWHM), positive gradient (PG, slope of the wash-in phase), peak intensity (PI), peak width (PW, full width at 90% of the maximum intensity), time-to-peak intensity (T_{PI}) and time-to-peak (TTP).

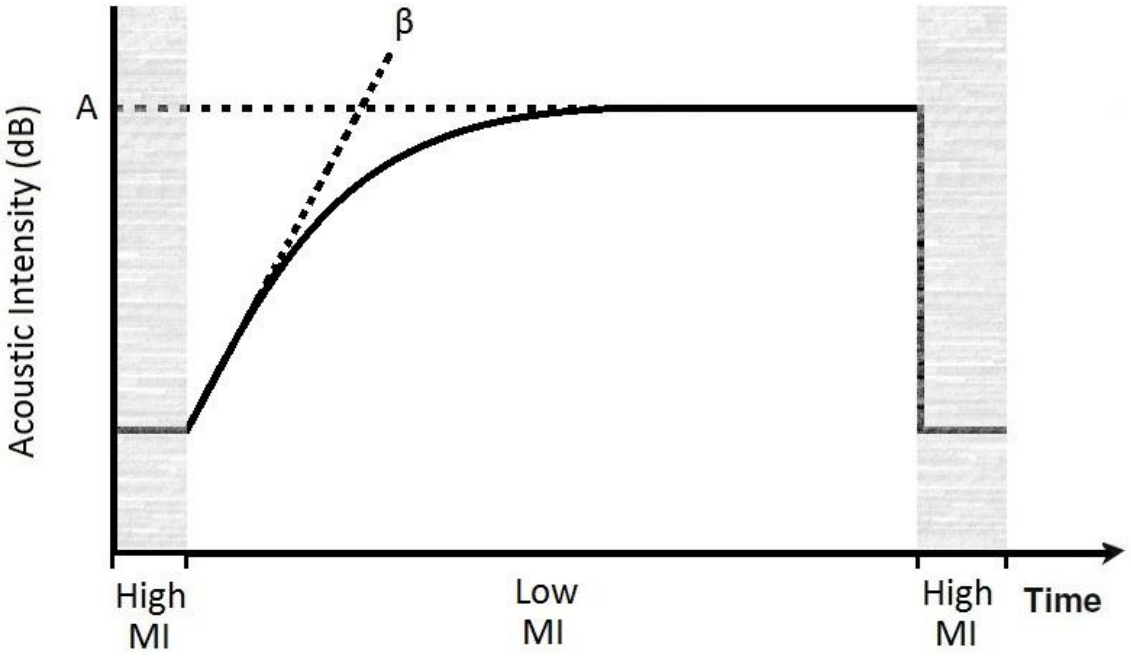

Figure 2: Intensity curve of the refill kinetics, resulting from high MI pulses followed by low MI pulses. The perfusion parameters are β, corresponding with the slope of the replenishment and A, corresponding with the asymptote of the refill curve.

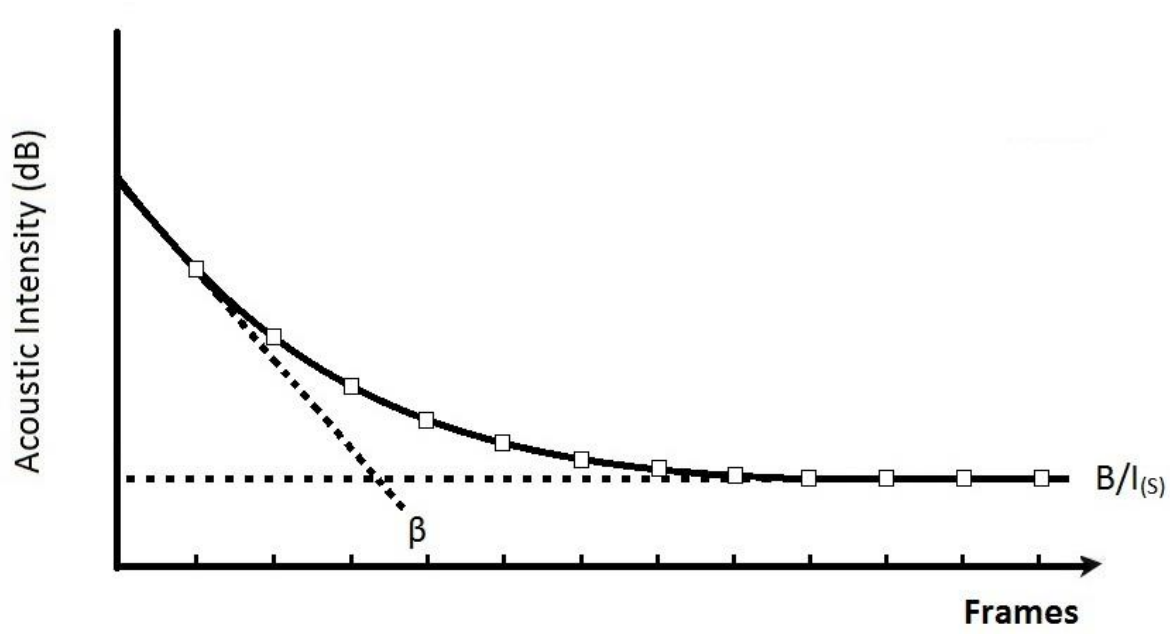

Figure 3: Scheme of contrast depletion kinetics of brain perfusion assessment. β= ln2/half life, B = baseline intensity (exponential model), equivalent to $I_{(S)}$ = intensity at the steady state (linear model). The dotted line indicates the two components of the complex exponential model.

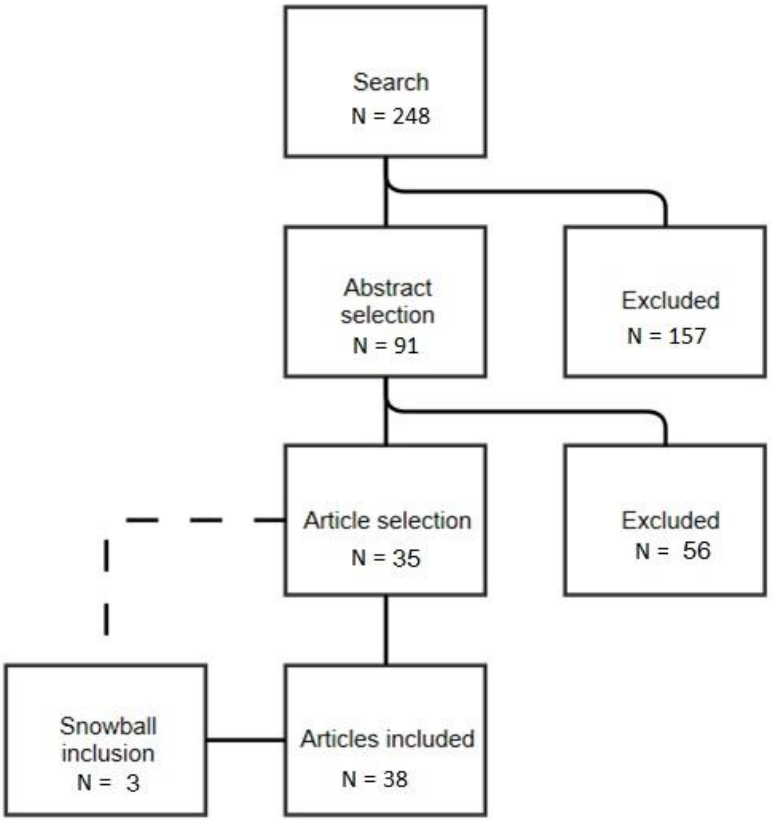

Figure 4: Flowchart of the literature review process.

Table 1: Search terms of the systematic review.

OR	cerebral blood flow cerebral circulation brain perfusion	contrast-enhanced ultrasound contrast enhanced ultrasound contrast-enhanced ultrasonography contrast enhanced ultrasonography contrast ultrasound ultrasound perfusion imaging ultrasound contrast agent ultrasound contrast agents

Table 2: Overview of the included studies and the study population.

Author	No. of patients; Type of disease	No. healthy subjects	Author	No. of patients; Type of disease	No. healthy subjects
Seidel et al. 1997[31]	0;	13	Seidel et al. 2004[17]	23; Acute ischemic stroke	0
Postert et al. 1998[10]	0;	18	Wiesmann et al. 2004[18]	30; Acute ischemic stroke	0
Federlein et al. 2000[13]	25; Acute ischemic stroke	14	Bartels et al. 2005[19]	6; Acute ischemic stroke	4
Seidel et al. 2000[26]	0;	12	Caruso et al. 2005[20]	20; Diabetes type II	20
Wiesmann and Seidel 2000[43]	0;	13	Hölscher et al. 2005[35]	0;	32
Postert et al. 2000[6]	0;	9	Krogias et al. 2005[21]	0;	20
Hölscher et al. 2002[32]	0;	13	Bartels and Bittermann 2006[22]	4; Intracranial space-occupying lesions	10
Meves et al. 2002[39]	0;	12	Eyding et al. 2006[23]	34; Hemispheric syndrome	0
Meyer and Seidel 2002[27]	0;	12	Heppner et al. 2006[45]	6, Traumatic brain injury	0
Stolz et al. 2002[14]	2; Moya-moya syndrome	10	Seidel et al. 2006[24]	22; Acute Ischemic stroke	0
Seidel et al. 2002[28]	0;	12	Engelhardt et al. 2007[54]	7; Brain tumour	0
Eyding et al. 2003 jan[29]	0;	17	Eyding et al. 2007[38]	10; Hemispheric syndrome	0
Eyding et al. 2003 oct[33]	0;	14	Meyer-Wiethe et al. 2007[40]	10; Acute Ischemic stroke	0
Seidel et al. 2003[11]	24; Acute ischemic stroke	0	Ickenstein et al. 2008[37]	6; Brain tumour	0
Bartels and Bittermann 2004[12]	10; Acute ischemic stroke	10	Kern et al. 2008[44]	12; Intracerebral hemorrhage	0
Eyding et al. 2004 apr[30]	0;	18	Vicenzini et al. 2008[25]	20; Brain tumour or brain hemorrhage	0
Eyding et al. 2004 jun[15]	4; Hemispheric Syndrome	0	Krogias et al. 2010[41]	10; Severe ICA stenosis	0
Eyding et al. 2004 aug[34]	0;	13	Kern et al. 2011[42]	23; Acute ischemic stroke	0
Kern et al. 2004[16]	15; Acute ischemic stroke	0	Bolognese et al. 2013[36]	24; Acute ischemic stroke	0

Table 3: Demographic data of the study population.

Study population	Total no. of subjects	Percentage (%)
Healthy subjects	296	
Patients:	327	100.00
Stroke	212	64.83
Hemispheric Syndrome	48	14.68
Brain tumor	28	8.56
Intracerebral hemorrhage	17	5.20
Moya-moya syndrome	2	0.61
Severe ICA stenosis	10	3.06
Traumatic brain injury	6	1.83
Intracranial space-occupying lesions	4	1.22
Diabetes type II	20	6.12

Table 4: Study population and the number of mentioned side effects for each UCA.

UCA	Subjects	Condition	No. Subjects	No. Subjects with side effects
Levovist	Controls		91	0
	Patients	Stroke	79	0
Optison	Controls		112	12
	Patients	Moya-moya syndrome	2	0
Definity	Controls		0	0
	Patients	Traumatic brain injury	6	0
Sonovue	Controls		44	0
	Patients		223	0
		Stroke	100	0
		Hemispheric Syndrome	44	0
		Brain tumour	28	0
		Intracerebral haemorrhage	17	0
		Severe ICA stenosis	10	0
		Intracranial space-occupying lesions	4	0
		Diabetes type II	20	0
Total			**555**	**12**

Table 5: Insonation approaches

Insonation approach	No. Of studies	No. Healthy subjects	No patients
Transtemporal	34	300	322
Onesided	20	151	128
Twosided	14	115	136
Onesided bilateral	6	34	58
Craniectomy	4	0	25

Table 6: Time between the CEUS examinations.

Time between examinations	No. Of studies	Bolus studies	Infusion studies
30 minutes	4	4	0
20 minutes	3	3	0
15 minutes	1	1	0
10 minutes	8	6	2
5-10 minutes	3	3	0

Table 7 a): Overview of the characteristics of the CEUS studies using the bolus kinetics approach. (Part 1) Abbreviations: mechanical index (MI), transducer type (TD), transmit frequency (TF), ultrasound contrast agent (UCA) and in case characteristics were not mentioned nm was notated.

Author	Study Population	US system, TD, TF	US method, depth, insonation plane, MI	UCA	Start after UCA, acquisition time	Insonation Side	Side effects	Reference	Perfusion parameters
Bolus (1)									
Seidel et al. 1997	13 healthy	SONOS 2500, 1.8/3.6 MHz, nm	Harmonic Imaging (HI); grey scale; depth unknown; axial; MI nm	Levovist 6.5 ml (1ml/s)	nm	Onesided	nm	x	Nr of visible segments, time of signal enhancement, maximal investigation depth
Postert et al. 1998	18 healthy	SONOS 5500, 2.5 MHz, nm	Harmonic Imaging (HI); grey scale; 10 cm; axial; MI nm	Levovist 6.5 ml (0.65 ml/s)	direct, 244 cardiac circles (61 images)	Twosided	0;	x	AUC, PI, TPI
Federlein et al. 2000	25 Acute ischemic stroke; 14 healthy	SONOS 5500, 1.8/3.6 MHz, nm	Harmonic Imaging (HI); grey scale; 10 cm; axial diencephalic plane; MI nm	Levovist 10 ml	direct, 2 minutes (0.5 Hz)	Onesided	nm	CT, CTA or DSA, TCCS	
Seidel et al. 2000	12 healthy	SONOS 5500, 1.8/3.6 MHz, nm	Harmonic Imaging (HI); Integrated backscatter (IBS); grey scale; 10 cm; axial; MI 1.0-1.1	Optison 0.5 and 1.5 ml (1ml/s)	direct, 248 cardiac cycles (62 images)	Twosided	2 subjects with mild side effects	x	AUC, PI
Wiesmann and Seidel 2000	13 healthy	SONOS 5500, 1.8/3.6 MHz, nm	Harmonic Imaging (HI); Integrated backscatter (IBS); grey scale; 10 cm; axial; MI 1.0-1.1	Optison 0.5 &1.5 ml (1ml/s)	direct, 248 cardiac cycles (62 images)	Twosided	nm	x	API, PPI
Postert et al. 2000	9 healthy	Sonoline Elegra, 2.5 MHz, nm	Contrast burst imaging (CBI) and Time variance imaging (TVI); Power Doppler (funcamental), 10 cm, axial diencephalic plane; MI >1	Levovist 10 ml	direct, 90-140 seconds (0.5 Hz)	Onesided	0;	x	PI, TPI
Hölscher et al. 2002	13 healthy	Sonoline Elegra, 2.5 MHz, nm	Contrast burst imaging (CBI) and Time variance imaging (TVI); Power Doppler (funcamental), unknown depth, axial; MI >1	Optison 0.7 ml (2ml/s)	nm, 130 seconds (0.5 Hz)	Twosided	nm	x	TPI, PI

Table 7 b): Overview of the characteristics of the CEUS studies using the bolus kinetics approach. (Part 2) Abbreviations: mechanical index (MI), transducer type (TD), transmit frequency (TF), ultrasound contrast agent (UCA) and in case characteristics were not mentioned nm was notated.

Author	Study Population	US system, TD, TF	US method, depth, insonation plane, MI	UCA	Start after UCA, acquisition time	Insonation side	Side effects	Reference	Perfusion parameters
Bolus (2)									
Meves et al. 2002	12 healthy	Sonoline Elegra, 2.5 MHz, nm	Contrast burst imaging (CBI) and Time variance imaging (TVI); Power Doppler (funcamental), 10 cm, axial diencephalic plane; MI CBI <1.5; TVI <1	Levovist 10 ml (8 ml/s)?	direct, 100-140 seconds (0.5 Hz)	onesided	0;	PWI	PI, TPI, PW
Stolz et al. 2002	2 Moya-moya syndrome; 10 healthy	SONOS 5500, 1.8/3.6 MHz, nm	Power Modulation Imaging (PM); 11 cm; axial; MI nm	Optison 2 ml	nm, 240 cardiac cycles (60 images)	twosided	nm	x	PI, TTP, AUC, MTT, RT
Eyding et al. 2003 oct	14 healthy	Sonoline Elegra, 2.5 MHz, TF 2.0 MHz	Pulse Inversion Harmonic Imaging (PIHI); grey scale; 10 cm; axial; MI nm	Sonovue; Optison	nm (0.5 Hz)	ipsi and bilateral (onesided)	0;	x	TPI, PI, PW
Seidel et al. 2003	24 Acute ischemic stroke	SONOS 5500, 1.8/3.6 MHz, nm	Harmonic Imaging (HI); Integrated backscatter (IBS); grey scale; 10 cm; axial midthalamic plane; MI nm	Levovist 5 ml	direct, >160 cardiac cycles (>40 images)	twosided	nm	CCT	PI, AUC
Bartels and Bittermann 2004	10 Acute ischemic stroke; 10 healthy	Acuson Seqouia 512, 2-4 MHz, nm	Harmonic Imaging (HI) (single-pulse transmission technology); grey scale; unknown depth; axial mesencephalic brainstem and diencephalic plane; MI stroke (craniectomy) 1.0-1.1, healthy 1.6	Sonovue 5 ml	nm, patients: 4 minutes	patients: craniotomy, onesided	0;	CT/MRI	Time between application of UCA and appearance, TTP, bolus duration, mean intensity before, during bolus, and steady state plateau (dB), mean bolus perfusion quotient, steady state perfusion quotient (%)
Eyding et al. 2004 jun	4 Hemispheric Syndrome	Sonoline Elegra, 2.5 MHz, TF 2.0 MHz	Pulse Inversion Harmonic Imaging (PIHI); grey scale; 15 cm (bilateral approach); axial diencephalic plane; MI >1	Sonovue 2.5 ml	90 seconds, nm (0.5 Hz)	onesided bilateral	nm	PWI	TPI, PI, PW

Table 7 c): Overview of the characteristics of the CEUS studies using the bolus kinetics approach. (Part 3) Abbreviations: mechanical index (MI), transducer type (TD), transmit frequency (TF), ultrasound contrast agent (UCA) and in case characteristics were not mentioned nm was notated.

Author	Study Population	US system, TD, TF	US method, depth, insonation plane, MI	UCA	Start after UCA, acquisition time	Insonation side	Side effects	Reference	Perfusion parameters
Bolus (3)									
Seidel et al. 2004	23 Acute ischemic stroke	SONOS 5500, 1.8/3.6 MHz, nm	Harmonic Imaging (HI); Integrated backscatter (IBS); grey scale; 10 cm; axial midthalamic plane; MI nm	SonoVue 2.4 ml	direct, nm (0.67 Hz)	onesided	nm	CCT	PPI,TTP
Wiesmann et al. 2004	30 Acute ischemic stroke	SONOS 5500, 1.8/3.6 MHz, nm	Harmonic Imaging (HI); Integrated backscatter (IBS); grey scale; 10 cm; axial midthalamic plane; MI nm	Levovist 5 ml	direct, 248 cardiac cycles (62 images)	twosided	0;	CCT	PPI, TTP
Caruso et al. 2005	20 Diabetes type II; 20 healthy	Duplex US system, 2 MHz, nm	Harmonic Imaging (HI); grey scale; 10 cm; axial diencephalic plane; MI nm	SonoVue 2.5 g (1 ml/s)	direct, 2 minutes (0.5 Hz)	onesided	0;	x	PI, PG
Hölscher et al. 2005	32 healthy	Sonoline Elegra, 2.5 MHz, nm	Contrast burst imaging (CBI); Power Doppler (funcamental), unknown depth, axial diencephalic plane; MI nm	Optison	nm (36-40 frames)	twosided	nm	x	TPI, PI
Krogias et al. 2005	20 healthy	Sonoline Elegra, 2.5 MHz, TF 2.0 MHz	Pulse Inversion Harmonic Imaging (PIHI); grey scale; 15 cm (bilateral approach); axial diencephalic plane; MI >1	SonoVue 2.5 ml (5ml/s)	direct, nm (0.5 Hz)	onesided bilateral	0;	x	PI, TPI, PW
Bartels and Bittermann 2006	4 Intracranial space-occupying lesions	Acuson Seqouia 512, 2-4 MHz, nm	Harmonic Imaging (HI) (single-pulse transmission technology); grey scale; unknown depth; axial mesencephalic brainstem and diencephalic plane ; MI craniectomy (2 subjects) 1.1, other 1.6	SonoVue 2x 2.5 ml (slow)	nm (1 Hz)	onesided, 2 craniotomy	0;	CT/MRI	API
Eyding et al. 2006	34 Hemispheric syndrome	Sonoline Elegra, 2.5 MHz, TF 2.0 MHz	Pulse Inversion Harmonic Imaging (PIHI); grey scale; 15 cm (bilateral approach); axial midthalamic plane; MI >1	SonoVue 2.5 ml	90 seconds, nm (0.5 Hz)	onesided bilateral	0;	CCT	TPI

Table 7 d): Overview of the characteristics of the CEUS studies using the bolus kinetics approach. (Part 4) Abbreviations: mechanical index (MI), transducer type (TD), transmit frequency (TF), ultrasound contrast agent (UCA) and in case characteristics were not mentioned nm was notated.

Author	Study Population	US system, TD, TF	US method, depth, insonation plane, MI	UCA	Start after UCA, acquisition time	Insonation side	Side effects	Reference	Perfusion parameters
Bolus (4)									
Seidel et al. 2006	22 Acute Ischemic stroke	SONOS 5500, 1.8/3.6 MHz, nm	Harmonic Imaging (HI); grey scale; 10 cm; axial diencephalic plane; MI nm	SonoVue 2.4 ml	direct, nm (0.67 Hz)	onsided	nm	CT	PPI, AUC, PG, TTP
Engelhardt et al. 2007	7 Brain tumour	Sonoline Elegra, 6.5 MHz, TF 3.0 MHz	Pulse Inversion Harmonic Imaging (PIHI), grey scale, unknown, resection area (craniotomy); Transmission power 5%	SonoVue 1.5 ml	nm, 70 seconds (1Hz)	onesided	nm	MRI	PI, TTP PW
Eyding et al. 2007	10 Hemispheric syndrome	Sonoline Elegra, 2.5 MHz, TF 2.0 MHz	Pulse Inversion Harmonic Imaging (PIHI), grey scale, 15 cm (bilateral approach), axial diencephalic plane; MI >1	SonoVue 2.5 ml	nm (0.5 Hz)	onesided bilateral	0;	CCT	TPI
Meyer-Wiethe et al. 2007	10 Acute Ischemic stroke	SONOS 5500, 1.8/3.6 MHz, nm	Harmonic Imaging (HI); grey scale; 10 cm; axial diencephalic plane; MI 1.6	SonoVue 2.4 ml	nm, 93 seconds (0.67 Hz)	onesided	nm	MRI	PI, TPI, AUC
Ickenstein et al. 2008	6 Brain tumour	Sonoline Elegra, 2.5 MHz, TF 1.2-2.4 MHz	Contrast burst imaging (CBI); Power Doppler (funcamental); 10 cm; axial; MI 1.8	SonoVue 5 ml (2ml/s)	nm, 60 seconds (1 Hz)	twosided	0;	CT	AUC, TTP, PI
Vicenzini et al. 2008	15; Brain tumour, 5; intracerebral hemorrhage	Acuson Sequoia 512, 2.5 MHz, nm	Contrast Pulse Sequencing (CPS); Power Doppler (fundamental); unknown depth; axial mesencephalic and diencephalic plane; MI 0.9	SonoVue 2.5 ml	direct, 120 seconds (30 Hz)	onesided	nm	CT/MRI	PI,TTP, full width, MTT, AUC, perfusion index
Krogias et al. 2010	10 Severe ICA stenosis	Sonoline Elegra2.5 MHz, TF 2.0 MHz	Pulse Inversion Harmonic Imaging (PIHI); grey scale; 15 cm (bilateral approach); axial diencephalic plane; MI 1.6	SonoVue 2.5 ml	direct, nm (0.5 Hz)	onesided bilateral	0;	MRI	PI, TPI, PW

Table 8: Overview of the characteristics of the CEUS studies using the refill kinetics approach. Abbreviations: mechanical index (MI), transducer type (TD), transmit frequency (TF), ultrasound contrast agent (UCA) and in case characteristics were not mentioned nm was notated.

Author	Study Population	US system, TD, TF	US method, depth, insonation plane, MI	UCA	Start after UCA, acquisition time	Insonation side	Side effects	Reference	Perfusion parameters
Refill									
Seidel et al. 2002	12 heathy	SONOS 5500, 1.8/3.6 MHz, nm	Harmonic Imaging (HI); grey scale; 10 cm; axial diencephalic plane; MI 1.0-1.6	Optison 4.5 ml total (0.5 ml/min en 1.0 ml/min)	90 seconds, 16 min total examination	onesided	0;		A, β, Axβ
Bartels et al. 2005	6 Acute ischemic stroke; 4 healthy	Acuson Seqouia 512, 2-4 MHz, nm	Contrast pulse sequencing technology (CPS) (single-pulse transmission technology); grey scale; unknown depth; axial mesencephalic brainstem and diencephalic plane; MI 1.1 and stroke 0.28, healthy 0.29	SonoVue 2x 2.5 ml (slow)	nm (0.5 and 1 Hz)	onesided	0;	MRI	Time between application of UCA and appearance, TTP, bolus duration, mean intensity before, during bolus, and steady state plateau (dB), mean bolus perfusion quotient, steady state perfusion quotient (%)
Heppner et al. 2006	6, Traumatic brain injury	SONOS 5500, nm, TF 1.7 MHz	Power Modulation Imaging (PM); unknown depth; sagittal and coronal planes through bur hole (craniotomy); MI 0.7, (2 frames) and 0.2	Definity 0.1 ml/min	nm, 10 seconds	Craniectomy	nm	x	A, β, Axβ
Kern et al. 2011	23 Acute ischemic stroke	iU22 xMatrix, 1-5 MHz, nm	Contrast Pulse Sequencing (CPS); Power Doppler (fundamental); unknown depth; axial 20 degrees cranial from mesencephalic plane; MI 1.32 (10 flashes) and 0.17	SonoVue 2.5 ml	direct, 10 seconds (15 Hz)	twosided	0;	PWI	A, β, rt-TTP
Bolognese et al. 2013	24 Acute ischemic stroke	iU22 xMatrix, 1-5 MHz, nm	Contrast Pulse Sequencing (CPS); Power Doppler (fundamental); unknown depth; axial 20 degrees cranial from mesencephalic plane; MI 1.47 (10 flashes) and 0.17	SonoVue 2,5 ml	direct, 10 seconds	twosided	nm	DWI &TCCD	rt-TTP, A, β, Axβ

Table 9: Overview of the characteristics of the CEUS studies using the depletion kinetics approach. Abbreviations: mechanical index (MI), transducer type (TD), transmit frequency (TF), ultrasound contrast agent (UCA) and in case characteristics were not mentioned nm was notated.

Author	Study Population	US system, TD, TF	US method, depth, insonation plane, MI	UCA	Start after UCA, acquisition time	Insonation side	Side effects	Reference	Perfusion parameters
Depletion									
Meyer and Seidel 2002	12 healthy	SONOS 5500, 1.8/3.6 MHz, nm	Harmonic Imaging (HI); Integrated backscatter (IBS); grey scale; 10 cm; axial diencephalic plane; MI 1.6	Optison 4.5 ml total (0.5 ml/min, 1.0 ml/min)	90 seconds, 2 seconds	onesided	0;	x	Acoustic Intensity
Eyding et al. 2003 jan	17 healthy	Sonoline Elegra, 2.5 MHz, nm	Contrast burst imaging (CBI); Power Doppler (funcamental), 10 cm, axial diencephalic plane; MI 1.8	Levovist: 8ml (2ml/s); Optison: 0.5 ml (0.5 ml/s)	40 seconds, nm (at 1 Hz)	twosided	4 subjects (Optison) with local effects	PWI	PC, DC
Eyding et al. 2004 apr	18 healthy	Sonoline Elegra, 2.5 MHz, nm	Contrast burst imaging (CBI); Power Doppler (funcamental), 10 cm, axial diencephalic plane; MI 1.8	Levovist: 8ml (2ml/s); Optison: 0.5 ml (0.5 ml/s)	40 seconds, 10-35 seconds (T1/2)	onesided	4 subjects with local effects (Optison)	x	Tmin, PC
Eyding et al. 2004 aug	13 healthy	Sonoline Elegra, 2.5 MHz, nm	Contrast burst imaging (CBI) and Pulse Inversion Harmonic Imaging (PIHI); unknown depth; axial diencephalic plane; MI 1.8	Optison 0.5 ml; 0.5 ml/s	40 seconds, nm (1 Hz)	onesided	2 subjects with local effects	x	PC, Tmin, RE
Kern et al. 2004	15;Acute ischemic stroke	HDI 5000, 2-4 MHz, nm	Power pulse inversion contrast harmonic imaging (PPICHI); Power Doppler; axial 20 degrees cranial from mesencephalic plane; MI 1.2 (20 frames) and low	SonoVue 2.5 ml	30 seconds, 1.4 seconds (14 Hz)	twosided	0;	PWI	δ I, I(t0), I(tbaseline)
Kern et al. 2008	12 Intracerebral hemorrhage	HDI 5000, 2-4 MHz, nm	Pulse Inversion Harmonic Imaging (PIHI); grey scale; 12 cm; axial; MI 1.3	SonoVue 2 ml bolus and 1 ml/min	30 seconds, 1.4 seconds (14 Hz)	twosided	0;	CT	PI, TTPI, PC, DC